HYDROLOGIC RESPONSE TO CONIFER REMOVAL FROM AN ENCROACHED MOUNTAIN MEADOW

A Thesis
presented to
the Faculty of California Polytechnic State University,
San Luis Obispo

In Partial Fulfillment
of the Requirements for the Degree
Master of Science in Forestry Sciences

by
Gregory Van Oosbree
June 2015

COMMITTEE MEMBERSHIP

TITLE:	Hydrologic Response to Conifer Removal from an Encroached Mountain Meadow
AUTHOR:	Gregory Van Oosbree
DATE SUBMITTED:	June 2015

COMMITTEE CHAIR:	Christopher Surfleet, Ph.D., Graduate Coordinator, Natural Resources Management and Environmental Sciences Department
COMMITTEE MEMBER:	John Jasbinsek, Ph.D., Associate Professor, Physics Department
COMMITTEE MEMBER:	Bwalya Malama, Ph.D., Associate Professor, Natural Resources Management and Environmental Sciences Department

ABSTRACT

Hydrologic Response to Conifer Removal from an Encroached Mountain Meadow

Gregory Van Oosbree

Meadows in the Sierra Nevada Mountains are an important ecological resource that have degraded in quality and distribution due to several environmental and anthropogenic stressors. The encroachment of conifers beyond forest meadow ecotones is largely responsible for the decline of meadow habitat throughout the past century. Currently, there is little research that quantifies the hydrologic response to removal of conifers encroaching meadows in terms of implicating successful meadow restoration. This study has implemented a before after control intervention (BACI) study design to determine the hydrologic response associated with the removal of conifers from a historic meadow encroached by conifers. The primary goals of this research were to: (1) establish a method to evaluate the weekly water balance of an encroached meadow before and after conifer removal (restoration) (2) characterize the hydrology of an encroached meadow and a nearby control meadow prior to restoration (3) assess the effectiveness of electrical resistivity tomography in improving the spatial interpretation of subsurface hydrology on our study site. A water budget approach was developed to quantify the hydrology of a control and study meadow (Marian Meadow) before and after restoration. In order to determine weekly changes in groundwater depth, 14 Odyssey water level capacitance instruments were installed to a 1.5 meter depth in PVC wells. In order to quantify changes in soil moisture storage, 14 soil moisture probes were installed to a ~1 ft (30 cm) depth. Both sets of instruments were installed using a spatially balanced random sampling approach. Electrical resistivity tomography was conducted on both meadows on three separate dates during: September 9-10 2013, May 5 2014 and September 6-7 2014. A method to quantify runoff from a stream that drains Marian Meadow (Marian Creek) was also established. The Priestley Taylor model was used to estimate daily evapotranspiration from both meadows. Electrical resistivity tomography improved the spatial interpretation of groundwater recharge and facilitated the use of a recession curve analysis to model groundwater recharge when the water table receded beyond instrument detection depths. Electrical resistivity also demonstrated a change in hydrologic characteristics across a forest –meadow ecotone. Analysis of the pre-removal hydrologic characteristics from September 2013 to December 2014 indicates that Marian Meadow may be a favorable candidate for restoration (in terms of hydrology). On Marian Meadow, volumetric soil moisture was higher than the Control Meadow from May-November 2014. Sufficient soil moisture in the summer months is thought to be critical to the maintenance of endemic meadow flora. The water table depth on Marian Meadow and the Control Meadow was similar throughout the analysis period, but Marian Meadow had a shallower water table during the summer months. The Control Meadow had near surface groundwater during short periods from February-April 2014 and December 2014. If conifer removal from Marian Meadow causes an increase in seasonal volumetric soil moisture and a decrease in seasonal groundwater depth, an augmented version of the stable hydrologic system already present on Marian Meadow may result in hydrologic conditions more favorable to meadow restoration.

ACKNOWLEDGMENTS

The research presented in this thesis could not have occurred without the close assistance and encouragement provided by many individuals. I would like to principally thank my major adviser Dr. Christopher Surfleet for his patience and commitment of time throughout the process of conducting this research and preparing this document. My committee members Dr. John Jasbinsek and Dr. Bwalya Malama also contributed invaluable assistance to this research and the preparation of this document. I would also like to thank all of the Cal Poly faculty that have supported my growth and development as a scientist and scholar. I would like to particularly thank Dr. Christopher Appel for his encouragement over the last two years and the large time commitment he made to help me through my 'crash-course' in soil science quarter during the spring of 2014. I would like thank my colleague Thomas Sanford for his assistance to this research and I look forward to seeing his future work. This research would not have been possible without funding made available by the California State University Agricultural Research Initiative (ARI) and the United States Department of Agriculture McIntire-Stennis Forestry Research Grant. The Collins Pine Company on whose land we are conducting this research has also played a critical role in supporting this study. Lastly, I would also like to thank my friends and family who have provided irreplaceable moral support throughout the process of completing my Master's Degree.

TABLE OF CONTENTS

Page

APPENDICES

LIST OF TABLES

LIST OF FIGURES

CHAPTER 1 INTRODUCTION

This study has developed a water budget approach to quantify the hydrologic response to vegetation removal on a meadow encroached by lodgepole pine (*Pinus contorta*) and other conifer species. Marian Meadow (MM), a 46-acre (0.186 km^2) historic meadow will have all encroaching conifers removed during the summer of 2015. An additional harvest of conifers from the watershed surrounding MM (2046 acres (8.28 km^2) will occur during the summer of 2016. Soil moisture probes and water level loggers have been installed to quantify the changes to soil moisture, groundwater depth and storage, and stream runoff associated with conifer removal on MM and a nearby control meadow (CM). Electrical resistivity tomography (ERT) was employed to characterize the existing seasonal subsurface hydrology of the two meadows. IRIS (Indicators of Reduction in Soils) tubes have also been used to determine the presence and extent (or lack thereof) of hydric soil on MM and CM. This study was performed with the close cooperation and assistance of the Collins Pine Almanor Forest (CPAF). The CPAF intends to facilitate the restoration of MM and other historic meadows on their land by completely removing encroaching conifers.

It is hypothesized that the removal of conifers will cause seasonal soil water content to increase and the seasonal water table to rise. Many studies have addressed meadow restoration and the hydrologic response to tree thinning or removal, but comparatively few specifically consider the role that the removal of conifers encroaching meadows in the western United States may play in facilitating meadow restoration. The assessment of the hydrologic response to conifer removal from encroached meadows and wetlands in quantitative terms provides an opportunity for land managers to determine

the effectiveness of efforts to restore historic meadows and wetlands. The goal of this research at MM, of which this thesis is part, is to determine if the removal of encroaching conifers from a historic meadow will (1) increase the quantity of seasonal soil moisture and (2) decrease the depth to the seasonal water table such that seasonal wetland (meadow) conditions are promoted. There are three objectives to the research comprising this thesis. First, to determine a robust method for evaluating the water balance for pre- and post-conifer removal on an encroached meadow. Second, to characterize the existing hydrology on Marian Meadow and a nearby Control Meadow prior to conifer removal. Three, to determine the effectiveness of using electrical resistivity tomography to improve the spatial interpretation of subsurface water on MM.

CHAPTER 2 LITERATURE REVIEW

2.1 Literature Review Overview

The quantification of the hydrologic response associated with conifer removal from encroached meadows is particularly important in terms of determining what actions are necessary to promote the return of meadow species because hydrology exerts the an influential control on the vegetative composition of meadows and wetlands (Lowry et al., 2011 and Lord et al., 2011). This literature review addresses the body of research pertaining to meadows in the western United States, threats to their persistence, conifer encroachment, the hydrologic response to vegetation removal on managed sites and the means by which the hydrologic response to conifer removal may be quantified.

2.2 Meadows in the Sierra Nevada and Cascades Mountains

Meadows in the Sierra Nevada and Cascade Mountains occur at elevations ranging from 918 to 12,910 ft (280-3935 m) (Gross and Coppoletta, 2013). Meadows serve several valuable hydrological and ecological functions integral to the maintenance of productive ecosystems such as promoting faunal and floral biodiversity and increasing late season base flow in streams (Viers et al., 2013). Meadows also provide several benefits to land managers including flood attenuation, increased plant forage, increased water quality in streams, and aesthetic/recreational values. The Sierra Nevada and Cascade Mountains encompass approximately 25% of the land area of California (Skinner and Taylor, 2006). Meadows comprise about 10% of the land area within the Sierra Nevada Mountains (Ratliff, 1985). Despite comprising less than a quarter of California's land area, the Sierra Nevada Mountains alone contain over 50% of

California's native flora (comprising of 405 taxa)), many of which are exclusive to meadow habitat (Shevock, 1996).

Meadow ecosystems tend to develop in basins or valleys that contain shallow layers of alluvial or colluvial deposits. Comparisons of meadow stratigraphy across the Sierra Nevada Mountains indicate that soils underlying meadows generally consist of coarse soil particles overlying bedrock that are in turn overlain by increasingly fine soils with organic matter towards the top of the soil column (Anderson and Smith, 1994). Generally, meadows possess the following attributes: the presence of one or more herbaceous plant communities, the presence of surface water or shallow groundwater during part or all of the growing season, fine textured surficial soil, and a lack of dense woody vegetation (Weixelman et al., 2011). Many sites throughout the southern Cascade and Sierra Nevada Mountains have historically been able to meet one or more of the aforementioned criteria, but are no longer able to do so due to environmental or hydrologic stressors. These sites may be considered degraded meadows that have the potential to be restored (Stillwater Sciences, 2012).

Previous efforts to establish a comprehensive classification system for meadows in the mountainous regions of the western United States have focused on one or several of the following characteristics: resident biological communities, elevation, site potential, site topography, geomorphic position, and moisture gradient (Ratliff, 1985). Meadows classified by moisture gradient are usually defined as either: wet, mesic, dry or sagebrush meadows. These classifications are based primarily on the depth to the water table (Chambers et al., 2011). A study in the Great Basin Region observed that the depth to the water table below dry meadows and mesic meadows ranged from 0.8-1.7 m and 0.5 -1.2

m respectively (Chambers et al., 2004) (Fig 2.1). Dry and mesic meadows tend to occur in areas where precipitation and runoff are the primary sources of soil moisture and groundwater inflow is a secondary input (Weixelman et al., 2011). In the Sierra Nevada and southern Cascade Mountains, this generally means that dry and mesic meadows have near surface groundwater during limited periods following precipitation and snowmelt (3-6 months of the year). These meadow types may occur in a variety of geomorphic settings, but must be able to retain moisture near the soil surface long enough following precipitation and snowmelt to enable perennial meadow flora to flower and reproduce (Weixelman et al., 2011). Dry meadows may occur in depressions with an underlying impervious layer that accumulates precipitation and retards the outflow of groundwater.

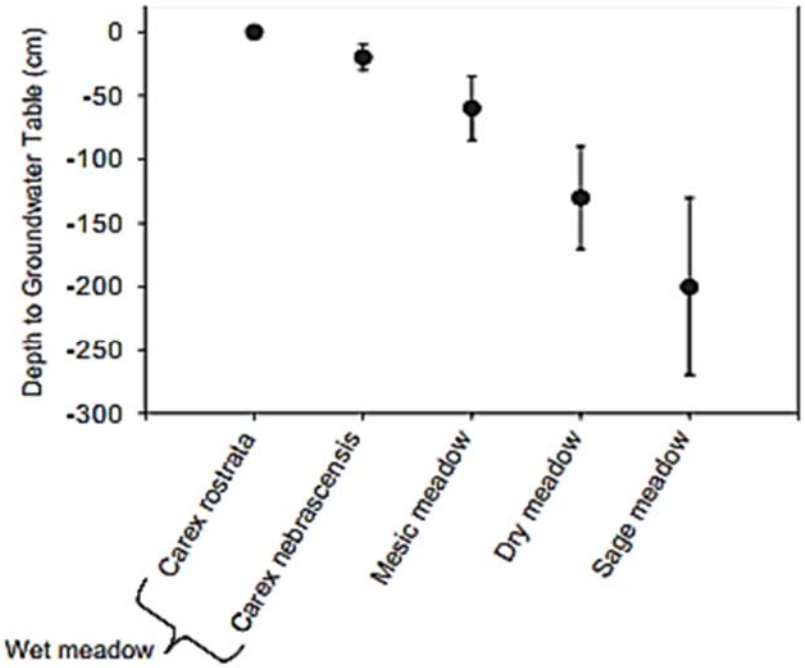

Figure 2.1 The seasonal groundwater depths associated with the moisture gradient meadow classification in the Great Basin region (Figure from Chambers et al., 2004)

The plant composition of meadows is strongly influenced by water and oxygen stresses (Lowry et al., 2011). Oxygen stress occurs when water in the root zone displaces oxygen, thereby preventing root respiration. Water stress occurs as a consequence of

drainage of gravitational and capillary water, evaporation and plant water uptake. Over time, if hydrologic inputs do not occur soil water limited conditions will cause water stress, culminating in permanent wilting point. Floral communities associated with dry and mesic meadows have a greater likelihood of occurring in regions that experience water stress, but, little to no oxygen stress. The species composition of dry and mesic meadows is characterized by the dominance of sedges, forbs and herbaceous species. Common flora associated with dry meadows in the western United States are common yarrow (*Achillea millefolium*), meadow larkspur (*Delphinium nuttallianum*), creeping wild rye (*Leymus triticoides*) and bluegrass (*Poa secunda*) (Engelhardt, 2009 and Weixelman and Zamudio, 1996).

2.3 Meadow Hydrology and Water Balance

There are several local conditions that govern the capacity of a meadow subsurface to store groundwater: the rate of inflow, the thickness and effective porosity of the underlying aquifer, the distribution of bedrock or other impermeable geologic substrata, and the ratio of the hydraulic conductivity of bedrock (or lower confining layer) to the saturated hydraulic conductivity of the aquifer (Hill and Mitchell-Bruker, 2010 and Stillwater Sciences, 2012). On a watershed scale, the size of the surrounding drainage area, topography, local microclimate, and existing stream morphology will all affect the subsurface hydrologic characteristics of meadows. The four primary inputs of water into meadows are infiltration of precipitation, snowmelt, subsurface flow from surrounding hill slopes, and inflow from streams and runoff (Lord et al., 2011). Outputs of plant available water from meadows include outflow from runoff and streams, seepage through the vadose zone and evapotranspiration (ET). In the United States, during the

summer months, ET generally accounts for the majority of losses from a hydrologic system. In the continental United States, approximately 67% of precipitation re-enters the atmosphere through ET (US Geological Survey, 1990). Evapotranspiration plays a particularly important role in the water balance of hydrologic systems during times of drought because it contributes to the depletion of already limited water resources in water bodies and soil (Hanson, 1991).

In mountainous regions with significant snowfall, groundwater recharge is largely driven by snowmelt. Snow tends to melt in pulses associated with diurnal heat fluxes and fluctuations in air temperature during the spring and early summer months. These processes promote a gradual infiltration of water into the subsurface, thereby promoting longer periods of near surface or excess surface groundwater in meadows (Lundquist and Roche, 2009). The transpiration rates of vascular plants determine which flora may colonize or persist within a given ecosystem. Plant species associated with dry meadows will generally have lower transpiration rates compared to plants that inhabit meadows that retain higher soil moisture and a shallower water table throughout the growing season (Aylward and Merill, 2012).

Evapotranspiration includes evaporation of water from soil, water bodies and snow cover and, and transpiration of water through leaf stomata. Climatic factors that govern ET rates include relative humidity, air temperature, net solar radiation, and wind speed (Allen et al., 1998). Local site factors that influence ET rates include vegetation distribution, species-specific characteristics such as rooting depth and stomatal resistance, soil moisture, and, the distribution of near surface groundwater or water bodies. Solar radiation provides the energy needed for evaporation to occur. Net radiation is the

difference between incoming radiation and reflected outgoing long wavelength radiation. The potential evapotranspiration (PET) of a land surface assumes uniform land cover by vegetation and unlimited soil moisture conditions. The actual evapotranspiration (AET) is a function of the actual soil moisture and vegetation present on a given land surface. Evapotranspiration is often modeled due to the complexity and expense of directly measuring ET. The lack of publically available site-specific atmospheric data complicates modelling ET. Five ET models that have been extensively utilized in forest ecosystems (in order of decreasing complexity) are the Shuttleworth-Wallace, Penman-Monteith, Penman, McNaughton-Black and Priestley-Taylor (PT) models. Despite its simplicity, a modified PT model has been shown to closely approximate physically measured ET in the Sierra Nevada Mountains and other Mediterranean climates (Fisher et al., 2005 and Utset et al., 2004). The success of modified PT models in forest environments led to its use in this study.

The PT model utilizes the coefficient α, (a dimensionless multiplier) to account for the percentage of surface and near surface moisture that is available for evaporation. The PT model was initially developed to estimate ET from sites with unlimited soil moisture conditions or other freely evaporating surfaces such as water bodies and wetlands. For such surfaces α is 1.26 (Priestley and Taylor, 1972). Subsequent studies have developed modified PT coefficients to account for soil water limited conditions and sites that do not possess uniform vegetation cover (Spittlehouse and Black, 1981 and Flint and Childs, 1991). Using the PT model, AET has also been modeled to be a function of field capacity and leaf area index by modifying the PT coefficient (Fisher et al., 2005 and Agam et al., 2010). Soil heat flux is often ignored when the PT model is

used to determine ET on a daily time scale (Fritschen and Gay, 1979). A statistical analysis comparing the empirically determined PT coefficient from 45 studies quantifying ET from temperate coniferous forests determined a mean constant PT coefficient of 0.65±0.25 for temperate coniferous forests (Komatsu, 2005).

2.4 Threats to Meadows in the Sierra Nevada and Southern Cascade Mountains

Currently, meadows in the Sierra Nevada face a myriad of threats including overgrazing, habitat degradation due to human recreation activities, fire prevention/regime alteration, residential/ commercial development, and climate change (Stillwater Sciences, 2012). Intensive livestock grazing can lead to excessive defoliation, trampling of sensitive vegetation, and a redistribution of nutrients within a meadow. Erosion of fertile top soil is a common consequence of intensive livestock grazing. Roads and trails also alter infiltration and runoff regimes and facilitate the introduction of invasive species. Degradation of meadow habitat generally manifests itself in the form of a reduction in seasonal soil moisture, an increase in seasonal water table depth, a loss of endemic meadow species, and the influx of pioneer vegetation such as conifers and xeric plant species.

2.4.1 Climate Change

Current trends toward warmer winters in the western United States indicate that snowpack will melt earlier in the year and more winter precipitation will occur as rain during the winter months (Stewart et al., 2005; Knowles, et al., 2006; Dettinger and Cayan, 1995). A consequence of the projected decreases in quantities of snowpack will be diminished groundwater recharge as a larger quantity of water moves through mountain watersheds as surface runoff following precipitation events (Loheide and

Lundquist, 2009). In many regions of the mountainous western United States, a deeper seasonal water table and decreased periods of field capacity will stress meadow vegetation with high transpiration rates and encourage the colonization of meadows by non-meadow species (Loheide and Gorelick, 2007). Meadows and wetlands in the northern Sierra Nevada and southern Cascade Mountains are the most vulnerable to the hydrologic regime change caused by climate change, because a higher rate of precipitation change from snow to rain will occur in this region (Stewart et al., 2004). Additionally, snowmelt timing on the western slope of the Sierra Nevada Mountains is more sensitive to small increases in temperature than the higher elevation eastern half of the range (Pupacko, 2007)

2.4.2 Conifer Encroachment

Conifer encroachment (or invasion) is a term used for movement of conifers beyond forest-meadow ecotones (a transitional zone between two ecosystems) into meadow biotic communities. Conifer encroachment is neither strictly a phenomenon associated with autogenic (governed by biotic factors) nor allogenic (governed by abiotic factors) forest succession. Analysis of meadow stratigraphy, radiocarbon dating, and tephrochronology indicate that some meadows in the Sierra Nevada Mountains have been converted cyclically to conifer forests in the past 12,000 years (Wood, 1975). In the Cascade and Sierra Nevada Mountains, soil moisture and composition often favor the establishment of *Pinus contorta* over other tree species due to its tolerance of a wide range of hydrologic and chemical conditions (Burns and Honkala, 1990). This tolerance plays a key role in its ability to colonize meadows while other tree species maintain their current position. Depending on elevation, and geomorphic position, *Pinus contorta* may

colonize meadows opportunistically during times of drought to avoid plant water stress (Gross and Coppoletta, 2013). During wetter and colder periods, soil water may act as a limiting factor on the expansion of most conifer species into wetlands and meadows due to their intolerance for prolonged oxic stress in their root zone. Alternatively, in the Cascade Mountains, successful recruitment of pioneer trees into dry and mesic meadow habitats has been tied to the onset of wetter summers and discontinuation of sheep grazing in the early 20th century (Miller and Halpern, 1998).

Research addressing 20th century conifer encroachment indicate that changes in seasonal soil moisture may play a larger role than climate in the current trend of encroachment in the Cascade Mountains (Haugo et al., 2011). Conifers can draw large quantities of water from soil. For example, the quantity of soil moisture depletion associated with a lone sugar pine (*Pinus lambertina*) in a surrounding 61.0 ft (18.6 m) radius of soil during the summer has been quantified as an equivalent depth of 22.57 in. (0.6 m) of water (Ziemer, 1968). As initial pioneer trees draw water from the soil, 'islands' of pioneers trees form and expand eventually leading to a feedback process that promotes the succession of other tree species associated with mid elevation pine forests such as ponderosa pine (*Pinus ponderosa*), *Psuedotsga menziesii*, and white fir (*Abies concolor*). Research focusing on the soil evolution of meadow forest ecotones has demonstrated that meadow soils undergo rapid biogeochemical changes as meadows are encroached by conifers (Griffiths et al., 2005). These changes are thought to be initiated by the trees themselves to facilitate a favorable environment for seedling recruitment. A number of biotic factors including tree-to-tree interactions in the root zone also play a

role in the initial encroachment and recruitment of seedlings following initial encroachment (Rice et al., 2012 and Haugo et al., 2013).

Fire management policies resulting in decreased fire frequency are partially responsible for an observed increase in the density of mid-elevation pine forest and the encroachment of *Pinus contorta* into meadows in the Sierra Nevada and Cascade Mountains (Vankat, 1977 and Hadley, 1999). Currently, approximately 60% of montane meadows in Sequoia Kings Canyon National Park and upwards of 42% of meadows in the Lake Tahoe basin contain both saplings and seedlings of *Pinus contorta* (Gross and Coppoletta, 2013). In Lassen National Park, conifer encroachment began following a dramatic change in fire regime and grazing practices associated with the parks establishment in 1916 (Taylor, 1990). It suffices to say that conifer encroachment is a highly complex phenomenon tied to a wide range of extrinsic and intrinsic factors responsible for each incidence of encroachment.

2.5 Hydrologic Response to Vegetation Removal

Many studies have addressed the effects of tree removal on stream discharge, water yield and soil water content (Keppeler and Ziemer, 1990; Adams et al., 1991; Surfleet, et al., 2013; Bigelow and North, 2012). The majority of surveyed research indicates that vegetation removal has a quantifiable effect on the hydrology of a watershed, during at least a short period between removal and re-vegetation. A study applying fuzzy linear regression analysis to data collected from 145 hydrologic experiments conducted in forest environments demonstrated a 10% reduction in canopy cover from a conifer forests was correlated with an increase in water yield of 20-25 mm (Sahin and Hall, 1996).

Studies that quantify the hydrologic response to vegetation removal generally follow a similar experimental design. A before and after control intervention (BACI) study design is implemented and a control or reference site with similar climate, soil, geology, and topography is selected. A study conducted within a 101-hectare watershed of the H.J. Andrews Experimental Forest provides a good representation of the methodological approach to quantifying soil moisture and groundwater trends following vegetation removal from a managed forest site (Adams et al., 1991). A treatment transect was located within 75 m of a nine hectare clearcut patch while the control was in an un-harvested area. A two-year calibration of no treatment was established to define pre-treatment conditions. The area comprising the clearcut harvest was broadcast burned and planted with Douglas fir (*Pseudotsuga menziesii)* seedlings following logging operations. Soil moisture was monitored at depths of 0-30, 30-60, and 60-120 cm every three weeks for three years on five separate locations on both transects. In the summer following clearcutting, the upper 120 cm of soil on the nine-hectare clearcut site contained 10 cm more water than the control site. Five years following the clearcut, the quantity of water in the upper 120 cm of soil was at least 2 cm lower than the water contained at this range on the control site.

Another study monitoring water yield, soil moisture and storm runoff before and after a clearcut on the Caspar Creek Watershed (CCW) (located in northwestern California), reported statistically significant increases in pore water pressure and soil moisture following tree removal from a second growth forest (Keppeler, et al., 1994). A similar study performed on the CCW found that stream flow was augmented for a five-year period following selective logging of a second-growth *Pseudotsuga menziesii* and

redwood (*Sequoia sempervirens*) forest (Keppeler and Ziemer, 1990). These increases occurred during both peak and base flow conditions. The growth of saplings and early successional plants was thought to be responsible for the return of pre-removal base flow and peak flow peaks. Another study conducted on the CCW found that that the hydrologic response to storm events occurring less frequently than 8 times per year, following a selective harvest (67% removal of timber volume), did not correspond with higher storm flow volumes (Wright et al., 1990).

2.6 IRIS Tubes

Hydric soils are soils that are saturated for a large enough period during the growing season to cause persistent anaerobic soil conditions. The indicators of hydric soils are primarily characterized by the aggregation or depletion of iron, manganese, sulfur or carbon compounds (Vasilas et al., 2010). IRIS tubes are used to determine the relative probability of hydric soil conditions in wetland environments (Jenkinson and Franzmeier, 2006). IRIS tubes can be inexpensively manufactured and employed to monitor the extent and distribution of hydric soils both temporally and spatially. They are constructed from ½-in. schedule 40 polyvinyl chloride (PVC) pipe that is cut to 60 cm (2.0 ft) lengths. The bottom 55cm (1.8 ft) of each IRIS tube is coated with a mixture of goethite (FeO(OH)) (to improve durability) and ferrihydrite ($Fe_5HO_8 \cdot 4H_2O$) paint (Rabenhorst and Burch, 2006). They are installed in the field using a soil push probe and must be placed within an area comprising a diameter less than six feet (1.8 m) in groups of five. A minimum of 15 IRIS tubes are required to determine a hydric soil boundary (five above, below, and within the anticipated boundary).

Upon immersion in hydric soil conditions, ferrihydrite paint (solid phase Fe (III)) is gradually reduced to soluble Fe (II). Depending on soil temperature, this process takes place over a 2-4 week period, and can only occur in hydric soils (Rabenhorst, 2008). A decrease in temperature below 'biologic zero' can retard the metabolic processes of microbes thereby limiting the use of IRIS tubes below temperatures of 8 °C (Rabenhorst, 2005). A general protocol has been established to analyze reduction of IRIS tubes. To make an interpretation of paint reduction from IRIS tubes, three of the five tubes in a set must exhibit the criteria described below (Table 2.1). Interpretation of IRIS tubes is generally done using digital visual software, but visual estimates by trained individuals can also be appropriate (Rabenhorst, 2011). Although employing IRIS tubes in less than three sets or for periods such as three to six months may limit quantitative interpretation of reduction, they can still be implemented to indicate that hydric conditions may develop in soils of interest.

Table 2.1 Protocol for interpreting the reduction of Fe^{3+} from IRIS tubes. (Figure from Rabenhorst, 2005)

Paint removed from a 10-cm section	Interpretation
%	
0	not reducing
1–5	probably not reducing
5–10	possibly reducing
10–25	probably reducing
>25	definitely reducing

2.7 Electrical Resistivity Tomography

Electrical resistivity surveying is a non-invasive geophysical method of interrogating subsurface geological material and structural properties, including surface soil and rock composition, subsurface layering, identification of faults, groundwater

depth, soil moisture, and the presence of contaminants (Burger et al., 2006). The application of electrical resistivity surveying to groundwater studies is well established (Frohlich et al., 1994 and Ravindran and Prabhu, 2012). In recent years, electrical resistivity surveys have been increasingly applied as a complementary tool in soil science and vadose zone studies (Samouelian et al., 2005). With respect to groundwater studies, such as estimating the depth to the water table, a principal advantage of electrical resistivity surveying is the ability to quickly collect spatially distributed data in a non-invasive manner, i.e. without installation of wells deep into the subsurface. A single electrical resistivity measurement consists of inserting four electrically conducting stakes (or nodes), connected to a battery into the ground. Nodes are inserted about 0.5 ft (0.15 m) into the ground. When the battery is activated, a circuit is made with the earth, which is the resistive element of the circuit, and the stable current, I, (measured in Amperes), is recorded. Simultaneously, two additional nodes are used to measure the potential difference, or voltage (measured in Volts, V), between the equipotential lines induced by the current (Fig 2.2).

The electrical resistance, R (units of Ohms, Ω), of the subsurface along the electrical path is then calculated by Ohms Law as $R = \frac{V}{I}$. The desired material property, however, is not electrical resistance, but, electrical resistivity (Fig 2.3). The electrical resistance of a material depends on its length and cross sectional area. Electrical resistance (R), and electrical resistivity (ρ), are by definition, proportional to length and area (Equation 1). Electrical resistivity is an inherent property of a given material that also depends on the presence of other conductive materials such as water. Electrical resistivity measures the inherent resistance of a given material to electrical flow over a

given distance. Consequently, electrical resistivity is measured in units of Ohm meters ($\Omega \cdot m$). In an electrical resistivity survey, this constant of proportionality is a function of the relevant current and potential electrode positions along with electrode spacing and thus depends on the geometry of the given array method implemented for a survey (Burger et al., 2006).

$$\rho = R\frac{A}{L} \quad (\mathbf{1})$$

Where: ρ= resistivity ($\Omega \cdot m$)

R= Resistance (Ω)

A= cross sectional area (m^2)

L = Cross sectional length (m)

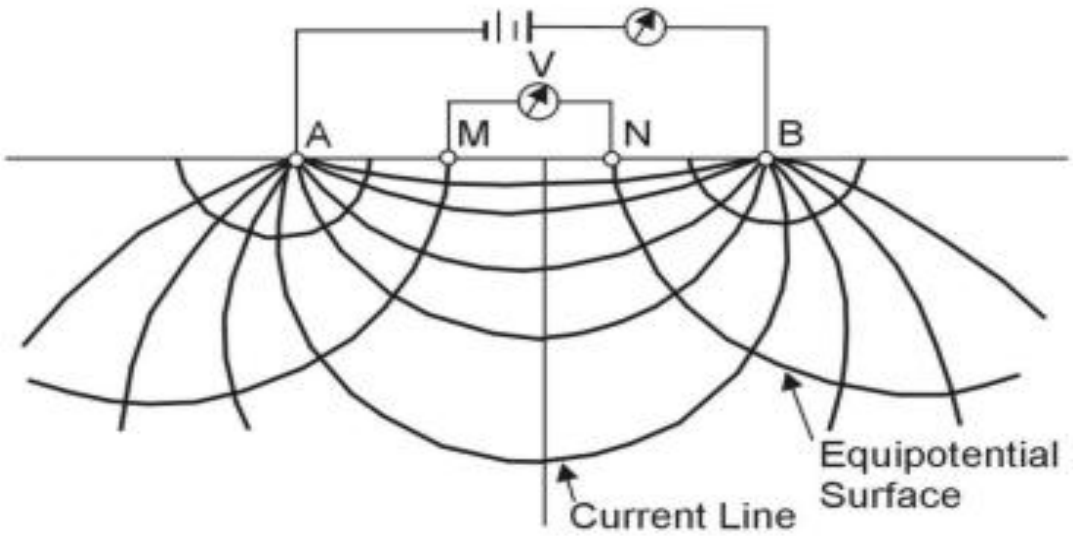

Figure 2.2 Measurement of subsurface electrical resistivity. Electrodes A and B inject electrical current into the ground. Resulting equipotential lines are measured at nodes M and N to determine electrical potential difference. (Accessed 3/22/15): www.epa.gov/esd/cmb/GeophysicsWebsite /pages/reference/img/fig270.jpg

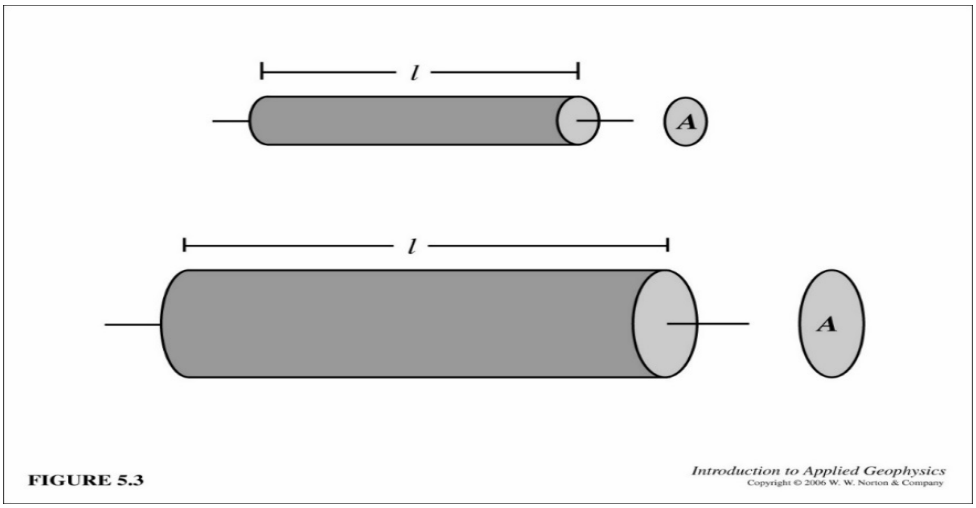

Figure 2.3 The relationship between electrical resistance and the geometrical properties of an electrically conducting material. Increasing length increases resistance, increasing area reduces resistance (Figure from Burger et al., 2006).

2.7.1 Electrical Resistivity Survey Arrays

Historically, electrical resistivity surveys were conducted by collecting individual measurements of resistivity with a set of four electrodes. Each subsequent resistivity measurement changed the electrode spacing about a center point to change the depth of current penetration and thus create a one-dimensional profile of electrical resistivity with depth. This procedure is referred to as vertical electrical sounding. Laterally moving electrodes in addition to changing electrode spacing about a center point allows a two-dimensional profile of resistivity to be developed (Fig 2.4). This labor-intensive practice is now most commonly conducted in a multi-electrode format, where a large number of electrodes may be connected to an automatic resistivity meter using a multi-core cable. Along with a multi-electrode format, a roll along method (Fig 2.5) is often implemented to lengthen the profile length of a resistivity survey, but does not increase the depth that electrical current is able to penetrate. A computer with an electronic switching element (multiplexer) selects which four electrodes are used to

make each measurement. This method allows a variety of different electrode configurations to be applied. The dipole-dipole, Schlumberger and Wenner methods are the most commonly used electrode array configurations used in resistivity surveys concerned with two-dimensional imaging of the subsurface (Fig 2.6).

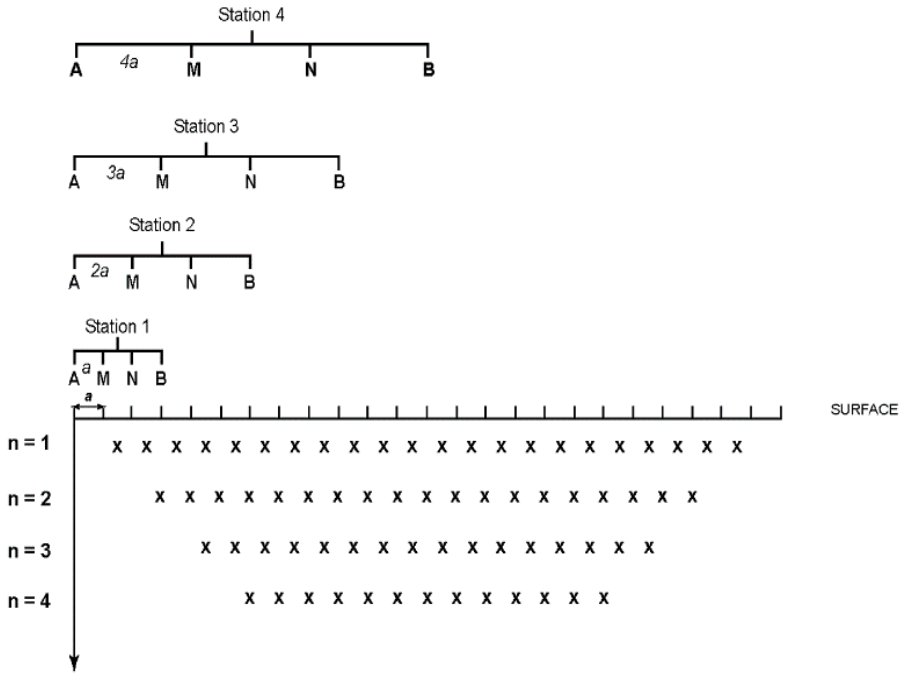

Figure 2.4 Schematic of a Wenner Array. Increasing electrode spacing with a common value provides deeper image points while laterally moving the center of the array build up a cross-section of image points. (Figure from Samoulian et al., 2005)

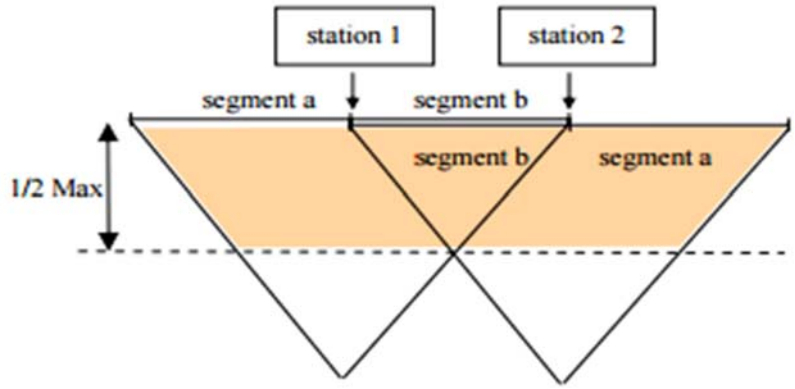

Figure 2.5 Roll Along technique used in a resistivity survey to increase profile length (Adapted from: Bernard et al., 2006).

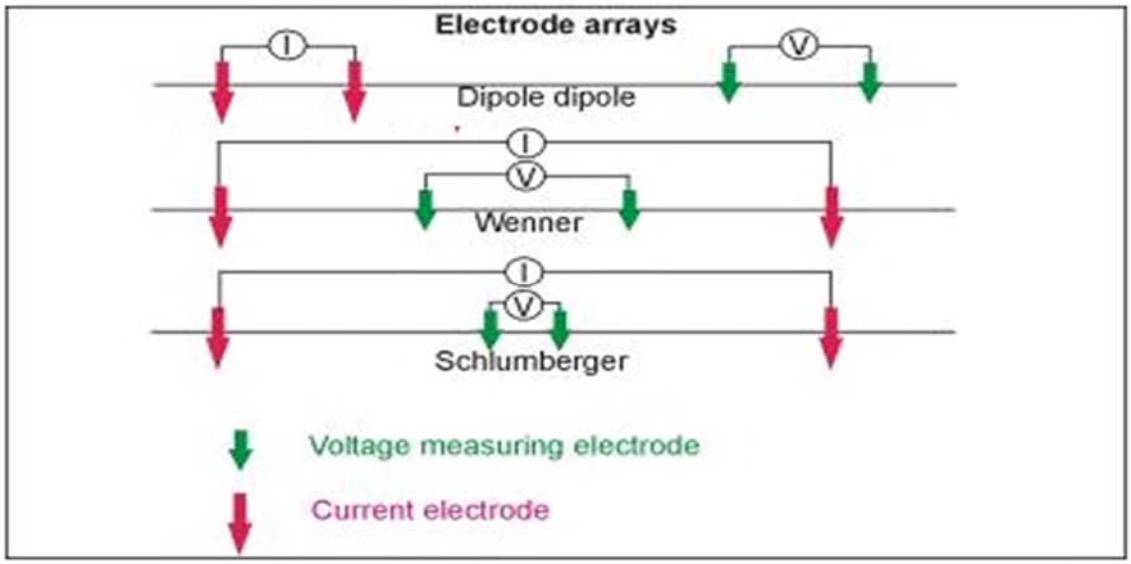

Figure 2.6 The three most common electrode arrays: dipole-dipole, Wenner and Schlumberger (Adapted 2/14/14): http://www.cflhd.gov/resources/agm/engApplications/RoadwaySubsidence/522IndentRoadbedExpanClays.cfm

The dipole-dipole array uses an asymmetrical arrangement of electrodes (voltage and current electrodes are adjacent to one another) and the Schlumberger uses an unequal spacing of two inner voltage electrodes and two evenly spaced outer current electrodes. The Schlumberger and dipole-dipole arrays are generally best at detecting lateral changes in electrical resistivity, which aids in distinguishing vertical structures in the subsurface (Samouelian et al., 2005). The Wenner array is a special case of the Schlumberger array with even node spacing. The Wenner array is frequently used in investigations of groundwater processes such as recharge (Frohlich et al., 1994 and Ravindran and Prabhu, 2012). The Wenner array provides several benefits to studies that emphasize interpretation of subsurface water. First, this array type provides good resolution for horizontally layered structures (Burger et al., 2006). Second, the Wenner array is provides an image that encompass depths of approximately 20% of the electrode profile length. Third, Wenner array also allows for deeper imaging of the subsurface

compared dipole-dipole Array. Lastly, for practical considerations, the Wenner Array is often used because collection of resistivity data can be completed in less time than other common arrays.

Compared to the dipole dipole array, the Wenner array has a higher signal strength because it needs a smaller number of measurement points to achieve the same coverage (Neyamadpour et al., 2010). An electrical resistivity arrays signal strength is inversely proportional to its geometric factor ($\frac{A}{L}$) (Herman, 2001). Signal strength can play an important role in array choice if the survey is conducted in areas with high background noise or high resistivity. The most appropriate array for a given survey is dependent on the desired depth of investigation, the type of structure defined, the level of background noise, and the sensitivity of the resistivity meter (Herman, 2001). In multi-electrode surveys, a larger number of electrodes will allow a greater depth and amount of data to be collected because a larger number of possible combinations may be used. The Wenner array was chosen for this study due to a primary emphasis on the analysis of horizontal sub surface hydrologic structures.

2.7.2 Interpretation of Electrical Resistivity Data

It is important to note that the values of electrical resistivity, ρ, determined in a field survey are regarded as apparent resistivity (ρ_a). This is due to the inhomogeneity and layered structure of the subsurface. A current path will generally encounter more than one type of material and so the calculated value of resistivity at any image point is typically a combination of more than one value. In a two-dimensional survey (as employed in this study), this uncertainty cannot be overcome by manual data analysis methods. Instead, software uses a combination of stochastic analyses (kriging) and mathematical inversion

of field data to develop a subsurface model of resistivity which best fits (in a least-squares sense) the field data. In this study, RES2DINV software was used to process field data into electrical resistivity diagrams (or cross sections) (RES2INV, geotomosoft.com). Electrical resistivity values yielded by data inversion can be correlated to potential subsurface materials or material properties such as rock or soil type, and depth to groundwater table. Interpretation of electrical resistivity data values alone is not unique and knowledge of the local geology is necessary to constrain the set of possible interpretations (Fig 2.7). In geologic materials, the nature and distribution of soil constituents, soil moisture, pore fluid composition, soil temperature, and the presence of conductive metal ores will all influence the estimated electrical resistivity in the subsurface (Samouelian et al., 2005).

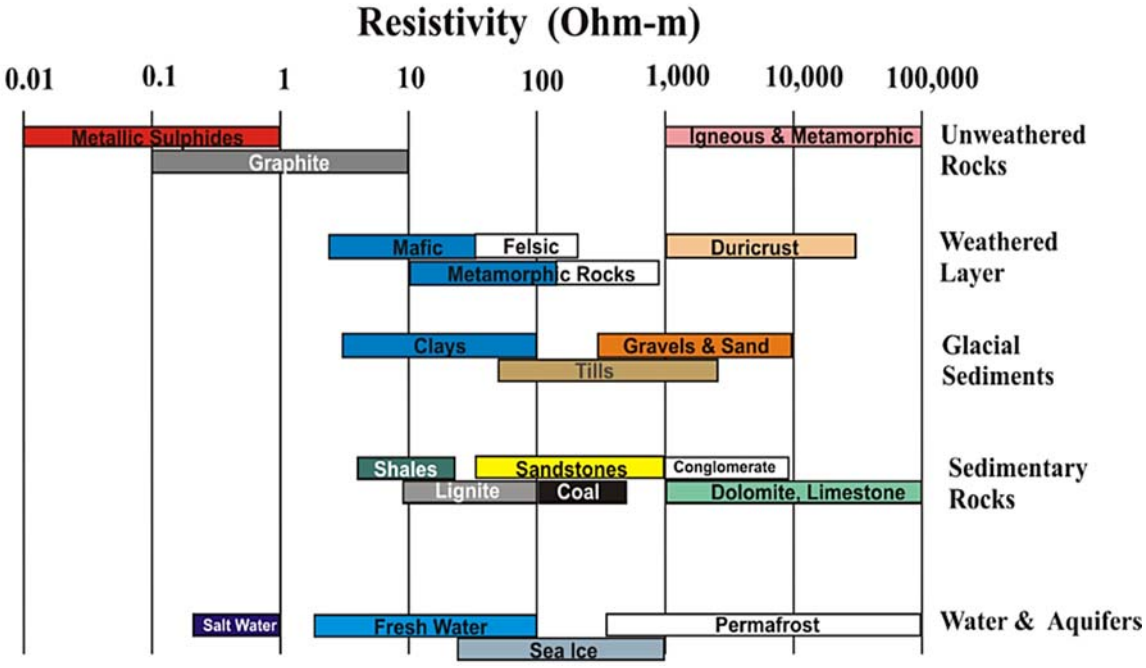

Figure 2.7 Electrical resistivity of common geologic materials. Values of electrical resistivity are not unique to a material and have a wide range of values for a given material depending primarily on water content (Adapted 3/22/2015): http://www.haylesgeoscience.ca/images/Palacky1988_ec_diag.png

Electricity flows through the Earth's subsurface due to electrolytic and electrical conduction (Burger et al., 2006). Electrical conduction is the flow of electrons through a conductive medium. Electrolytic conduction is the flow of electrical current through the movement of ions. In most geologic environments, electrolytic conduction through soil and bedrock pore water is the primary conductor of electrical current. In the case of subsurface water, the electrolytes and conductive constituents in solution with pore water that are primarily responsible for waters low resistance to current. Pure water is a poor conductor of electricity. Several studies have successfully used ERT to quantify temporal variations in subsurface hydrologic processes (Jayawickreme et al., 2008 and Goyal, et al., 1996). Assuming the soil water is not limited; materials with a higher porosity will have lower electrical resistivity (Adli.et al., 2010). Empirical relationships have been developed to quantify the effects that particle size distribution, mineral composition, and soil moisture saturation have on electrical resistivity (Fig 2.8) (Hong Jiung et al., 2014; Mccneil, 1980; Fukue et al., 1999; Archie, 1942).

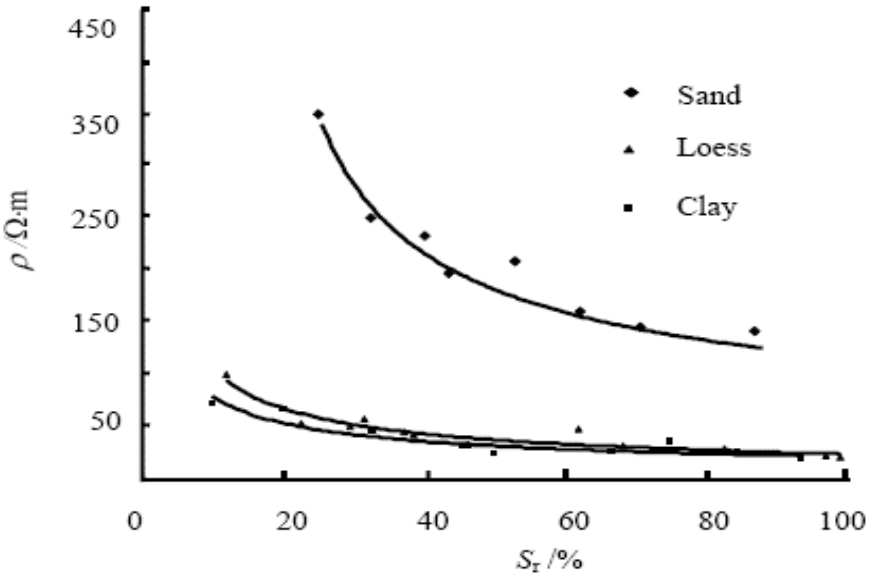

Figure 2.8 Relationship between saturation percentage, soil texture and electrical resistivity determined empirically. (Figure from Hong Jiung et al., 2014).

In addition to inversion of field measurements, soil samples are often collected and their resistivity is measured using a soil box apparatus to calibrate field measurements. Apparent resistivity may also be corrected for varying soil temperatures (Amidu and Dunbar, 2007). Electrical resistivity surveying has also been used to characterize the hydrologic disparities between forest-grassland ecotones and vadose zone water movement in forest soils (Jayawickreme et al., 2011 and Oberdörster, 2010). In a two-layer soil system, most soils will have an upper region of the subsurface with higher apparent resistivity and a lower region with lower apparent resistivity. This situation is commonly encountered in this study, with the vadose zone layer overlying the saturated soil layer. In this case, current will preferentially flow into the lower resistivity layer. However, if instead resistivity increases with depth, then electrical current will be preferentially confined to the upper layer (Fig 2.9).

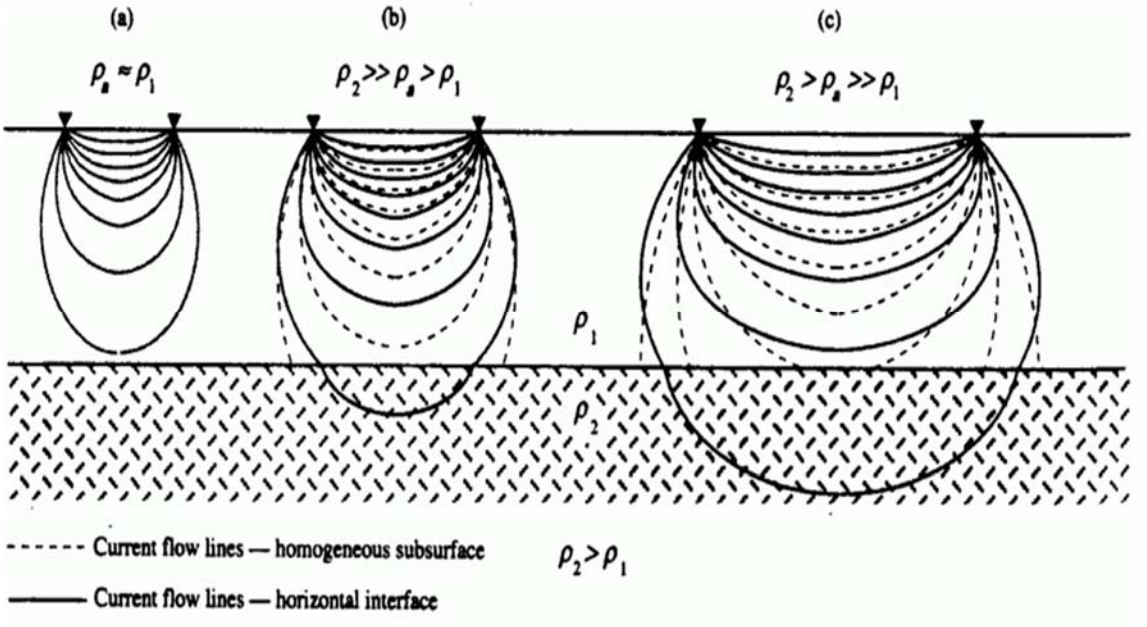

Figure 2.9 The effect of layered resistivity on current flow (Figure from Burger et al., 2006).

When current flows through a region of lower resistance, the distance between equipotential lines increases, as a larger proportion of the current will flow through a less resistant medium (Fig 2.10). Consequently, a survey with a wider electrode spacing will allow more current through layers with lower resistivity (Herman, 2001). The measured apparent resistivity will therefore become lower as electrode spacing is increased, assuming a more resistant medium overlies a less resistant medium. In the case of increasing resistivity with depth, current will preferentially flow in the upper layer. If resistivity decreases with depth then more electrical energy will be refracted into the lower layer.

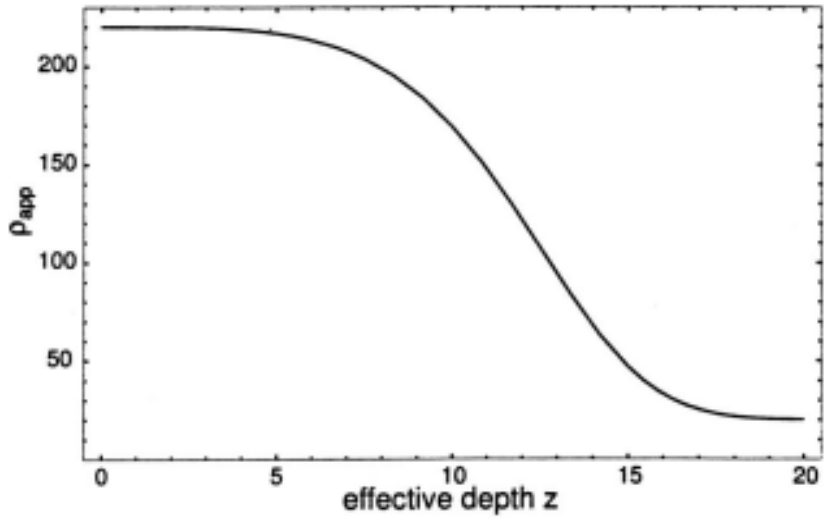

Figure 2.10 Apparent resistivity as a function of imaging depth. Apparent resistivity decreases nonlinearly as the node spacing increases (Figure from Herman, 2001)

In summary, ERT is a non-destructive subsurface mapping technique that is useful for temporal modeling of subsurface hydrologic processes and soil water content. Electrical resistivity tomography allows for analysis of subsurface hydrologic processes at a relatively low cost at varying resolutions. In terms of quantifying changes in the hydrologic properties of meadows, ERT offers researchers a means to inexpensively

calibrate or corroborate observations performed with other more traditional methods that directly monitor water table depth and quantify soil moisture.

2.8 Meadow Restoration

Successful restoration of a degraded meadow could be signaled by a higher seasonal water table, improvement of water quality in streams, increases in seasonal soil moisture and the return of endemic meadow species. Benefits to the restoration of degraded meadows may include an increase in plant and animal biodiversity, increased late summer water storage, increased forage, flood attenuation, and, increased aesthetic values (Stillwater Sciences, 2012). A number of challenges face land managers attempting to restore meadows encroached by conifers. One key impediment to meadow restoration is the occurrence of biogeochemical alterations to meadow soils following initial conifer encroachment. These alterations may be responsible for a feedback system that favors the re-establishment of conifers in a meadow following vegetation removal (Halpern et al., 2010 and Griffiths et al., 2005).

If conifer encroachment has occurred over a long time scale, the soil seed bank may no longer contain viable seeds of species targeted for restoration that are able to germinate successfully (Lang, 2006). Analysis of the soil seed banks below encroached meadows in western Oregon indicates that 75% of the native meadow species are either absent or contain seeds that are no longer viable (Swanson et al., 2007). Furthermore, the species that are represented in these seed banks are often primarily early successional forbs and grasses. Forest understory and ruderal (plants that opportunistically proliferate on disturbed land) species may also be well represented within encroached meadow seed banks. However, following conifer removal, forest understory species will be at a

disadvantage because of the lack of shade following removal of the conifers that create overstory shading. The lack of a soil seed bank is a major limitation to restoration of encroached meadows (Lett and Knapp, 2005). Soil disturbance caused by tree harvesting equipment may also facilitate the arrival of additional unwanted species.

Consequently, successful restoration of meadow species may require dispersal of seeds and continued removal of unwanted vegetation. Previous research indicates that the establishment of early successional shrubs, forbs and conifer seedlings following initial conifer removal efforts generally reverses increases in soil moisture, stream flow and water yield (Keppeler et al., 1994 and Adams et al., 1991). The removal of pioneer vegetation following conifer removal is usually necessary to preserve the hydrologic response to initial conifer removal. In some regions, fire in addition to removal of encroaching vegetation may be the most effective management tool to promote the restoration of degraded meadow habitat because it was the primary mechanism associated with removal of encroaching vegetation before changes in fire regime (Caprio and Graber, 1999). However, meadow restorations performed by removing encroaching vegetation without the subsequent implementation of selective slash or broadcast burning have demonstrated that conifer removal alone is sufficient for short-term restoration of some encroached meadows, especially meadows with a history of infrequent wildfire (Swanson et al., 2007 and Halpern et al., 2012). Furthermore, broadcast burning and slash burning may be counterproductive to meadow restoration because of the attendant increases in soil nitrogen content and exposure of mineral soil, which induces conditions favorable to the establishment of ruderal species.

If current climate trends continue, it may also become increasingly difficult to restore encroached meadows, as conifer encroachment into some meadows may represent a transition to a new stable state tied to climate change rather than a temporary ecosystem fluctuation (Haugo and Halpern, 2007). Lastly, although studies have observed a hydrologic response to conifer removal on encroached meadows and wetlands, it is important to remember that the hydrologic response to conifer removal will ultimately be governed by site-specific characteristics such as: stand composition, soil series, microclimate, time elapsed since initial conifer encroachment, and the volume of vegetation removed. Due to the challenges associated with restoration of encroached meadows, the most effective method to preserve mountain meadows threatened by conifer encroachment is to stop conifer encroachment in its early stages (Lang, 2006 and Kremer et al., 2014). Regardless of how effective conifer removal from an encroached meadows is in terms of promoting restoration efforts, any step towards restoration of an encroached meadow must begin with the removal of encroaching vegetation.

CHAPTER 3 METHODS

3.1 Study Area

Marian Meadow and CM are located within the eastern portion of the South Cascades Bioregion (SCB), which comprises about 4% of California's land area (Skinner and Taylor, 2006). Control Meadow is located approximately four miles directly west from MM (Fig 3.1). Control Meadow was 'treated' by removing the majority of encroaching conifers during the summer of 2012. For the purposes of this study, CM comprises approximately 20.3 acres (0.082 km^2) (Fig 3.3), and MM comprises approximately 45 acres (0.182 km^2) (Fig 3.2). Marian Meadow is located within the Upper Feather River Watershed (UFRW). Control Meadow is located within the Deer Creek Watershed (DCW) (Sacramento River Watershed Program (SRWP), 2015). The DCW drains 229 square miles (593 km^2) and the UFRW drains approximately 3200 square miles (8288 km^2); both watersheds form tributaries to the Sacramento River. Mixed conifer pine forest comprises about 70% of the land area in the UFRW. Deer Creek supports significant populations of anadromous fish, including salmonids, in part because of its consistent supply of cold water and a lack of major downstream dams (SRWP, 2014).

The climate of the SCB is Mediterranean, which means that the majority of precipitation occurs from November to April (California Cooperative Snow Surveys (CCSS), 2002). The average yearly historical precipitation recorded at Chester Flat (approximately five miles (1.6 km) from MM at an elevation of 4600 ft (1402 m)) is 33.9 in. (860 mm). Depending on fluctuations in climate, a large proportion of this precipitation may occur as snow. The average snowpack recorded on April 1st (the period

when snowpack generally peaks in the Sierra Nevada Mountains) at Chester Flat is 16 in. (0.4 m) (CCSS, 2002). The tree species composition of mixed conifer forests in the eastern portion of the SCB, below the subalpine zone primarily consists of *Pinus ponderosa*, jeffery pine (*Pinus jeffreyi*), incense cedar (*Calocedrus*), *Abies concolor* and *Pinus contorta* (Fites-Kaufman et al., 2007). Historically, stand composition in the SCB and surrounding areas was controlled by a variety of factors including: elevation, slope aspect, local soil moisture conditions, geologic substrate, fire frequency, and fire intensity (Griffin, 1967 and Griffin and Critchfield, 1976).

During the 20th century, fire suppression in combination with logging of fire resistant trees and, a climactic warming trend have significantly altered the stand composition of forests in the SCB (Skinner and Chang, 1996). Hydrologic and vegetative changes associated with fire suppression, grazing practices, climate change and soil biology have encouraged the loss of historic meadow and wetland habitat as coniferous forests expand beyond historic ecotone boundaries (Halpern et al., 2010). In 1905, large areas of land in the SCB were established as the Lassen National Forest. Fire frequency and, the portion of land area grazed by sheep and cattle dramatically decreased following its establishment (Skinner and Taylor 2006).

These changes are partially responsible for a modern-day critical shortage of late seral stage and old growth forest, which many plant and animal species depend on for habitat (Franklin and Fites-Kaufman 1996). Marian Meadow and CM are located in a transitional zone between the Cascade and Sierra Nevada Mountains. The terminus of the Sierra Nevada Mountain range is defined by the subsidence of the titled fault block associated with the Sierra Nevada batholiths below the younger volcanic formations

associated with the Cascade Mountains near Lake Almanor (Durrell, 1988). Soils in the SCB region are primarily derived from volcanic material, yielding soil series such as Alfisols, Mollisols and, Inceptisols (Miles and Goudey, 1997). The soil series represented on MM is an Alfisol with moderate clay content. CM consists primarily of poorly consolidated alluvial materials with high sand content (classified as an Entisol) (USDA-NRCS), 2014).

The unconsolidated material on CM contributes to its high permeability. On MM, a higher clay content, and lower sand content contributes to lower permeability. The differences in soil composition between the two meadows, serve to emphasize a degree of disparity will exist between CM and MM in terms of their respective hydrology, irrespective of restoration efforts. Tables of relevant soil information pertaining to CM and MM are included in Appendix E. This distinction does not account for differences in vegetation between MM and CM. In the moisture classification schemes reviewed as part of this thesis, CM and MM most closely match a classification of a dry or mesic meadow. However, the depth to groundwater has a greater range in both directions relative to the ground surface compared to the depth range typically observed for these meadow types (Weixelman.et al., 2011 and Lord et al., 2004).

3.2 Study Design

This study implemented a BACI design to determine the hydrologic response to conifer removal on a historic meadow encroached by *Pinus contorta*. All encroaching trees on MM will have been removed by end of the summer of 2015. A partial removal of timber in the surrounding watershed (approximately 2043 acres (8.27 km^2) is scheduled to occur during the summer of 2016 (Fig 3.4 and 3.5). The defined boundaries of MM

spanned CA Highway 36, but instruments were only installed north of Highway 36, with the exception of a water logger placed near a culvert on Marian Creek (MC). Soil moisture probes and water level loggers were installed using a spatially balanced random sampling approach (after Stevens and Olsen, 2004). The placement of instruments was determined using a transect line starting near Highway 36 spanning 1250 ft (380 m) on a bearing of 315° (N45W). Ten lines perpendicular to the transect line were delineated in 125 ft (38 m) intervals; each of these lines was assigned a number from 1-10. Four of these ten lines were randomly chosen for placement of groundwater wells and soil moisture probes (lines 9, 3, 6, and 4).

These lines were paced across the lateral extent of MM to determine their respective lengths. Sub-sections of each line bisecting the transect line were delineated by 25 ft (7.6 m) intervals, starting from the western edge of MM. The terminus of each side of MM was considered the boundary where tree density became markedly higher than the concentration observed within what was hypothesized to be the extent of the encroached meadow. These numbered sub-sections were treated as integers that were selected by a random number generator (e.g., 20 numbered sub-sections would be established for a 500 ft (152.5 m) line). Four potential sites for instrument placement on each of these four lines were selected for instrumentation. This procedure was repeated on CM on two separate dates. Two lines were instrumented starting on September 10-13 2013 and two lines were instrumented during separate visits during June and September of 2014 (Fig 3.5). In total, 14 sites were chosen for instrument placement on MM and nine sites were chosen for instrument placement on CM (Tables 3.1 and 3.2).

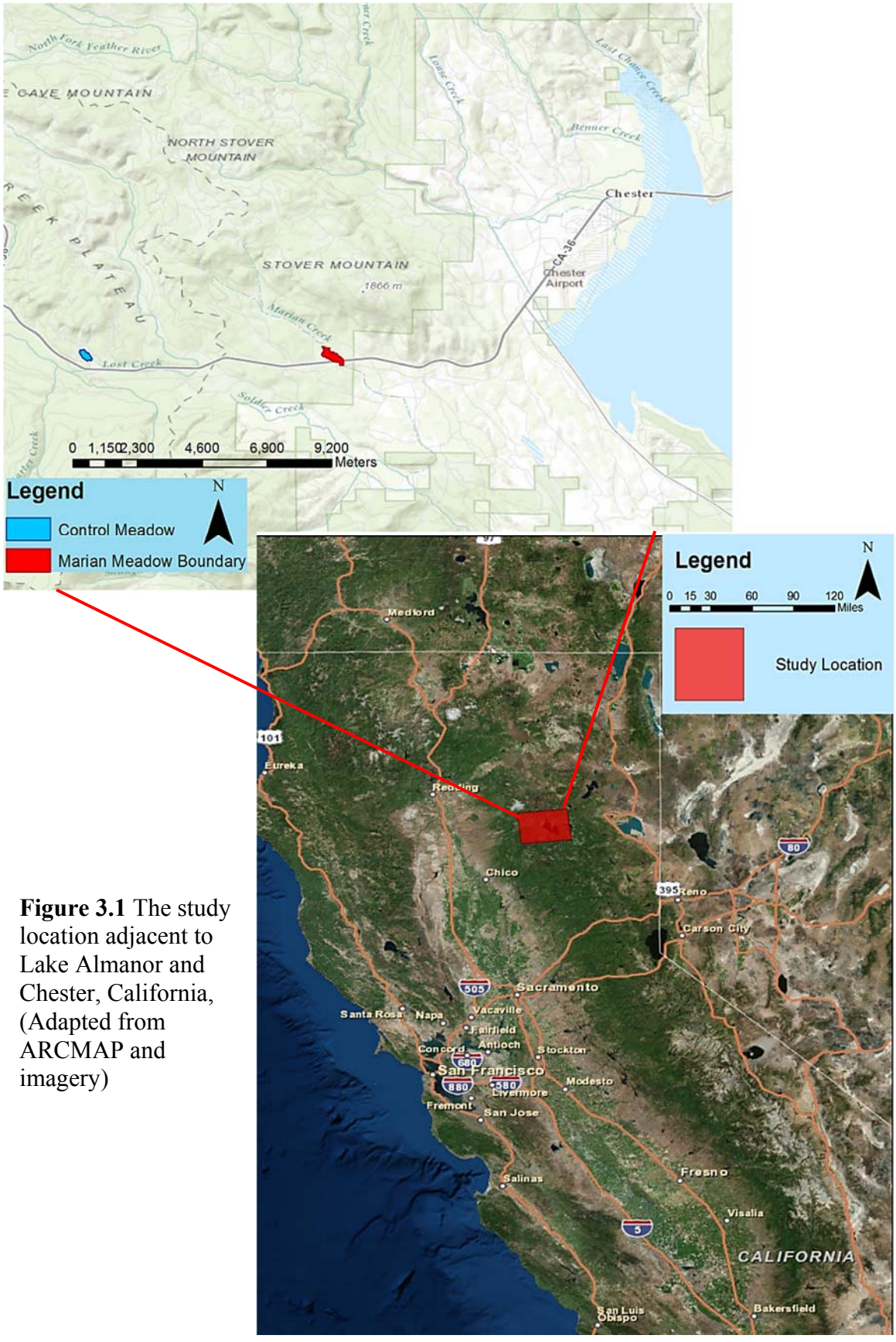

Figure 3.1 The study location adjacent to Lake Almanor and Chester, California, (Adapted from ARCMAP and imagery)

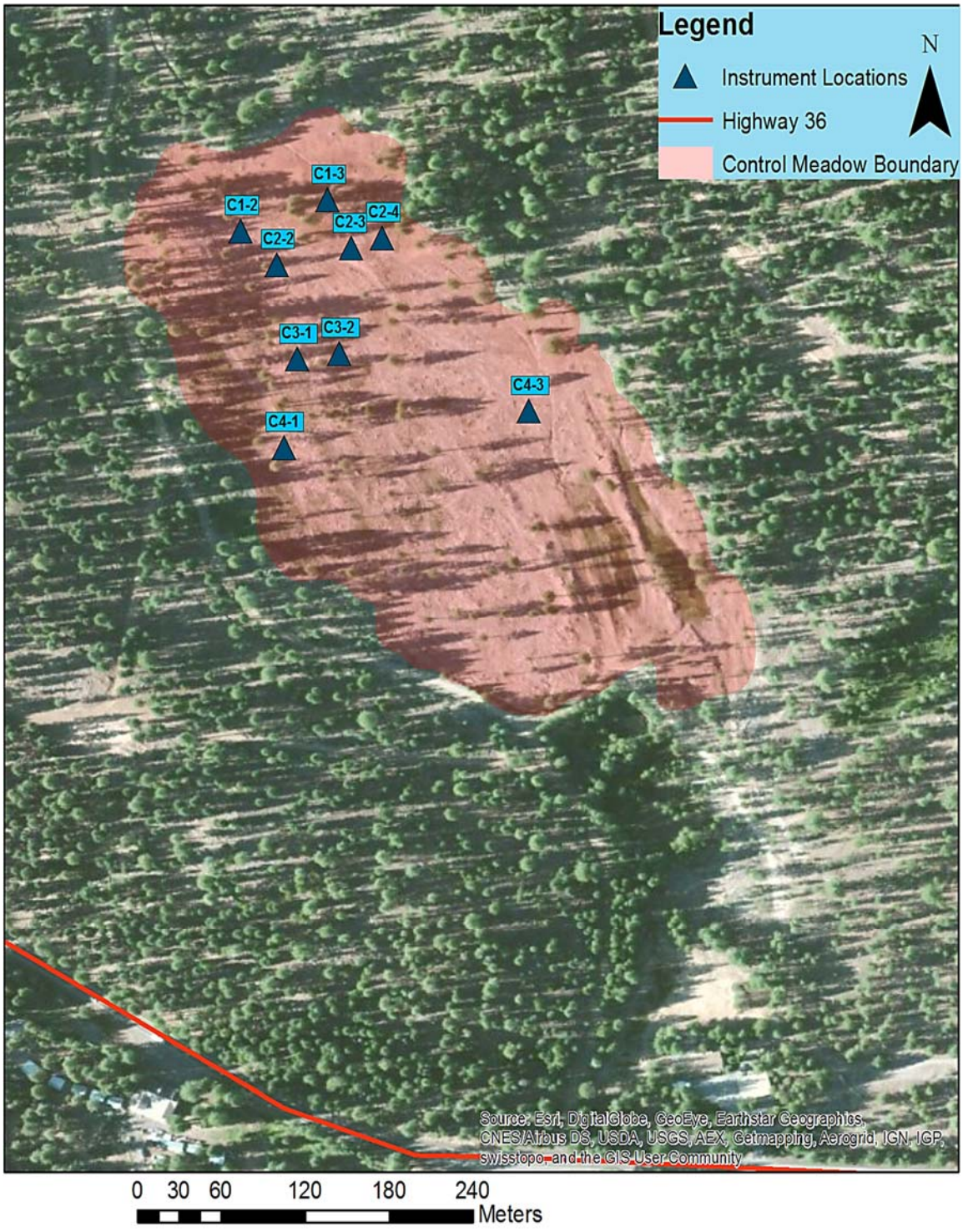

Figure 3.2 Locations of instruments on the Control Meadow. See Table 3.2 for coordinates and instrument descriptions for each site.

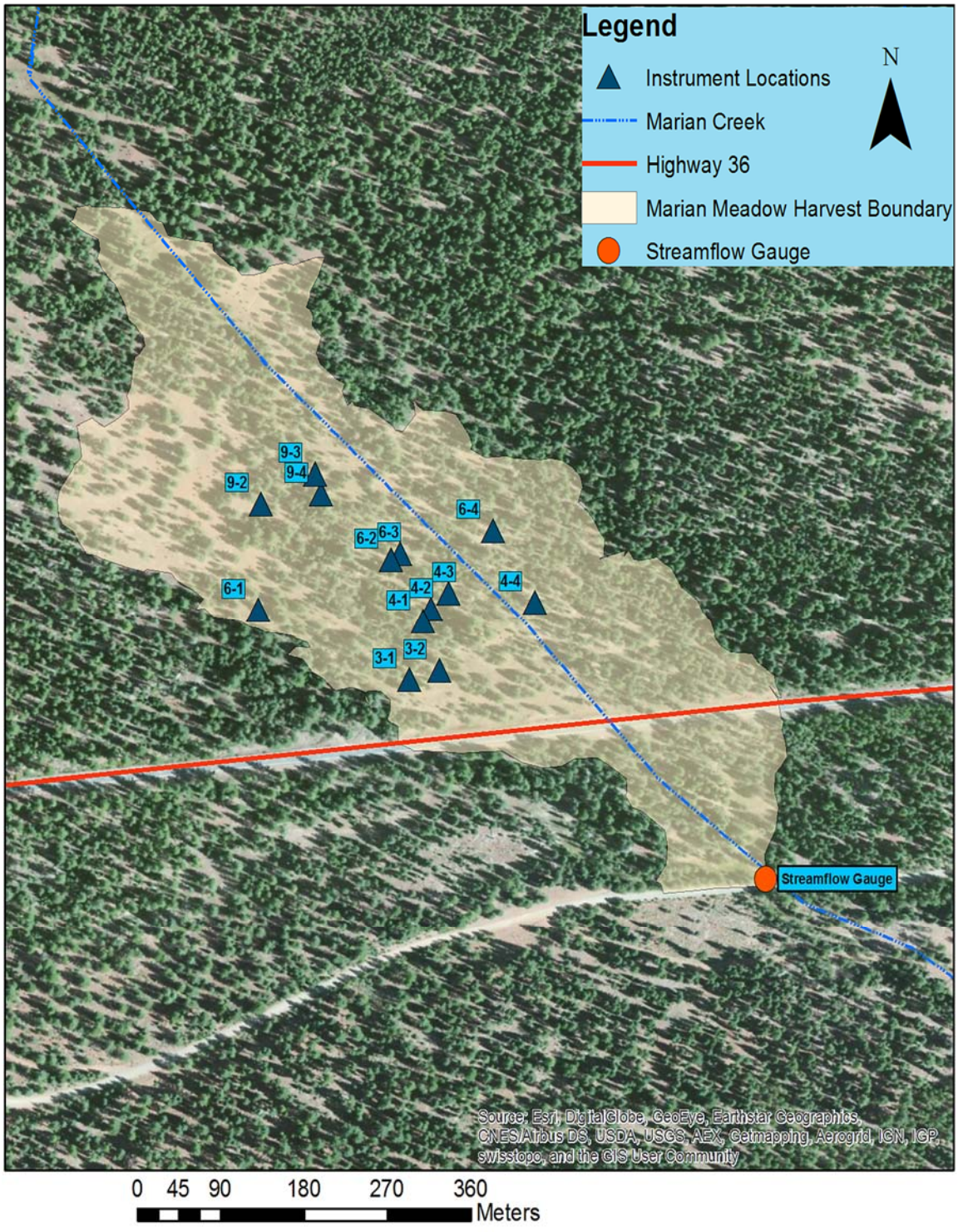

Figure 3.3 Locations of instruments on Marian Meadow. See Table 3.1 for coordinates and instrument descriptions for each site.

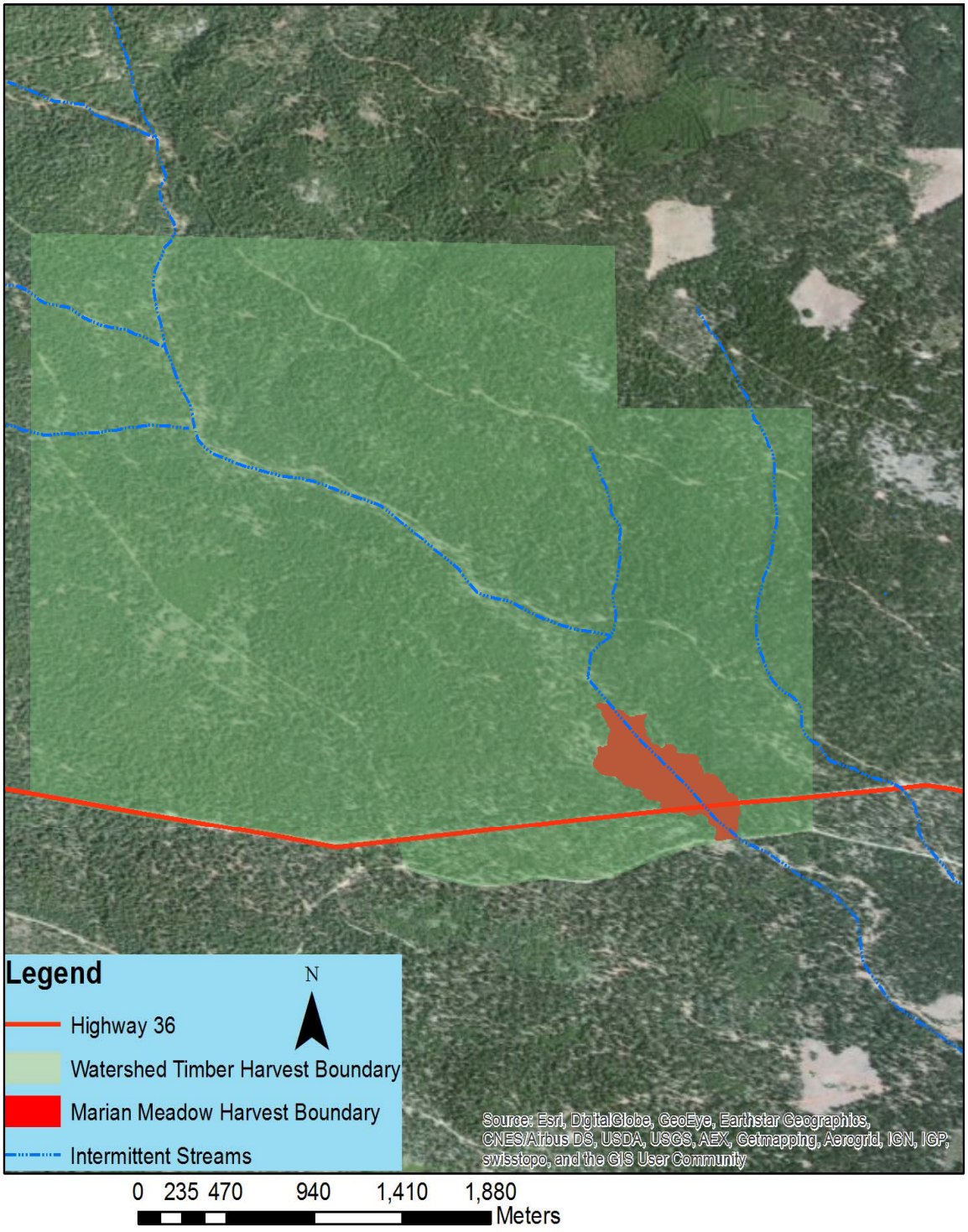

Figure 3.4 The watershed scale selective timber harvest relative to the extent of MM

Table 3.1 GPS location and type of instruments by site on Marian Meadow. All instruments in this table were installed during September 2013

Site	Longitude	Latitude	Soil Moisture Probe	Water Level Logger	Blank Well
9-4	-121.31594	40.26388			✔
9-3	-121.31600	40.26404	✔	✔	
9-2	-121.31652	40.26380	✔	✔	
6-4	-121.31427	40.26358	✔	✔	
6-3	-121.31517	40.26339	✔	✔	
6-2	-121.31526	40.26333			✔
6-1	-121.31655	40.26291			✔
4-4	-121.31386	40.26298	Not Instrumented		
4-3	-121.31470	40.26305			✔
4-2	-121.31487	40.26292	✔		
4-1	-121.31495	40.26282	✔	✔	
3-4	-121.31386	40.26282	✔	✔	
3-2	-121.31479	40.26241			✔
3-1	-121.31508	40.26233	✔	✔	

Table 3.2 GPS location of instruments by site on the Control Meadow *= SM Probe installed on 6/13/14 and/or water level logger installed 9/7/14

Site	Longitude	Latitude	Soil Moisture Probe	Water Level Logger	Blank Well
C4-3*	-121.39325	40.26373	✔	✔	
C4-1*	-121.39482	40.26353	✔		
C3-2*	-121.39446	40.26405	✔	✔	
C3-1*	-121.39474	40.26402	✔	✔	
C2-4*	-121.39419	40.26469	✔		✔
C2-3	-121.39439	40.26463			✔
C2-2	-121.39487	40.26454			✔
C1-3	-121.39454	40.26490	✔	✔	
C1-2	-121.39510	40.26473	✔	✔	

An additional water level logger was placed adjacent to a road culvert at the downstream end of MM on MC. Measurements from this instrument, along with known discharge measurements were used to quantify the discharge of water leaving the meadow as surface runoff on a weekly basis. The soil moisture probes and water level

loggers used in this study were manufactured by Dataflow Systems Limited. These instruments operate on lithium batteries (7.2 Volt, 8.6Wh) that were periodically replaced. The soil moisture probes and water level logger's main units are waterproofed to the manufacturer's specifications. Desiccants were placed within each instruments data recorder and regularly replaced to prevent condensation build-up within the data recorder housing.

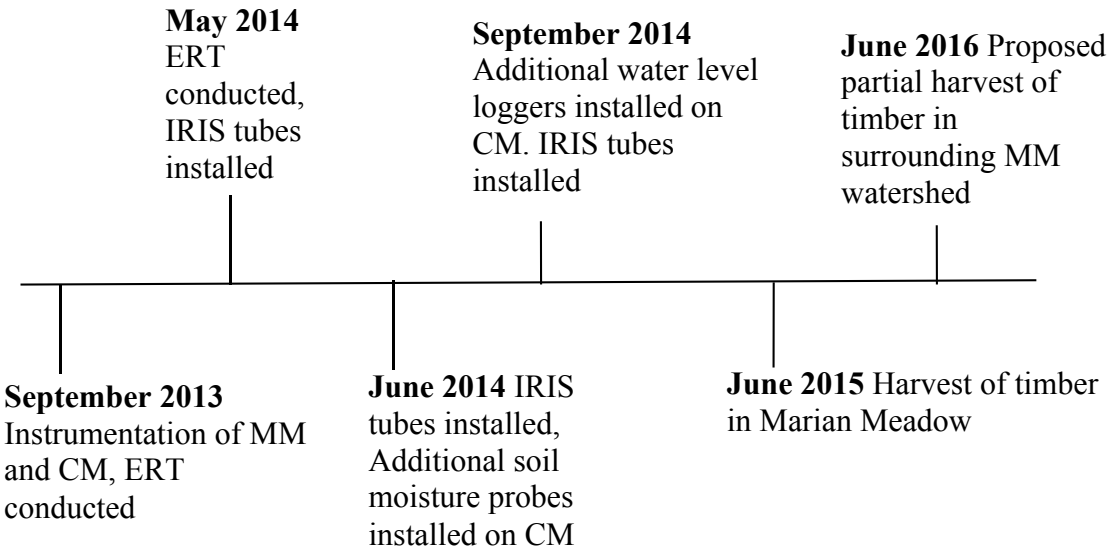

Figure 3.5 Timeline of events associated with study of Marian Meadow restoration.

The soil moisture probes used in this study quantify gravimetric soil moisture by measuring the relative dielectric constant of soil. The dielectric constant of oven-dried soil ranges from three to five that of water is 80. These empirically established values allow instruments that measure the relative dielectric permittivity of soil to make reliable in-situ determinations of soil moisture. The water level loggers used in this study determine depth to groundwater with a capacitor. The measuring element of the logger forms one plate of the capacitor and the water in contact with the measuring element forms the second plate. This allows a measure of groundwater depth to be determined because the quantity of water in contact with the measuring element is proportional to the

capacitance measured. A counterweight is attached at the bottom of the measuring element to allow current to flow between the two conductors, thus forming a capacitor.

3.3 Water Budget

A standard water balance equation (Equation 2) was used to construct a weekly water budget for MM and CM. Precipitation data were taken from a weather station located near Prattville, California maintained by Pacific Gas and Electric (PG &E) (CDEC,2014). Temperature data (daily minimums, maximums, and averages) were taken from a weather station maintained by the US Forest Service in Chester, California (CDEC, 2014). Gaps in precipitation and temperature data from these sources were amended from an additional weather station located near Chester, California (National Oceanic and Atmospheric Administration (NOAA), 2014). Evapotranspiration from CM and MM was modeled using the Priestley- Taylor method (PT). Net solar radiation data were taken from a climate station maintained by CIMIS (California Irrigation Management Information System) located approximately 55 miles from the study site near Buntingville, California (Lat: 40º17' N Long: -120º26W)) (CIMIS, 2013).

$$P = Q + ET + \Delta S + \Delta G \quad \textbf{(2)}$$

Where: P= Precipitation (ft)

ET= Evapotranspiration (ft)

ΔS= Change in soil moisture storage (ft)

ΔG= Change in groundwater storage (ft)

Q= Outflow (ft)

Average weekly volumetric soil moisture and depth to groundwater values were determined by compiling hourly measurements recorded by water level loggers and soil

moisture probes. During periods when groundwater receded past the detection depth of groundwater wells, interpretations of groundwater depth and by extension recharge were inferred from ERT data coupled with a recession curve analysis (Surfleet et al., 2013). Outflow from MM was determined by correlating measured stream discharge with stage measured in at the base of a culvert at the bottom of MC (Fig 3.3). In order to measure stream stage, a water level logger was installed in a PVC case clamped to a T-post. Measurements recorded by the logger will be correlated with physical measurements of stream discharge. Outflow from ephemeral stream channels on CM was not quantified.

3.4. Soil Moisture (ΔS)

3.4.1 Soil Moisture Probe Installation

Prior to installation in the soil, soil moisture probes were encased in an enclosed 1.5 in. (3.8 cm) diameter PVC pipe to protect the data recorder component from weather (Fig 3.6). A section of PVC pipe was cut to a length of approximately 1.0 ft (0.3 m). A PVC cap was attached to one side of the case with PVC cement. A hole was drilled into the attached cap in order to allow the soil moisture probes sensor and cable to be inserted through the case and into the soil column. In order to install the probe, a 14 in. (0.36 m) hole was excavated and a steel rod was hammered parallel to the ground surface at a depth of 1.0 ft (0.3 m). This hole acted as a pilot hole for the probes sensor. When the probe had been inserted snugly into this pilot hole, the excavated hole was refilled and the native material removed was lightly packed down to maintain the soils undisturbed bulk density. The top end of the case was left above the ground surface and painted to aid in probe location during subsequent field visits. When the instrument and PVC case were installed in the field, a cap whose inner walls had been greased with petroleum jelly was

fit to the top of the case end to prevent precipitation from entering the case. Silicone glue and duct tape were used in an attempt to prevent water from percolating through the hole drilled at the bottom end of the case. In some cases, flowing water was able to penetrate this barrier on probes installed on CM.

Figure 3.6 The soil moisture probe (1), case and (2) data recorder (duct tape has been removed from the PVC case)

3.4.2 Soil Moisture Data Calibration

To calibrate soil moisture measurements, the soil water content of soil adjacent to each soil moisture probe was empirically determined by using the gravimetric method (DeAngelis, 2007). Soil samples at each site were collected at a depth of 1.0 ft (0.3 m) and placed in sealed Ziploc bags. Within one week of being collected in the field, approximately 150-175 g of each soil sample was removed from the sealed Ziploc bags, placed in a weighing can and weighed on an analytical balance. The recorded mass was the field soil moisture mass. Following weighing, soil samples were inserted into a drying oven (with weighing can lids removed) set to 105 °C for 24 hours. Following removal

from the drying oven, the soil samples were immediately placed in desiccant cabinets to allow the weighing cans to cool to the touch without absorbing water vapor.

When the weighing cans had cooled to the touch (2-3 hours), they were weighed to determine the oven dry mass of each sample. The mass of water in each soil sample was determined by subtracting the mass at 'field soil moisture' from the oven dry mass of the soil (Equation 3).

$$W_m = F_m - D_m \ (\mathbf{3})$$

Where: W_m=Soil water mass (g)

F_m= Field moisture soil mass without mass of lidded weighing can (g)

D_m= Oven dry soil mass without mass of lidded weighing can (g)

The gravimetric wetness of each sample was determined by dividing the soil water mass from the mass of the oven dry soil. In this study, soil moisture probes were placed in the field prior to calibration (Equation 4). Consequently, the measured gravimetric soil moisture had to be correlated with the uncalibrated value the instrument recorded at the time and date each soil sample used for instrument calibration was collected in the field (Equation 5). When the calibration was performed, a calibration file was made within the instruments software so future values recorded by the instrument were calibrated.

$$\Theta_g = \frac{W_m}{D_m} \ (\mathbf{4})$$

Where: Θ_g= Gravimetric wetness (soil moisture) (%)

$$V_c = \frac{V_u - O_v}{\theta g - 0} \quad \textbf{(5)}$$

Where: V_u= Uncalibrated value (mm)

O_v= Offset value (mm) (factory installed into each instrument)

V_c = Calibrated value (mm)

3.4.3 Conversion of Gravimetric to Volumetric Soil Moisture

In order to establish the quantity of water stored as soil moisture, the gravimetric wetness of soil measured by each soil moisture probe was converted to a volumetric wetness. Gravimetric wetness is related to volumetric soil moisture by bulk specific gravity (synonymous with bulk density). The average bulk density of soil at a 1.0 ft (0.3 m) depth on MM and CM was determined by collecting soil samples near soil moisture probes using the core method (Black et al., 1965). Soil samples were taken using a soil core sampler that allowed undisturbed samples to be collected (Fig 3.7). The soil core sampler was driven into the ground horizontally at a depth of 1 ft (0.3 m), within 1.5 ft (0.45 m) of soil moisture probes. The inner concentric brass rings of the soil core sampler were removed from the sampler body. Each ring was trimmed of excess soil with a knife, so that the volume of soil collected within the ring was identical to the volume enclosed by the sides of the ring. Each sample was enclosed with tin foil and placed in a sealed Ziploc bag. Samples were collected in this manner at three separate locations on both CM and MM.

In a laboratory, soil samples were removed from each ring, placed in weighing cans and oven dried at 105 °C for 24 hours. The mass of each oven-dried sample was measured on an analytical balance. An average bulk density of soil on both meadows was

determined by calculating the ratio of the oven dry mass of soil to the bulk volume of the soil (Equation 6). The volumetric soil moisture could then be related to soil bulk density (Equation 7). Soil samples were also collected using the soil core sampler at a depth of 2.0 ft (0.6 m) at a single location on CM and two locations on MM to determine the bulk density of soil at 2.0 ft (0.6 m).

$$P_b = \frac{D_m}{V_s} \quad (6)$$

$$\Theta_v = \Theta_g * \frac{P_b}{P_w} \quad (7)$$

Where: Θ_v =Volumetric soil moisture (wetness) ($\frac{g}{cm^3}$)

Θ_g = Gravimetric wetness($\frac{g}{g}$)

P_w= Water bulk density ($\frac{g}{cm^3}$)

P_b= Soil bulk density ($\frac{g}{cm^3}$)

V_s= Soil volume (cm^3)

Figure 3.7 The soil core sampler parts; inner concentric rings are separated by spacer rings (seen in the picture above the sampler).

3.4.4 Conversion of Volumetric Soil Moisture to an Equivalent Water Depth

Volumetric soil moisture at a 1 ft (0.3 m) depth was used to determine the equivalent depth of water stored as soil moisture. In terms of soil water distribution, soil homogeneity was assumed, in that no distinction was made between the unsaturated zone and the capillary fringe. The soil moisture measured at a depth of 1.0 ft (0.3 m) was considered to be the average soil moisture for all parts of the soil column above the water table. This depth was chosen because it was considered a good compromise between drier surface soil and wetter soil in the vadose zone. This assumption allowed the equivalent depth of water to be calculated (Equation 8).

$$S_{Ed} = V_w * G_d \quad (\mathbf{8})$$

Where: S_{Ed} = Equivalent depth of water in the soil (ft)

V_w = Average weekly volumetric soil moisture (%)

G_d = Depth to groundwater (water table) (ft)

An arithmetic mean of soil moisture measurements recorded at each soil moisture probe was used to determine the quantity of water stored as soil moisture on CM and MM on a weekly basis. The weekly equivalent depth of water in soil was used to determine the Δ S component of the water budget (Equation 9).

$$\Delta S = S^1_{ED} - S^0_{ED} \quad (\mathbf{9})$$

Where: S_{ED}^1 = Current soil moisture equivalent water depth (ft)

S_{ED}^0 = Preceding soil moisture equivalent water depth (ft)

3.4.5 Determination of Porosity

The porosity of the soil on CM and MM was determined using an indirect method relating soil bulk and particle density to porosity (Equation 10) (Carter, 1993). The particle density of soil on MM and CM was assumed to be 2.65 g/cm^3 (Chesworth, 2008). The field capacity of soil on both CM and MM was considered to be half of the water content at saturation (Christensen and Peacock, 2000 and Sibbet and Ferguson, 2005). Although, this estimation provides the ability to relate volumetric soil moisture to the hydrologic properties of soils on CM and MM a more robust method is suggested to empirically determine field capacity on a volume basis for future comparisons or use in other aspects of the study (Cassel and Nielsen, 1986).

$$n = \left(1 - \frac{P_b}{P_s}\right) * 100\% \quad (\mathbf{10})$$

Where: n =porosity (%)

P_b = Bulk density of soil ($\frac{g}{cm^3}$)

P_s =Particle density of soil ($2.65\ \frac{g}{cm^3}$)

3.5 Groundwater Depth Measurement

3.5.1 Groundwater Well Fabrication and Installation

Water level loggers were installed on MM and CM within shallow groundwater observation wells constructed from 5.0 ft (1.5 m) lengths of 1 in. (2.5 cm) PVC pipe. A 6-8 in. (0.15-0.20 m) section of 1.5 in. (4 cm) PVC pipe was fit to one end of the 5 ft length of 1 in. (0.3 m) PVC pipe using a 1.0 to 1.5 in. (2.5-3.8 cm) junction and PVC glue. This attachment allowed the water level logger to sit above the main shaft of the well above

the ground surface. The bottom of the well casing was plugged with a rubber stopper to prevent soil from entering the bottom of the well. The bottom 1.0 ft (0.3 m) of the well casing was perforated using a cordless drill to allow water to enter the PVC well casing. The holes were covered with plastic window screening to prevent soil particles from entering the well. Groundwater wells installed without instruments followed the same procedure using 1 in. (2.5 cm) PVC but did not have the 1.0 to 1.5 in. (2.5-3.8 cm) junction attached. A cap (greased with petroleum jelly) was placed on top of each groundwater well to prevent precipitation from entering the well.

A tool with an inner core, outer sleeve and, a pounder was constructed to create the initial holes needed to install shallow groundwater wells (Fig 3.8). The core was constructed from solid iron. The top of the core had a 3 in. (7.6 cm) wide pounding cap welded on and the bottom of the core that was sharpened to a point so that it could be driven into the ground. The outer hollow sleeve was constructed to fit around the core. The bottom of the core was beveled so that the core and outer sleeve formed one point. The outer sleeve was fit around the core and the sleeve rod assembly was pounded into the ground using a fencepost pounder and a sledgehammer. To install groundwater wells, the inner core was removed from the ground. In most cases, the core had to be separated from the outer sleeve using a 48 in. farm jack. The PVC groundwater well was fit within the outer sleeve. The outer hollow sleeve was removed, taking care not to disturb the well. The outer hollow sleeve of the assembly had two holes adjacent to where it interfaced with the pounding cap so that it could be removed from the ground with a thick rod of steel rebar.

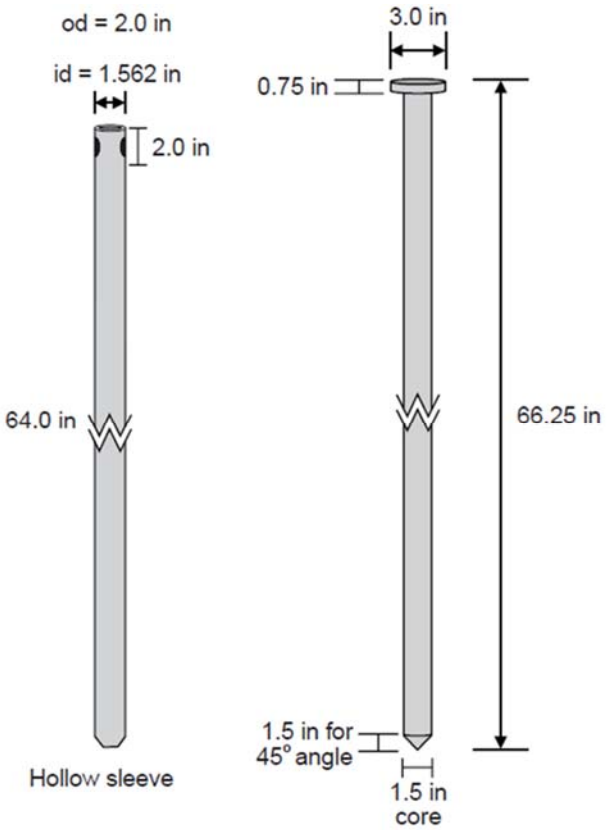

Figure 3.8 The outer sleeve and core used to install shallow groundwater wells (Figure from Bohn, 2001)

Disturbed areas on the sides of the well were filled with sand and native material. The interface between the groundwater well casing and the ground was lined with bentonite clay to prevent water from flowing down the sides of the well. Installing the core and sleeve with a fencepost pounder and hammer was problematic when sites possessed fine textured soil, low soil moisture or high concentrations of cobbles and pebbles. A hydraulic auger was needed to make many of the 4.9 ft (1.5 m) holes needed to install groundwater wells because the inner core could not be pounded more than 2.6 ft (0.8 m) into the soil using the fencepost pounder and sledgehammer. Two sets of the outer hollow sleeve and core assembly were constructed and used at the study site because this tool was susceptible to bending and warping after repeated use.

3.5.2 Water Level Logger Calibration

The water level loggers used in this study were 4.9 ft (1.5 m) in length. They were calibrated using a top down calibration procedure; this meant that the interface between the instrument element and the data recorder was the zero point for depth measurements. To calibrate the water level logger, two marks were made with a waterproof marker on the Teflon lined element 100 mm and 1000 mm from the interface between the counterweight and the instrument element (Fig 3.9).

Figure 3.9 A water level logger installed in a groundwater well on Marian Meadow

The water level loggers counterweight and instrument element were immersed in a bucket filled with tap-water at depths of 1000 mm and 100 mm and a setting in the instruments software that allowed real time measurements to be made was used to measure the values the logger measured at these immersion depths. These measurements were used to determine the slope of the water level logger calibration equation, offset

value and calibrated value (Equations 11, 12 and 13). As with the soil moisture probes, when the instruments were calibrated a calibration file was created within the instruments software that would automatically calibrate all future data downloaded from the instrument.

$$\Delta = \frac{V - V_o}{X - X_o} \quad (\mathbf{11})$$

$$\text{Offset} = V_o - (X_o * \Delta) \quad (\mathbf{12})$$

$$V_c = \frac{(V_u - O)}{\Delta} \quad (\mathbf{13})$$

Where: Δ= Slope of the calibration curve

V= Value at 1000 (mm)

V_o= Value at 100 (mm)

X= 1000 (mm)

X_o=100 (mm)

V_u= Uncalibrated Value

V_c= Calibrated Value (mm)

Calibrated groundwater depth values had to be corrected because the interface between the instrument element and the recorder did not occur at the ground surface (Equation 14).

$$G_d = V_c - X_g \quad (\mathbf{14})$$

Where: G_d= Actual groundwater depth (mm)

X_g= Distance from recorder interface to the ground (mm)

The recorded depth to groundwater value consisted of the depth to groundwater in addition to the height of the logger's data recorder- measuring element interface above the ground surface. A well sounder was used to take measurements of groundwater depth at all instrumented and un-instrumented groundwater wells during field visits. All groundwater depth values measured using the well sounder were cross referenced with calibrated values from each water level logger in an attempt to ensure that the groundwater wells were recording accurate groundwater depths. The arithmetic mean of depth to groundwater measured across CM and MM was used to determine the average depth to groundwater for each week of the water balance when known groundwater depth data was available.

3.6 Electrical Resistivity Tomography

Electrical resistivity tomography surveying was conducted on both CM and MM. An automatic resistivity meter (SYSCAL Kid Switch) with a 24-electrode string manufactured by IRIS Instruments was used to conduct electrical resistivity surveys. Resistivity measurements were collected using the Wenner PRF Switch array setting on all surveys. Field data was downloaded from the resistivity meter to a computer using PROSYSII software (http://www.iris-instruments.com/Support/support.html, Accessed 3/23/15) and processed into subsurface electrical resistivity models with RES2DINV software (geotomosoft.com). RES2DINV calculates the best-fitting subsurface electrical resistivity model using a least squares inversion method. This method proceeds in an iterative manner, updating the subsurface electrical resistivity model to minimize misfit between field data and calculated apparent resistivity data. Convergence to a final model

is achieved when successive models change by less than a specified percentage. The RES2DINV defaults were used to assess convergence.

During initial reconnaissance surveys on CM and MM, a variety of electrode spacings and survey locations were considered and implemented (Tables 3.3, 3.4 and 3.5). Ultimately, within the main portion of both meadows, one long transect with roll along lines and two lines bisecting this transect line were established as the consistent format for all future surveys (Fig 3.10 and 3.11). The transect lines running across CM and MM used a 5 m electrode spacing. Survey lines that bisected transect lines featured shorter electrode spacing (1.5 m) to provide a balance of near surface and deeper resistivity resolutions. The maximum total survey length for a single series of measurements was 115 m. This survey length at a 5 m electrode spacing using a Wenner PRF Switch setting yielded a maximum imaging depth of approximately 20 m. The shorter bisecting lines had an imaging depth of approximately 6 m. A transect and bisecting line adjacent to the MC road culvert was also selected to characterize the subsurface resistivity of the lower portion of MM. Logarithmic contour intervals were used exclusively to contour electrical resistivity values presented in electrical resistivity diagrams.

Table 3.3 GPS locations, orientations and lengths of resistivity survey lines on the Control Meadow

Date	Survey Line	Survey Center Lat and Long	Trend	Length(m)
5/6/2014	Ecotone Boundary	40.2650, -121.3940	55°	47
9/6/2014	Ecotone Boundary	40.2649, -121.3941	70°	54
9/6/2014	Upper Bisecting Line	40.2641, -121.3945	60°	34.5
9/6/2014	Lower Bisecting Line	40.2634 -121.3942	60°	34.5
9/6/2014	CM Transect	40.2640, -121.3944	335°	170

Table 3.4 GPS locations, trends and lengths of resistivity survey lines on Marian Meadow

Date	Survey Line	Survey Center Lat and Long	Trend	Length(m)
9/10/2013	Upper MM Transect Bisecting Long Line	40.2641, -121.3163	65°	115
9/10/2013	Upper MM Transect Bisecting Short Line	40.2641, -121.3163	65°	34.5
9/10/2013	Marian Meadow Transect	40.2642,-121.3164	340°	51.75
9/10/2013	Lower MM Transect Bisecting Line	40.2639, -121.3162	50°	51.75
5/6/2014	Marian Meadow Transect	40.2633, -121.3141	40°	175
9/7/2014	Marian Meadow Transect	40.2635, -121.3156	345°	115
9/7/2014	Lower MM Transect Bisecting Line	40.2633, -121.3153	25°	51.75
9/7/2014	Upper MM Transect Bisecting Line	40.2640, -121.3160	68°	51.75
9/7/2014	Lower Marian Creek Meadow Transect	40.2614, -121.3116	15°	92
9/7/2014	Lower Marian Creek Meadow Transect Bisecting Line	40.2610, -121.3117	278°	34.5

Table 3.5 Electrode spacings used for each electrical resistivity survey

Date	Survey Line	Node Spacing(m)
9/7/2013	Upper MM Transect Bisecting Line	1.5
9/7/2013	Upper MM Transect Bisecting Line	1.5
9/7/2013	Marian Meadow Transect	5
9/7/2013	Lower MM Transect Bisecting Line	1.5
5/6/2014	Marian Meadow Transect	5
9/7/2014	Marian Meadow Transect	5
9/7/2014	Lower MM Transect Bisecting Line	1.5
9/7/2014	Upper MM Transect Bisecting Line	1.5
9/7/2014	Lower Marian Creek Meadow Transect	4
9/7/2014	Lower Marian Creek Meadow Transect Bisecting Line	1.5
9/6/2014	Ecotone Boundary	1
5/3/2014	Ecotone Boundary	1
9/6/2014	Upper Bisecting Line	1.5
9/6/2014	Lower Bisecting Line	1.5
9/6/2014	CM Transect	5

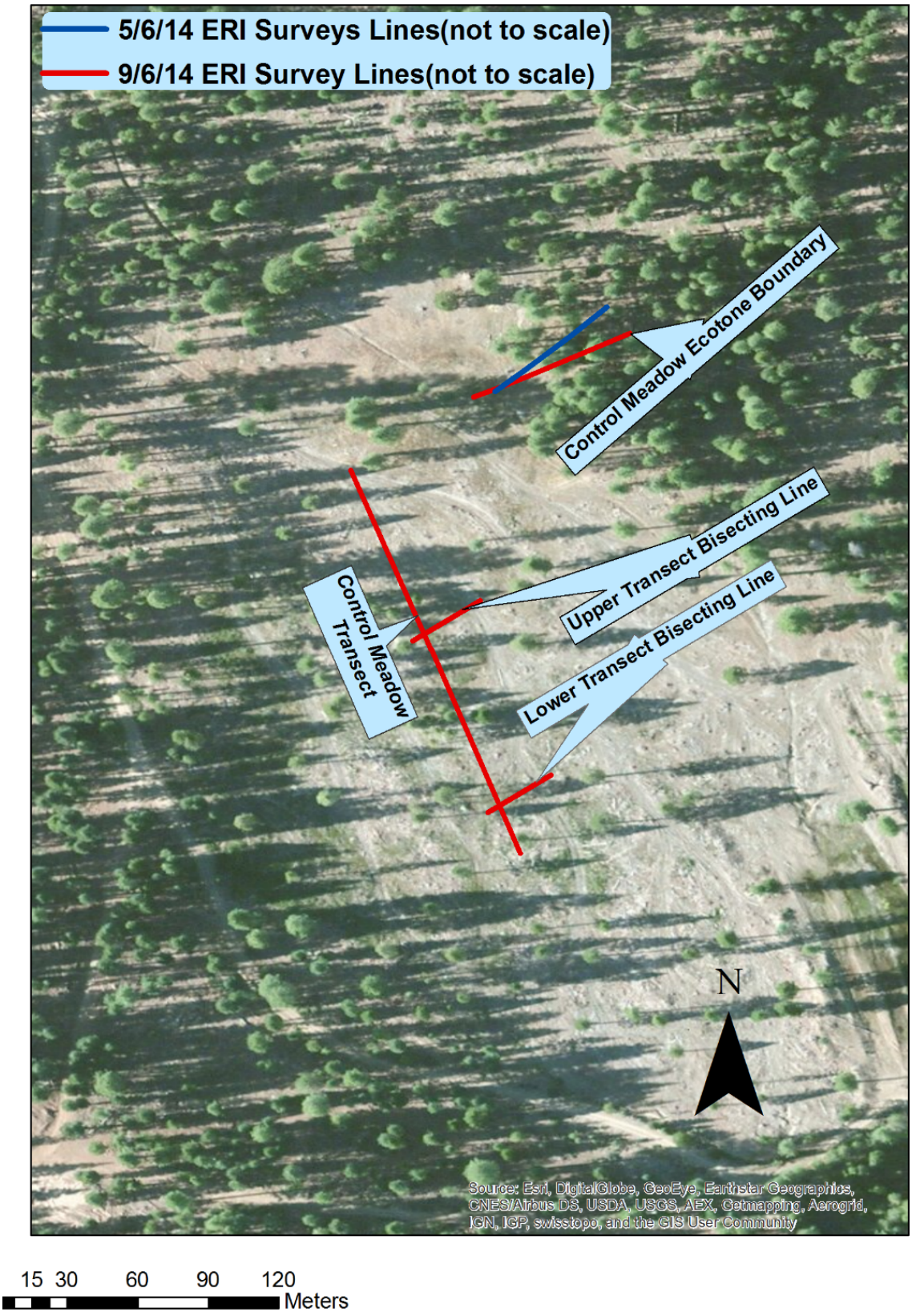

Figure 3.10 Electrical resistivity surveys conducted on the Control Meadow

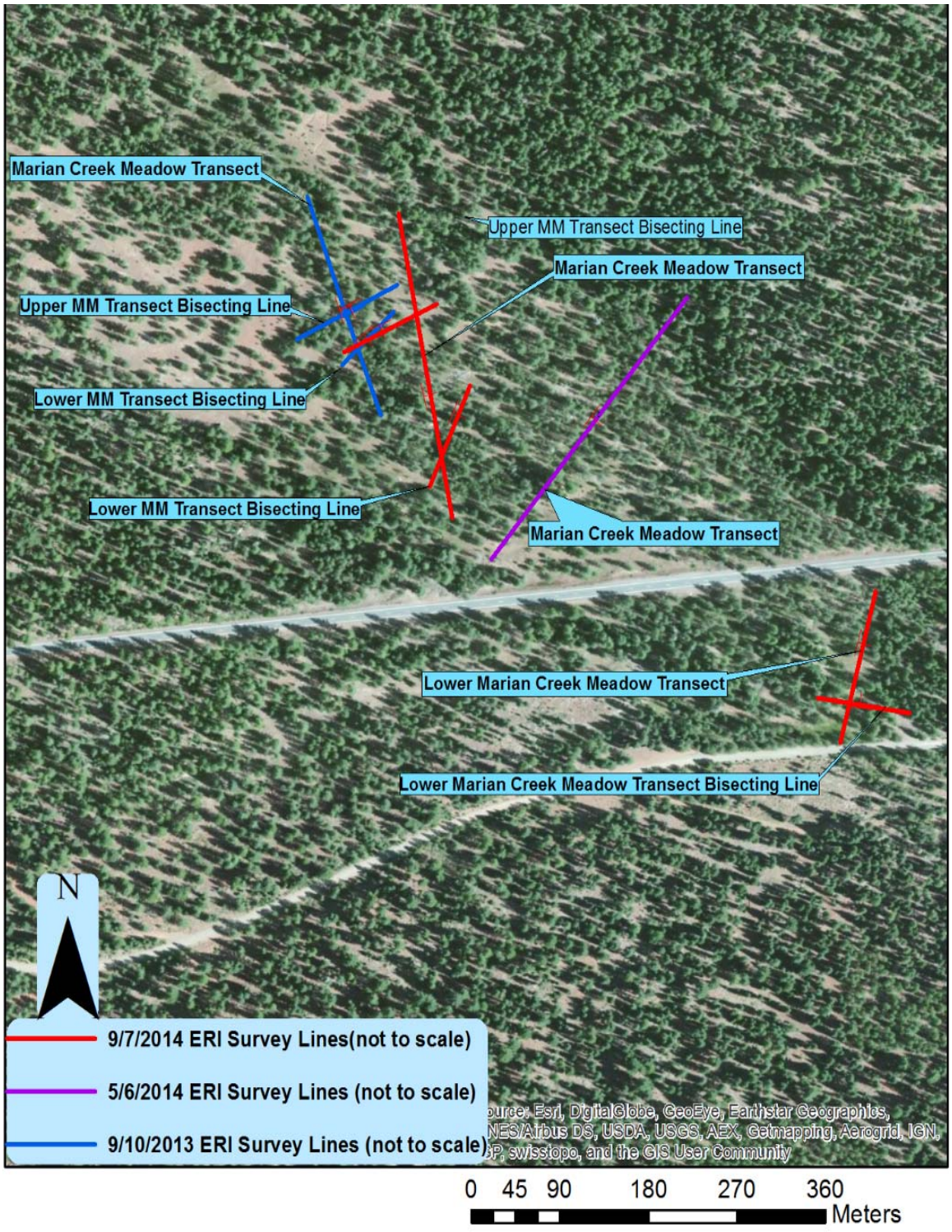

Figure 3.11 Electrical resistivity surveys conducted on Marian Meadow

3.7 Groundwater Recharge Recession Curve Analysis

Using the shallow groundwater wells alone, the depth to groundwater could not be determined during periods when the water table receded more than 3.5 ft (1.1 m) below the ground surface. A recession curve analysis that accounted for weekly precipitation was used to model groundwater recharge below MM and CM (Surfleet et al., 2013) (Equation 15). The recession curve was fit to model recharge from groundwater depths inferred from analysis of electrical resistivity diagrams to known depths recorded by each groundwater well. On MM, groundwater was interpreted as a region where consistent resistivity below 45Ω · m occurred in the upper boundary of the saturated zone and resistivity remained below 105-110 Ω · m in the lower boundary of the saturated zone. On CM, groundwater was interpreted as a region where resistivity consistently ranged from 100-180Ω · m. The resistivity ranges chosen to represent saturated soil were based largely on empirically derived electrical resistivity values of saturated soils similar to those present on MM and CM, and spatial interpretation of the distribution of resistivity values (see Section 2.7).

$$G_d = (k * m) - P \quad (\mathbf{15})$$

Where: G_d =Groundwater depth (ft)

k=Recession coefficient

m=Inferred groundwater depth (ft)

P= Precipitation (ft)

The spatial geometry of electrical resistivity in CM and MM subsurface factored heavily into how the electrical resistivity of the subsurface was interpreted in terms of indicating distinct hydrologic zones. The region of the subsurface considered

groundwater below both CM and MM had a narrower range of resistivity, compared to the resistivity observed above the saturated zone. This pattern could be observed visually in electrical resistivity diagrams regardless of the contouring criteria, unless a very broad non-logarithmic contouring scheme was implemented. Depths to groundwater were inferred from surveys conducted with a 1.5 m spacing because these surveys provided a better resolution of the first 10.0 ft (3.1 m) below the ground surface. A similar distribution of resistivity relative to depth below the ground surface was observed across MM. Consequently, the depths to groundwater inferred from each resistivity diagram were generally within 1.0 ft (0.3 m) of one another. Excluding the ecotone region, this was also true on CM.

On MM, a depth of 9.2 ft (2.8 m) was used as the known depth for the weekly period starting on 9/12/13 and a depth of 8.5 ft (2.30 m) was used as the known depth for the weekly period starting on 9/5/14. Groundwater depths were known from February 2014- May 2014 in most wells on MM and CM. On MM, the first recession equation modeled groundwater recharge from 9.2 ft to the first known groundwater depth, which occurred on varying dates during February 2014 on individual groundwater wells. The second recession equation modeled groundwater discharge from the last known groundwater depths which occurred on varying dates in June 2014 to 8.5 ft (2.30 m). The third recession equation modeled groundwater recharge from 8.5 ft (2.30 m) to known groundwater depth measured in December 2014 in all groundwater wells.

No ERT surveys were conducted during September 2013 on CM. On CM, the first recession curve had to model groundwater recharge ‘in reverse’ from February 2014 to September 2013. Known depth values measured by groundwater wells were used as

the initial known values for the recession curve analysis. An inferred groundwater depth of 10.7 ft (3.3 m) determined from an electrical resistivity survey conducted on September 6 2014 (Fig 3.13) was considered to be the target value for the February 2014-September 2013 recession equation. This assumption may have introduced uncertainty, but a choice of a different groundwater depth for the initial week of the water budget analysis on CM without corroborating data would have been arbitrary. The 2nd and 3rd recession curve equations used a methodology identical to that described in the previous paragraph and fit data to and from 10.7 ft (3.26 m). Appendices A and B include depictions of the measured apparent electrical resistivity pseudosections, calculated apparent electrical resistivity pseudosections, and inverse model electrical resistivity sections for each survey taken on MM and CM.

3.7.1 Groundwater Depth to Equivalent Groundwater Content (ΔG)

In order to determine the equivalent depth of water stored as groundwater, a total width of the saturated subsurface had to be determined. Electrical resistivity tomography was used to infer the depth to the base of the aquifer on MM (Fig 3.14). On MM, the base of the aquifer was considered to be a region where the electrical resistivity began to rise above 110-120Ω · m. This transition was considered to occur at approximately 41.0 ft (12.5 m). A depth to the base of the aquifer below CM could not be determined because this layer lay beyond our maximum detection depth of 20 m using the Syscal Kid Swtich 24 system with a Wenner PRF Switch setting. The reference datum of 41.0 ft (12.5 m) applied to MM, was also applied to CM.

The change in the quantity of water stored as groundwater during each week was determined relative to this reference datum and the average depth to groundwater

measured for each week. The fraction of the subsurface that contained water between these two boundaries was considered to be the same as porosity (Equation 16). The porosity of the layer comprising the water table was considered uniform (based on porosity at a 2.0 ft (0.6 m) depth). In the water budget analysis, the change in equivalent depth of groundwater was relative to each preceding week (Equation 17). Measurements of groundwater content from the first weekly period of the study (9/13/13-9/20/13) were used as the initial reference point to determine subsequent content variations. The determination of weekly groundwater storage thus allowed the determination of the ΔG component of the water budget.

$$G_{Ed} = p * (G_b - G_d) \quad (16)$$

Where: G_{Ed} = Equivalent depth of water stored in the aquifer (groundwater) (ft)

n= Porosity (determined from Equation 8 and P_b)

G_d= Depth to groundwater (ft)

G_b= Base of the aquifer (41.0 ft)

$$\Delta G = G^1_{Ed} - G^0_{Ed} \quad (17)$$

Where: G_{ED}^1= Current groundwater equivalent water depth (ft)

G_{ED}^0= Preceding groundwater equivalent water depth (ft)

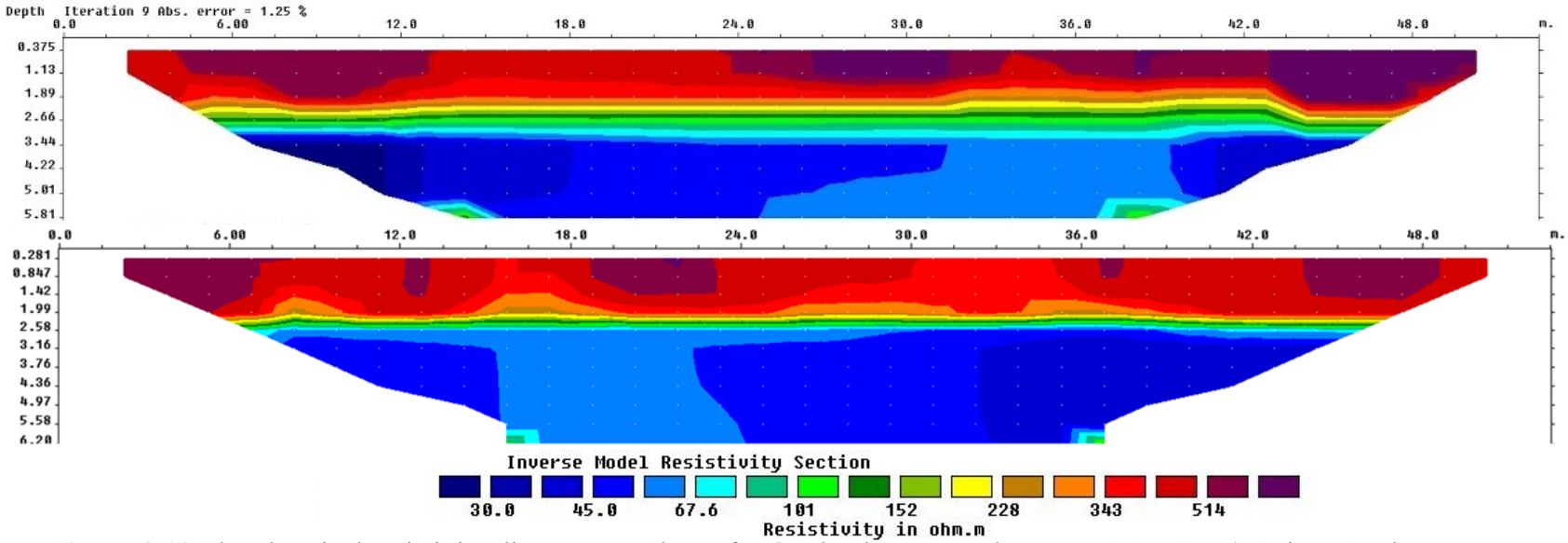

Figure 3.12 The electrical resistivity diagrams used to infer the depth to groundwater on MM Top (Marian Meadow Transect 9/10/2013, Abs Error=1.25) Bottom (Lower Marian Meadow Transect 9/7/2014, Abs Error=1.06)

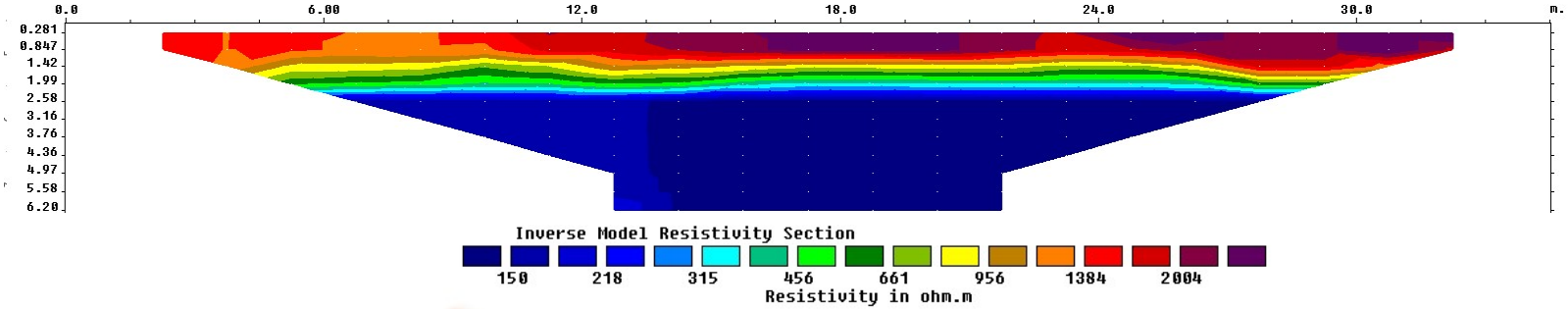

Figure 3.13 Electrical resistivity diagram used to infer the depth to groundwater below CM (Control Meadow Lower Bisecting Line 9/6/2014: Abs Error=1.9%)

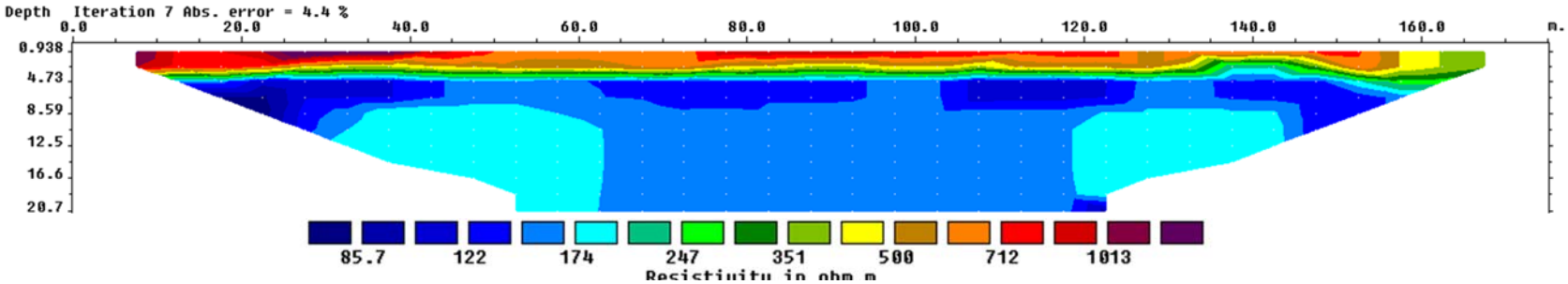

Figure 3.14 Electrical resisitvity diagram used in an attempt to determine a depth to the base of the aquifer below CM (Control Meadow Transect 9/7/2014: Abs Error=4.4%)

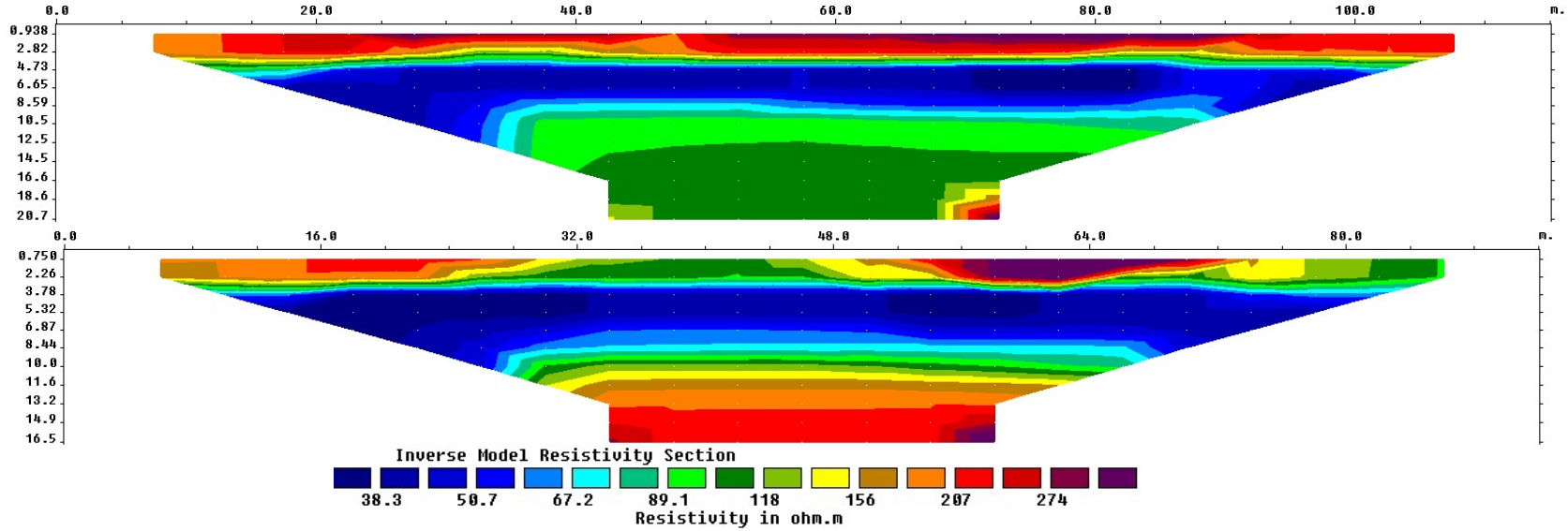

Figure 3.15 Resistivity surveys from September 2014 used to determine the depth to the base of the aquifer below Marian Meadow (Top MM Transect 9/10/2014, Abs Error=5.0%) Bottom: (Lower MM Transect 9/10/2014, Abs Error=3.3%)

3.8 Outflow (Q)

The water level logger used as a stream stage recorder was calibrated using a bottom-down calibration procedure. This meant that the zero point was the interface between the counterweight and the measuring element. Due to instrument failures, stage was not quantified prior to September 2014. During field visits, measurements of flow and discharge were performed 20.0 ft (6.1 m) upstream of the MC culvert using a Hach FH950 Handheld Flow-Meter. The height of water in the culvert was also manually measured. A discharge of 2.34 $\frac{ft^3}{s}$ (0.07 $\frac{m^3}{s}$) was determined on MC on 12/21/14. To calculate outflow from MC, the MC road culvert dimensions were measured to relate the cross sectional area and the hydraulic radius of the culvert to the depth of water measured within the culvert (Fig 3.16). The dimensions of the culvert were measured in the field and could be used in Manning's equation (Equation 18) to calculate discharge. An empirically derived Manning's coefficient for corrugated metal piping was used in Manning's equation to provide an alternative means to quantify outflow (American Concrete Pipe Association, 2009).

$$Q = \frac{1.486}{n} * A * R^{0.667} * S^{0.5} \quad (\mathbf{18})$$

Where Q= Discharge ($\frac{ft^3}{s}$)

n= Mannings roughness coeffidient

A= Cross sectional area of flow boundaries(ft^2)

S= Slope of the pipe

R= Hydraliuc radius (ft)

Figure 3.16 The Marian Creek road culvert during March 2015; the stage recorder is enclosed within a PVC case that is attached to a T post (indicated by the red arrow).

Discharge and flow through the road culvert could be determined by correlating physically measured stream discharge with the height of water measured by the stage recorder installed adjacent to the road culvert. Although these methods for quantifiyng outflow (Q) were established, outflow was not considered as part of the water budget analysis as it pertains to this thesis because of the lack of usable data prior to the replacment of a malfucntioning instrument installed as a stage recorder with a new water level logger in September 2014. The lack of quantified outflow prior to flow events first measured in December 2014 is a source of uncertainty in the water balance of MM. However, this uncertainty is probably only significant following large precipitation events because MC is an ephemeral stream. Outflow from CM was not measured.

3.9 Evapotranspiration (ET)

Evapotranspiration from CM and MM was modeled using the PT method (Equation 19) (Priestley and Taylor, 1972). Daily net radiation measurements were taken from a CIMIS station located near Buntingville, California (CIMIS, 2014). The PT coefficient used for both CM and MM was an average value of empirically derived PT coefficients developed for temperate coniferous forests (Komatsu, 2005). The slope of the saturation vapor pressure curve was determined using an equation developed from empirically derived relations between temperature and pressure (Equation 20) (Tetens, 1930 and Murray, 1967). The latent heat of vaporization was determined using an equation developed to relate temperature to the latent heat of vaporization (Equation 21) (Harrison, 1963). Atmospheric pressure on both meadows was estimated using an equation that relies on the established empirical relationship developed between elevation and atmospheric pressure (Equation 22) (Portland State Aerospace Society, 2004). The psychrometric constant (a relation the partial pressure of moist air to air temperature) was determined using an empirically derived equation that relates the psychrometric constant to several atmospheric parameters (Equation 23) (Brunt, 1939). Evapotranspiration was modeled on daily basis, and then compiled on a weekly basis to determine the net output of water in the form of ET for each week of the water budget.

$$\mathrm{PET} = \frac{\Delta_s(\mathrm{R} - \mathrm{G})}{\Delta_s + \gamma}\alpha \quad (\mathbf{19})$$

Where: R= Net solar radiation, $(\frac{\mathrm{mJ}}{(\mathrm{day})\mathrm{m}^2})$

G=Soil heat flux, $(\frac{\mathrm{mJ}}{(\mathrm{day})\mathrm{m}^2})$

Δ_s=Slope of the saturation vapor pressure curve, $(\frac{kPa}{^\circ C})$

γ =Psychrometric constant $(\frac{kPa}{^\circ C})$

α=PT coefficient (0.65±0.25)

$$\Delta s = \frac{4098(0.6108 * e^{(\frac{17.27T}{T+237.3})}}{(T^2 + 237.3^2)} \quad (\mathbf{20})$$

$$\lambda = 2.501 - 0.002361T \quad (\mathbf{21})$$

Where: T=mean daily air temperature in °C

$$P_1 = 100 * (\frac{44331.514 - x}{11880.516})^{5.256896} \quad (\mathbf{22})$$

$$\gamma = \frac{C_p * (1000P)}{\varepsilon * \lambda} \quad (\mathbf{23})$$

Where C_p = specific heat at constant pressure, $1.013\ 10^{-3}$ $(\frac{mJ}{kg*^\circ C})$

P = atmospheric pressure (Pa)

Ɛ =ratio molecular weight of water vapor to dry air (0.622)

λ= latent heat of vaporization $(\frac{mJ}{kg})$

x=elevation (m)

3.10 IRIS Tube Fabrication and Installation

IRIS tubes were installed on CM and MM in order to determine the incidence of hydric soils (Fig 3.17). The presence of hydric soils following restoration efforts on MM could be indicative of hydrologic conditions that favor meadow re-establishment. The presence of hydric soils on CM could be indicative of successful restoration following

conifer removal in 2012. IRIS paint was prepared using a recipe and application methodology adapted from M. C. Rabenhorst's 7 day IRIS paint recipe (University of Idaho Pedology Laboratory, 2014). When the IRIS paint had been prepared, it was stored in a refrigerator for two weeks before it was applied to the PVC tubing. The full methodology followed to prepare the IRIS paint is provided in Appendix F. Fifty centimeter lengths of PVC were prepared for paint application by using acetone to remove ink from the outer surface of each tube (under a fume hood). When labelling had been removed, the tubes were sanded in a well-ventilated space to provide a surface for the IRIS paint to adhere to. Prior to applying the IRIS paint to the tubes, supernatant liquids were poured from the paint solution until it had reached the viscosity of house paint. The prepared tubes were coated with a layer of IRIS paint using a lathe device consisting of a cordless drill with a rubber stopper, shaft, and buret holder. A standard foam brush was used to apply the paint. Each IRIS tube was left to dry for at least a week prior to installation in the field.

Figure 3.17 IRIS tubes installed on Marian Meadow from 5/6/14-9/7/2014

Prior to installation in the field, IRIS tubes were individually enclosed in wrapping paper to prevent paint loss from abrasion. The IRIS tubes were installed manually using a soil push probe to create a pilot hole for each tube. In each set, IRIS tubes were placed within one meter of one another. A number 1-5, set number (1-2), and the time and date of installation were recorded on the unpainted portion of each IRIS tube. IRIS tubes were deployed in two sets of groups of five on MM during June 2014 and September 2014. On CM, one set of IRIS tubes was installed during June 2014. IRIS tubes were installed adjacent to groundwater wells at sites that seemed to possess the greatest likelihood of possessing hydric soils. Due to this distance and time involved in reaching the field site, IRIS tubes were left in place for a period of approximately four to six months. In the future, if a formal hydric soil boundary is desired IRIS tubes should be deployed in three sets, one set above, below, and within a suspected hydric soil zone over a shorter period of time (see Section 2.6).

CHAPTER 4 RESULTS

4.1 Results Overview

Although data collection on MM and CM is ongoing, data presented as part of this thesis span from 9/13/13 to 12/21/14 (referred to as the analysis period). Some data pertaining to the water balance will also be presented in a cumulative yearly format (9/13/13-9/12/14, referred to as the first year of study). The study results presented as part of this thesis are presented in such a manner as to allow a comprehensive evaluation of the pre-restoration hydrologic characteristics of MM and CM. The compiled weekly data (reported in 7-day intervals starting from initial date of installation) used to construct figures and tables in this section is included in Appendices C, D and G. During many of the weekly periods, compiled average weekly values of depth to groundwater and soil moisture do not comprise data from the entirety of the soil moisture probes and groundwater wells outlined in Tables 3.1 and 3.2. This was due to several instrument malfunctions on both meadows.

4.2 Hydrologic Characterization of Marian Meadow

4.2.1 Marian Meadow Groundwater Characteristics

The depth to the base of the aquifer below MM was determined to occur at an approximate depth of 41.0 ft (12.5 m) (see Fig 3.15). This depth is the 'reference datum', above which weekly and monthly changes in depth to groundwater (and by extension the weekly quantity of groundwater storage) were evaluated. On MM, the shallowest average depth to groundwater (1.26 ±0.39 ft (0.38 ±0.12 m)) was measured during an incomplete weekly period of the water budget analysis from 12/19/2014-12/21/14 (Fig 4.1). During

the first year of study, the shallowest depth to groundwater on MM, over a weekly period, was 1.62±0.65 ft (0.49±0.20 m) (spanning from 4/4/14-4/11/14). Saturated excess surface water was not measured by any groundwater wells on MM. The maximum depth to groundwater inferred from ERT was 9.2 ft (2.18 m) (see Methods section 3.6).

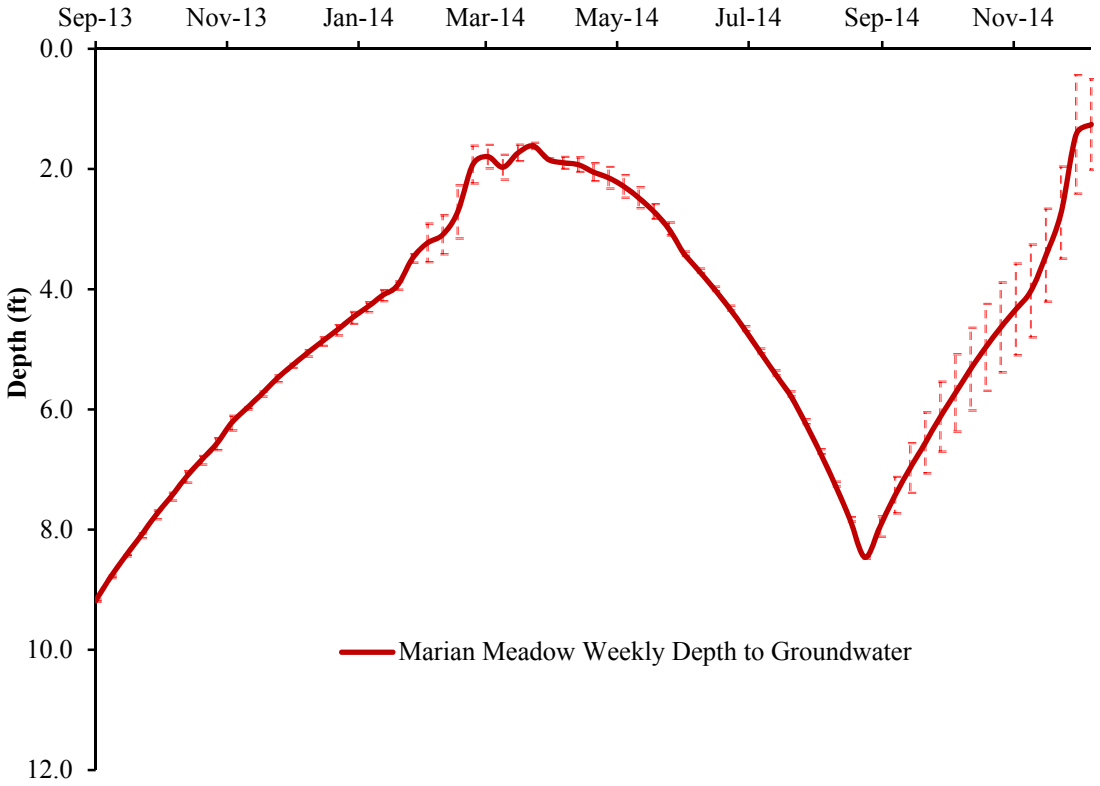

Figure 4.1 Weekly variations in average depth to groundwater on Marian Meadow

During the analysis period, depths to groundwater were consistently measured within 2.00 ft (0.61 m) of the ground surface from the periods of 3/7/14-4/25/14 and 12/12/14-12/21/14. All of the groundwater wells installed on MM detected groundwater from 2/28/14-5/23/14 and 12/5/14-12/21/14. The average weekly depth to groundwater during the analysis period was 4.74 ±2.16 ft (1.45±0.66 m). The bulk density of soil at a 2.00 ft (0.61 m) depth was determined to be 1.48 ±0.12$\frac{g}{cm^3}$, yielding a porosity of 44.3%. The average weekly quantity of water stored as groundwater above the reference datum

during the analysis period ranged from 12.08-16.08 ft (3.69-4.91 m). The average weekly quantity of water stored as groundwater during the analysis period was 14.36±0.18 ft (4.35±0.05 m).

4.2.2 Marian Meadow Soil Moisture Characteristics

The average weekly volumetric soil moisture on MM was 20.7±6.0%. On MM, the highest average weekly volumetric soil moisture (31.7±4.7%) was measured during the last incomplete weekly period of the water budget analysis: 12/19/2014-12/21/14 (Fig 4.2). The lowest average weekly volumetric soil moisture was 10.0±3.0% (from 9/27/13-10/4/14). Volumetric soil moisture remained above 25.00% from 1/31/2014-5/30/2014.The average weekly volumetric soil moisture on MM during the first year of study was 20.1±6.2%. With a few exceptions, the standard deviation of volumetric soil moisture measurements ranged between values of ±2.8% and ±4.0% during the analysis period. The bulk density of soil at a 1.0 ft (0.3 m) depth on MM was 1.40±0.13$\frac{g}{cm^3}$, yielding a porosity of 47.0%.

Weekly and monthly volumetric soil moisture was analyzed for significance of correlation to precipitation (signifcane as defined by Dancey and Reidy, 2007). Monthly averaged volumetric soil moisture measurements had a moderate correlation (R=0.61) with precipitation (Fig 4.11). Average weekly volumetric soil moisture had a weaker correlation (R=0.35) with precipitation (Fig 4.10), indicating that there may be a lag between precipitation and soil water uptake on MM. The quantity of water stored as soil moisture during the analysis period ranged from 0.4-1.5 ft (0.15-0.46 m). The average quantity of water stored as soil moisture on MM during the analysis period was 0.87±0.26 ft (0.27±0.08 m). The quantity of water stored as soil moisture during the first

year of study was 0.84±0.25 ft (0.26±0.08 m). The field capacity of soil on MM was estimated to occur at a volumetric soil moisture of 23.6%. On MM, soils were estimated to be at or above field capacity from 1/15/15- 5/20/15 and 10/15/15-12/21/15.

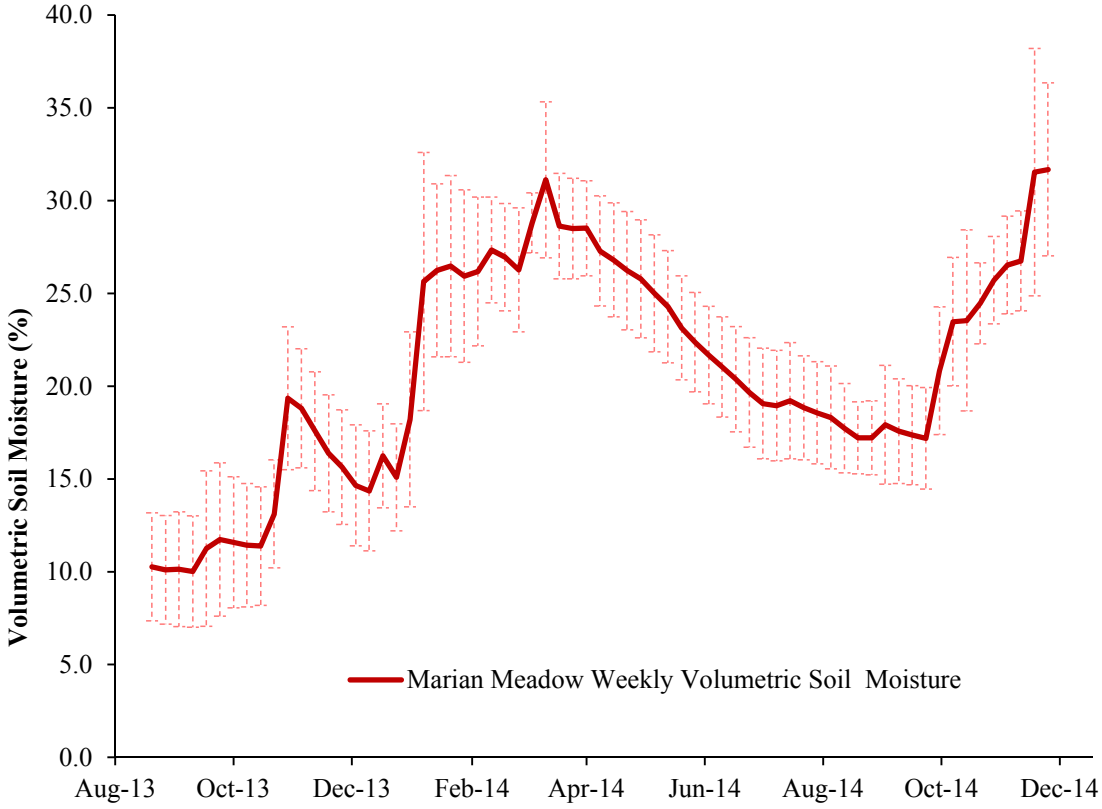

Figure 4.2 Average weekly volumetric soil moisture of soil on Marian Meadow

4.3 Hydrologic Characterization of the Control Meadow

4.3.1 Control Meadow Groundwater Characteristics

On CM, the shallowest average weekly depth to groundwater measured was 0.71±0.74 ft (0.22±0.23 m), from 12/19/2014-12/21/14). Depths to groundwater were shallower on the lower portion (lines 3 and 4) of CM relative to the upper portion of CM (lines 1 and 2). Saturation excess surface water was measured in groundwater wells on lines 3 and 4 from 12/10/14 -12/19/14. The maximum depth to groundwater inferred from

ERT surveys was approximately 10.7 ft (3.26 m) (see Fig 3.13). During 2014, depths to groundwater were consistently within 2.0 ft (0.6 m) of the ground surface from: 3/14/14-5/16/14 (Fig 4.3). Groundwater wells made groundwater depth measurements from 3/14/14- 6/6/14 and 12/12/12/21/14. The average depth to groundwater during the analysis period was 5.03±2.86 ft (1.53±0.87 m). The bulk density of soil at a depth of 2.00 ft (0.61 m) was 1.59$\frac{g}{cm^3}$, yielding a porosity of 39.9%. The average weekly quantity of water stored as groundwater during the analysis period was 14.35±1.14 ft (4.37±0.35 m). The average weekly quantity of water stored as groundwater during the first year of study was 14.35±1.18 ft (4.37 ±0.36 m). The total quantity of water stored as groundwater on CM ranged from 13.20-18.88 ft (4.02-5.76 m)

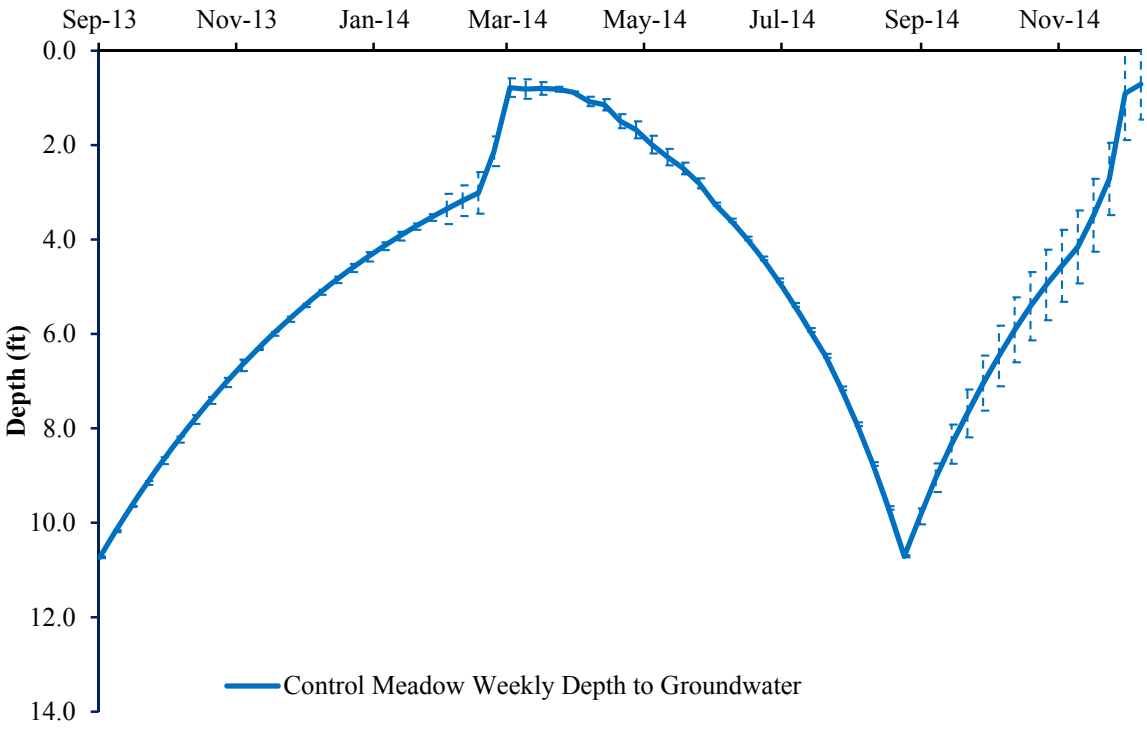

Figure 4.3 Average weekly depth to groundwater on Control Meadow

4.3.2 Control Meadow Soil Moisture Characteristics

The bulk density of soil at a depth of 1.0 ft (0.3 m) on CM was 1.53±0.13$\frac{\mathbf{g}}{\mathbf{cm^3}}$, yielding a porosity of 42.0%. On CM, the highest average weekly volumetric soil moisture was 39.8±15.3% (from 12/19/2014-12/21/14). The lowest volumetric soil moisture measured was 4.6% during the initial weekly period of analysis in September 2013. This value may be an anomaly associated with the soil moisture probe equilibrating with the soil because volumetric soil moisture rose to 17.1% within two weeks of installation and no value below 11.0% was measured after the first two weeks of data collection. The average weekly volumetric soil moisture measured on CM during the analysis period was 20.2±6.5%. Many of the lowest average weekly volumetric soil moisture measurements occurred during a period when only two soil moisture probes were installed near the top portion of CM on line 1.

The average volumetric soil moisture measured from 6/13/14-12/21/14 (starting with the installation of additional soil moisture probes on lines 3 and 4) was 17.8±7.4%. The average volumetric soil moisture measured during the first year of study was 20.08±5.88%. The field capacity of soil on CM was estimated to occur at a volumetric soil moisture of 21.0%. Soil on CM was estimated to be at or above field capacity from 1/15/15-5/20/15 and 11/15/15-12/21/15 (Fig 4.9). The average quantity of water stored as soil moisture during the analysis period and first year of study was 0.85±0.35 ft (0.26±0.08 m). Soil moisture probes C4-1, C3-2, C3-1 and C4-3 were installed prior to installation of adjacent groundwater wells during September 2014. Consequently, the depth to groundwater depth at these instrument locations was inferred from the C1-3 groundwater well to make measurements of stored soil moisture from 6/13-9/13/14 at

these probe locations. The average weekly quantity of water stored as soil moisture from 6/13/14-12/21/14 ranged between 0.30-1.65ft (0.09-0.50 m). Weekly volumetric soil moisture remained above 25.0% from 3/7/2014-5/7/2014 (Fig 4.4). The standard deviation of volumetric soil moisture measured on CM following installation of additional soil moisture probes on lines 3 and 4 ranged from ±1.09-16.8%. The highest standard deviations were associated with weeks when precipitation events occurred.

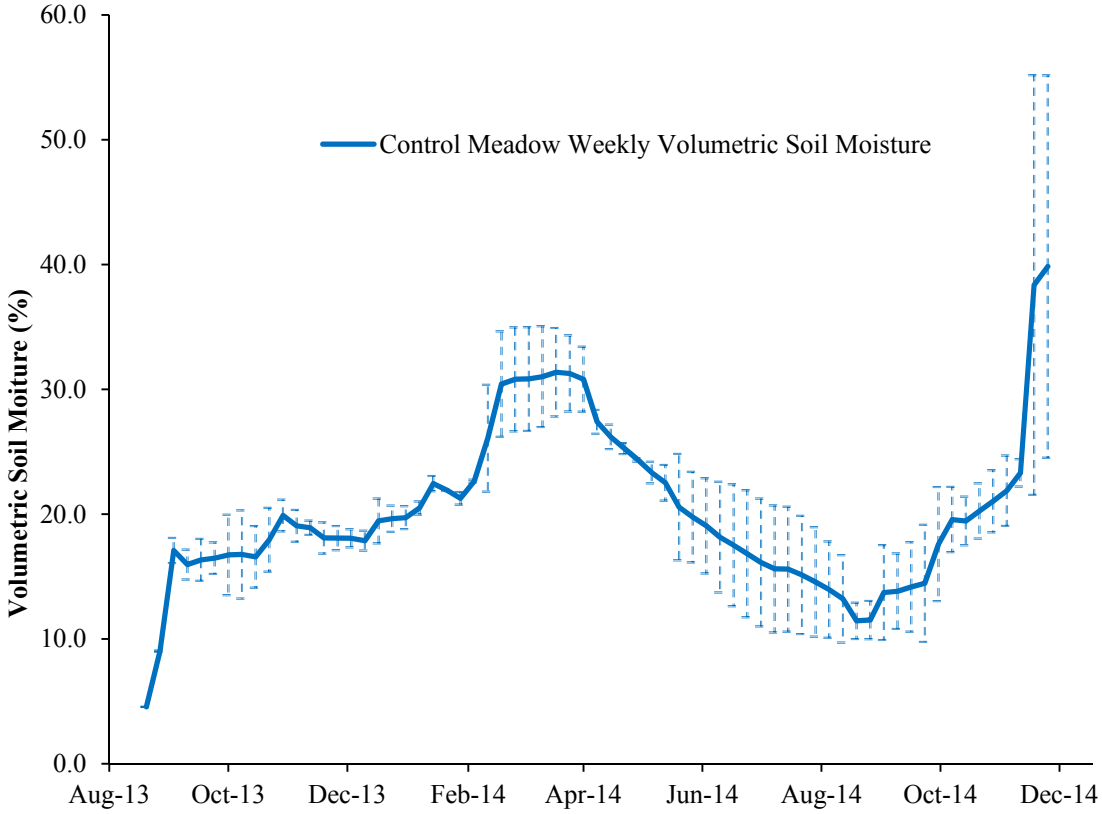

Figure 4.4 Weekly average volumetric soil moisture on Control Meadow

4.4 Hydrologic Comparison Figures

4.4.1 Groundwater Comparison Figures

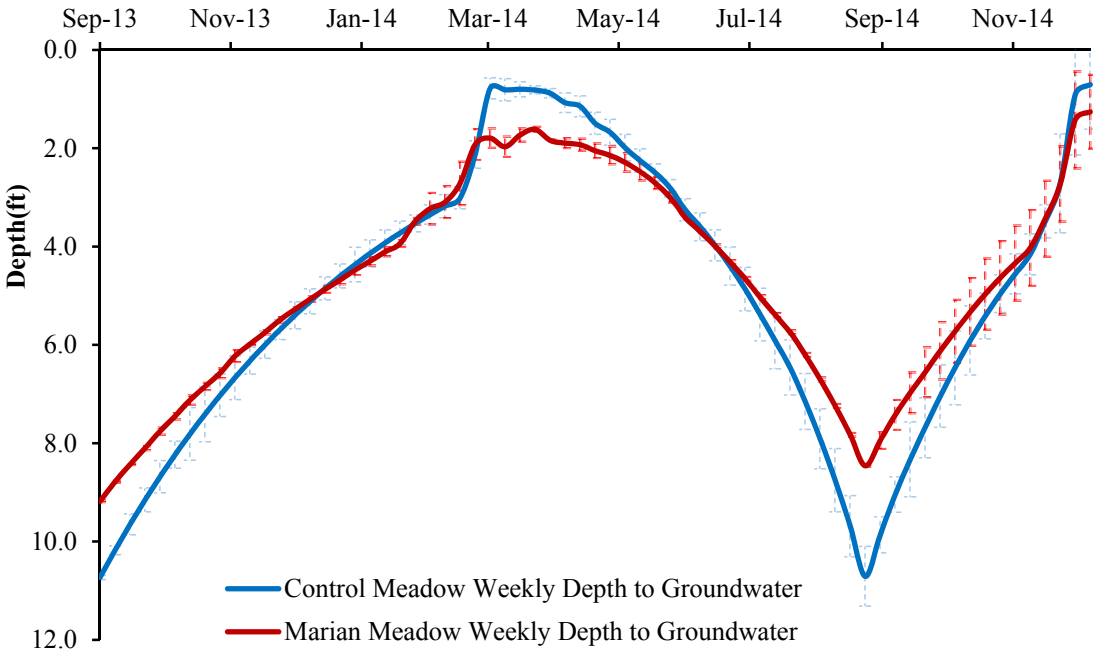

Figure 4.5 Comparison of the average weekly depth to groundwater below Control Meadow and Marian Meadow

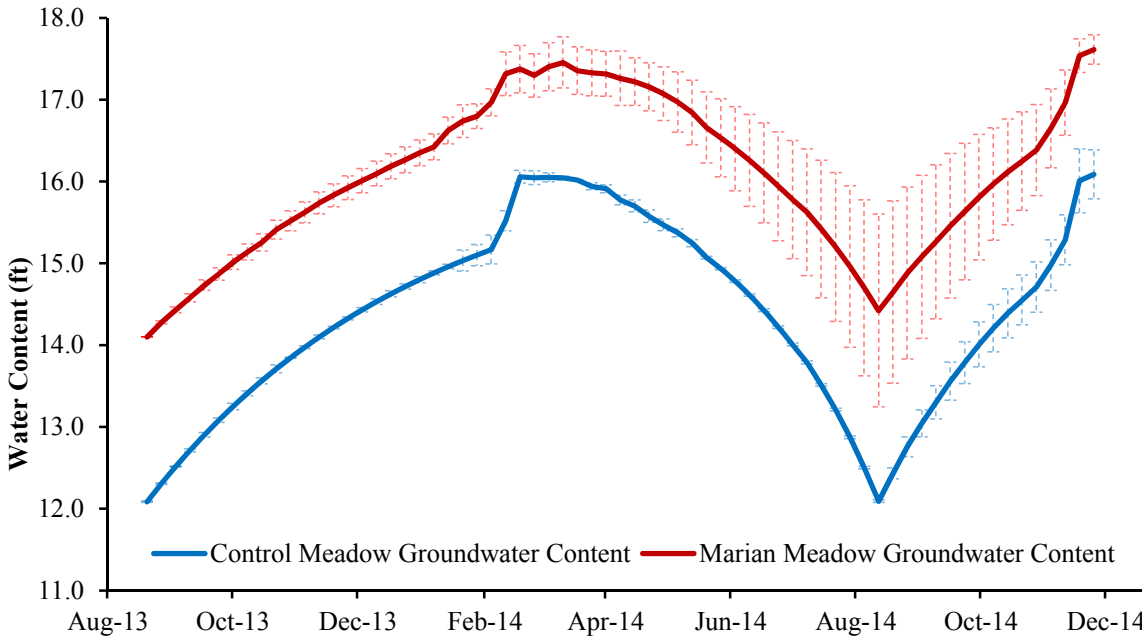

Figure 4.6 Comparison of the quantity of water stored as groundwater between the reference datum and the potentiometric groundwater surface on Control Meadow and Marian Meadow

4.4.2 Soil Moisture Comparison Figures

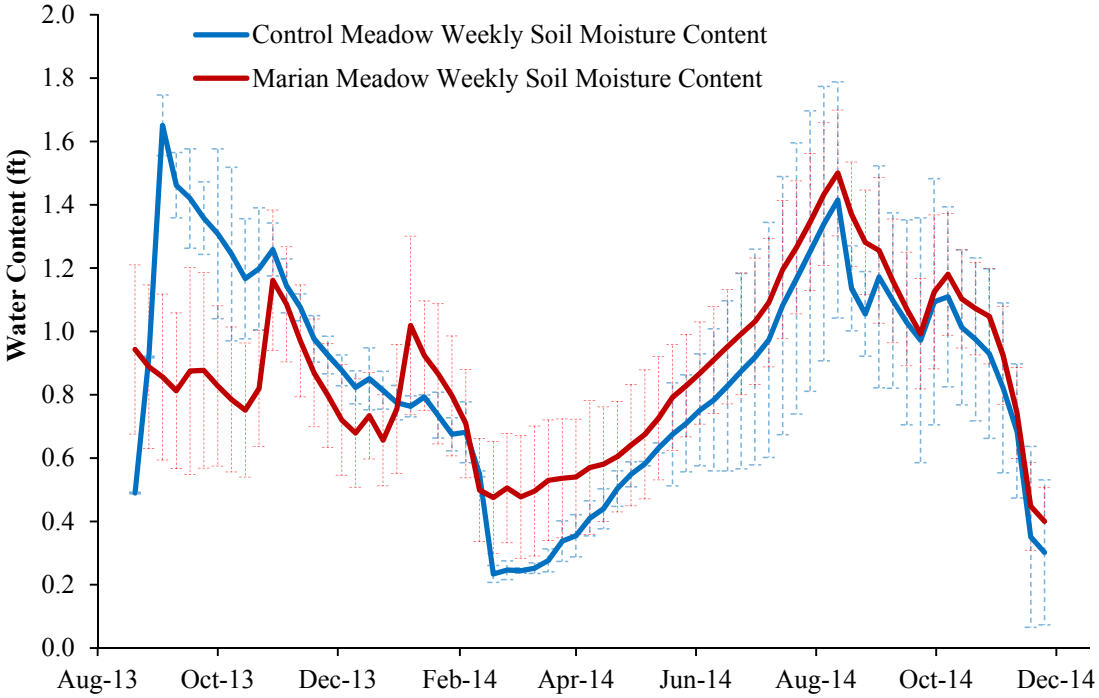

Figure 4.7 Comparison of the average weekly quantity of water stored as soil moisture below Control Meadow and Marian Meadow

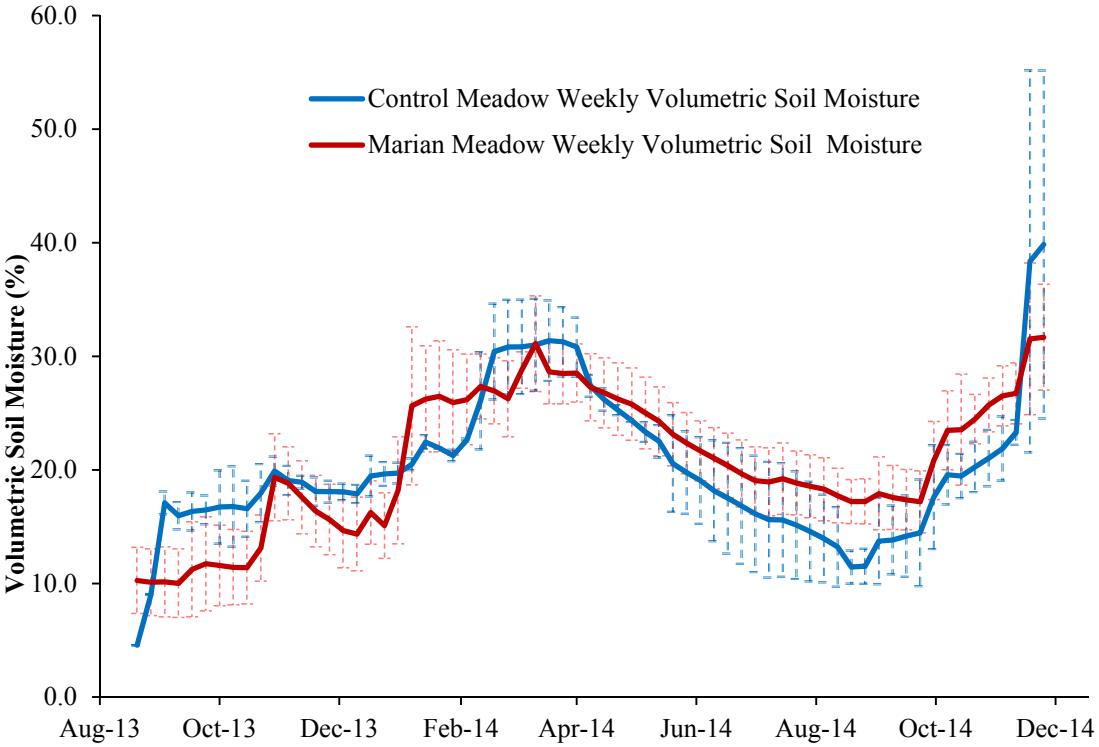

Figure 4.8 Average weekly quantity of water stored as soil moisture on Control Meadow and Marian Meadow

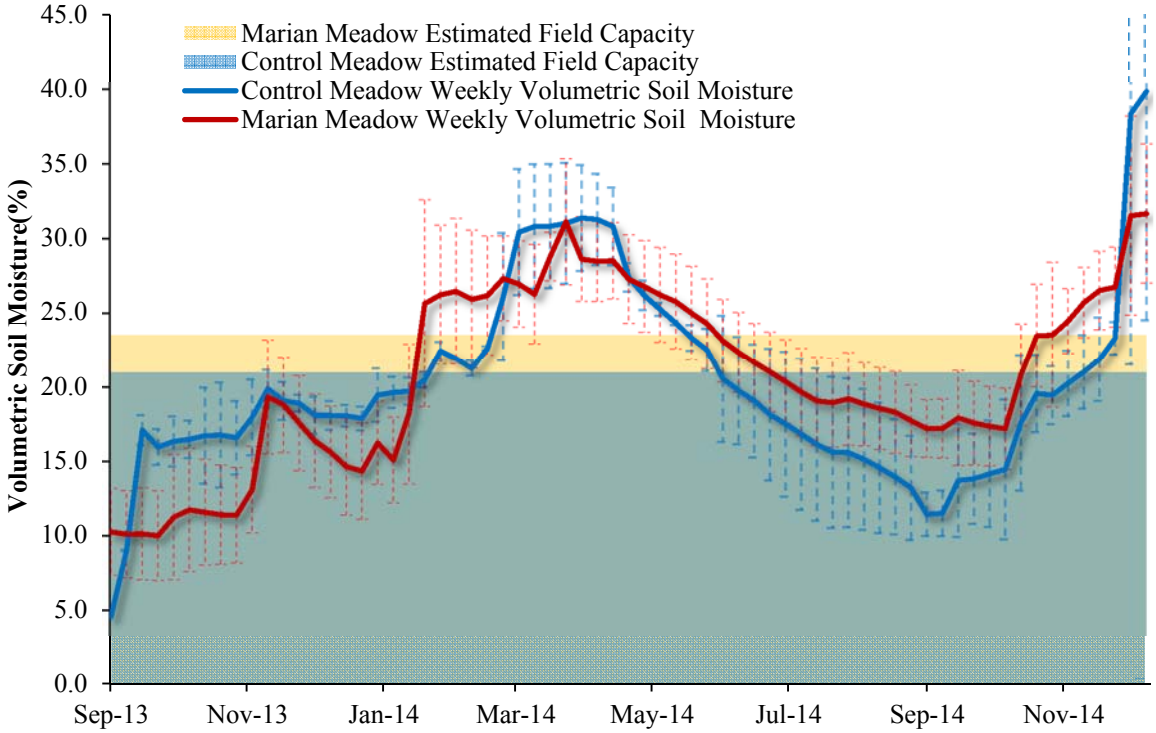

Figure 4.9 Average weekly volumetric soil moisture compared to the estimated field capacity of soil on Control Meadow and Marian Meadow

4.4.3 Hydrologic Response to Precipitation Inputs

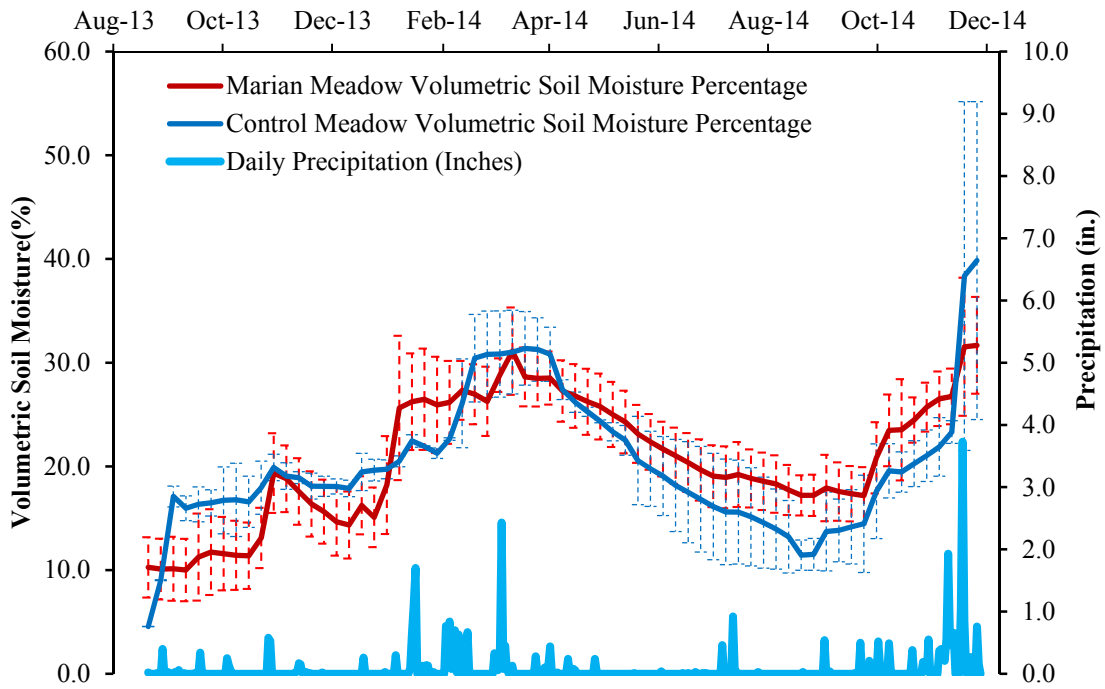

Figure 4.10 Average weekly depth to groundwater compared to daily precipitation on both meadows

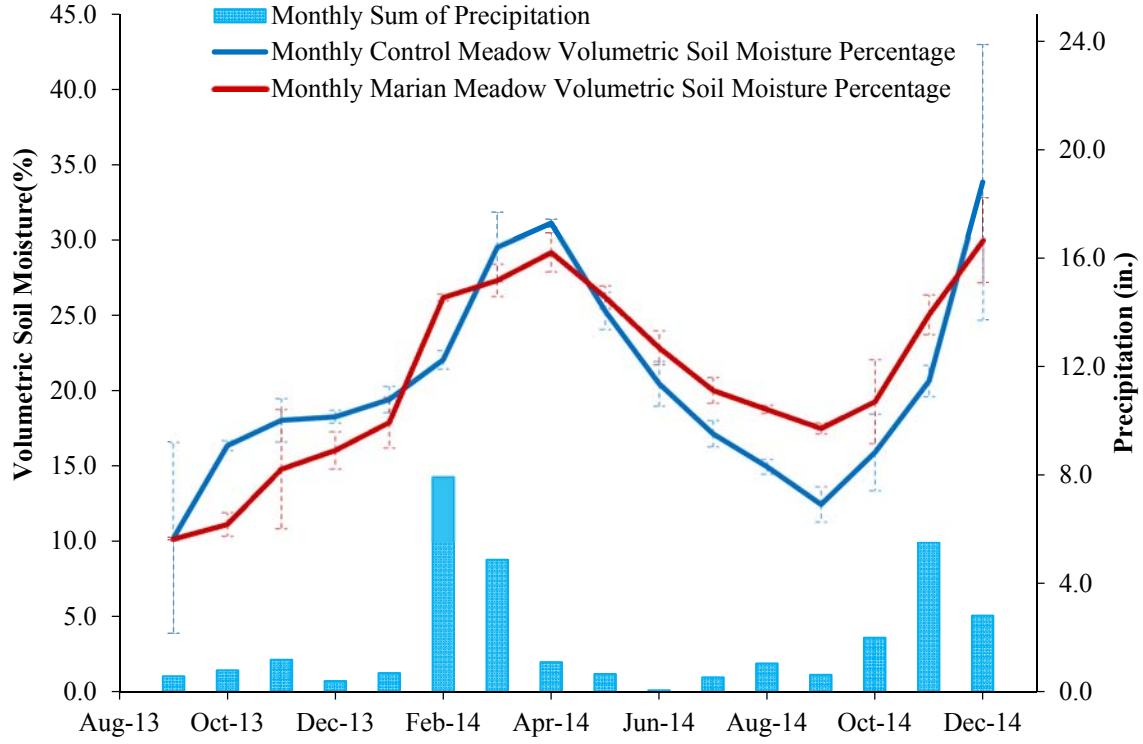

Figure 4.11 Average monthly volumetric soil moisture on both meadows compared to monthly precipitation

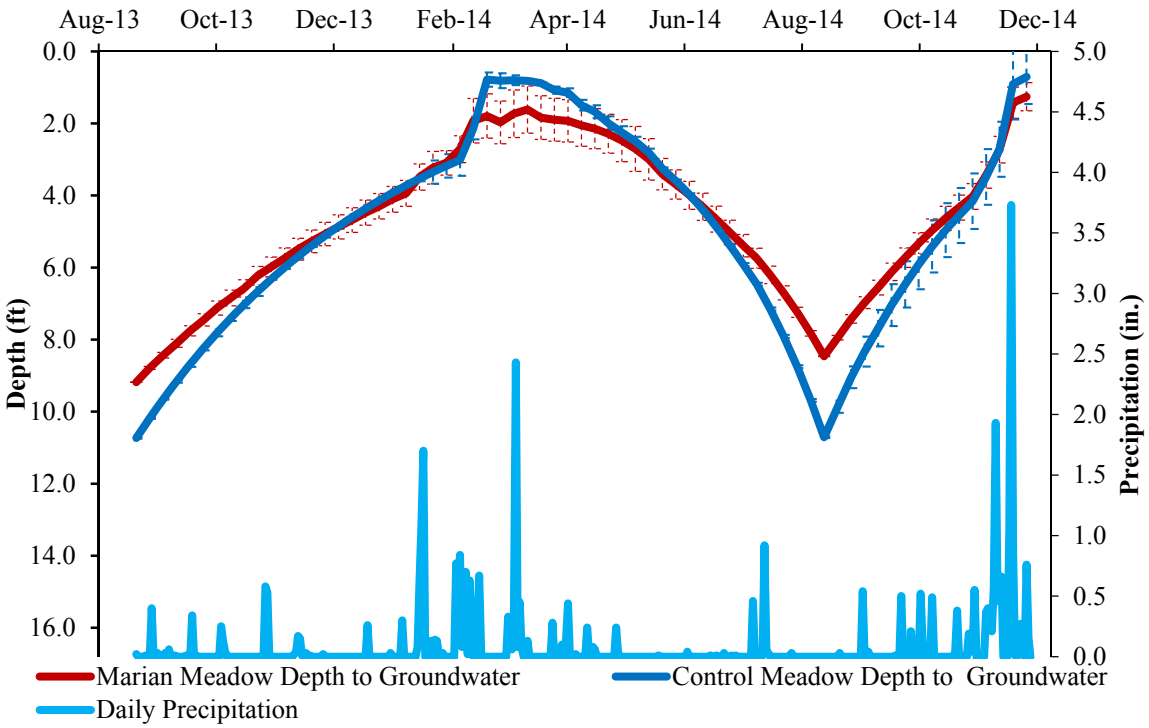

Figure 4.12 Comparison of average weekly groundwater depth on both meadows compared with daily precipitation totals

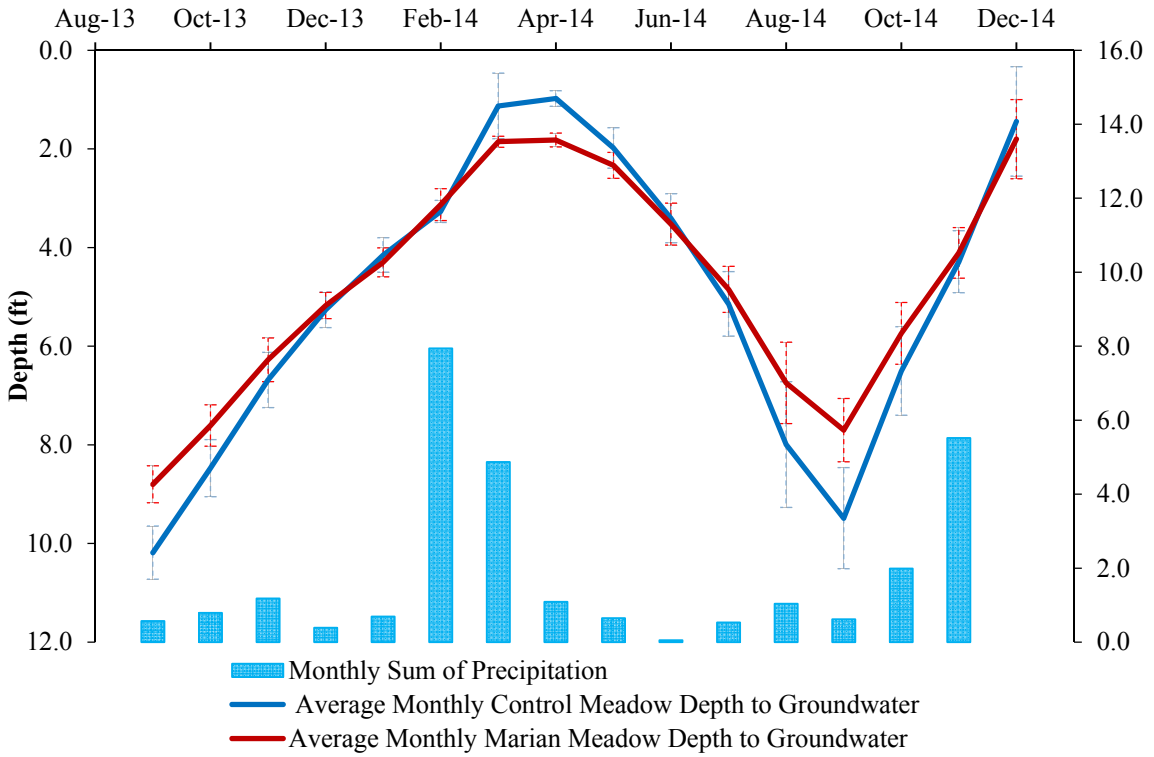

Figure 4.13 Comparison of average monthly groundwater depth on both meadows compared with monthly precipitation totals

4.4.4 Total Water Comparison Figures

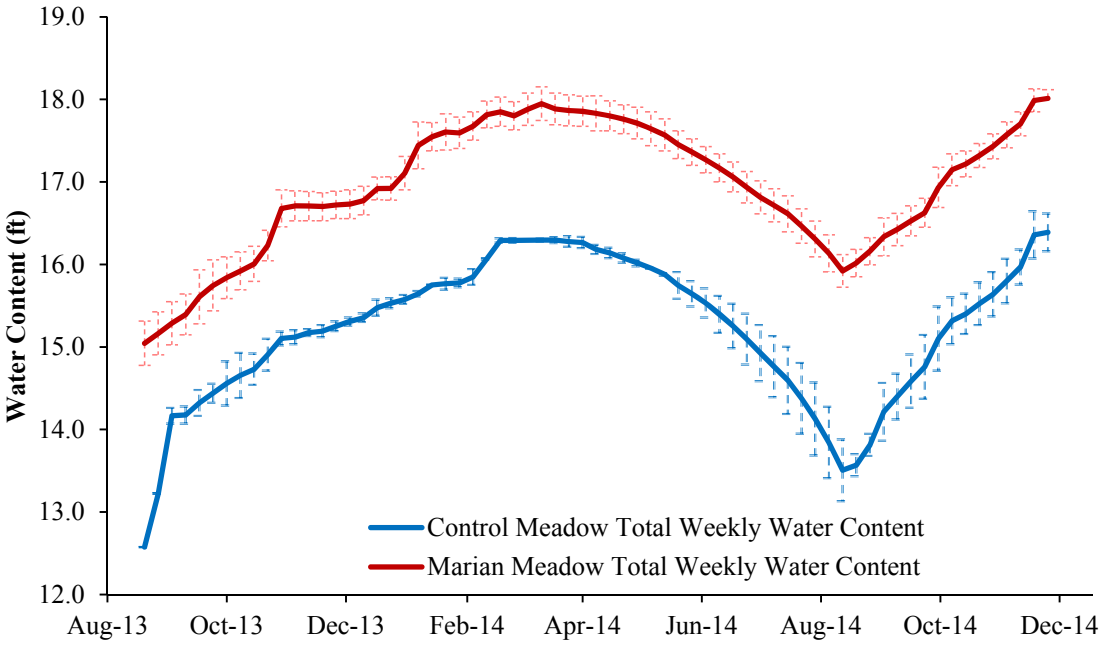

Figure 4.14 Comparison of total average weekly water content on Marian Meadow and Control Meadow

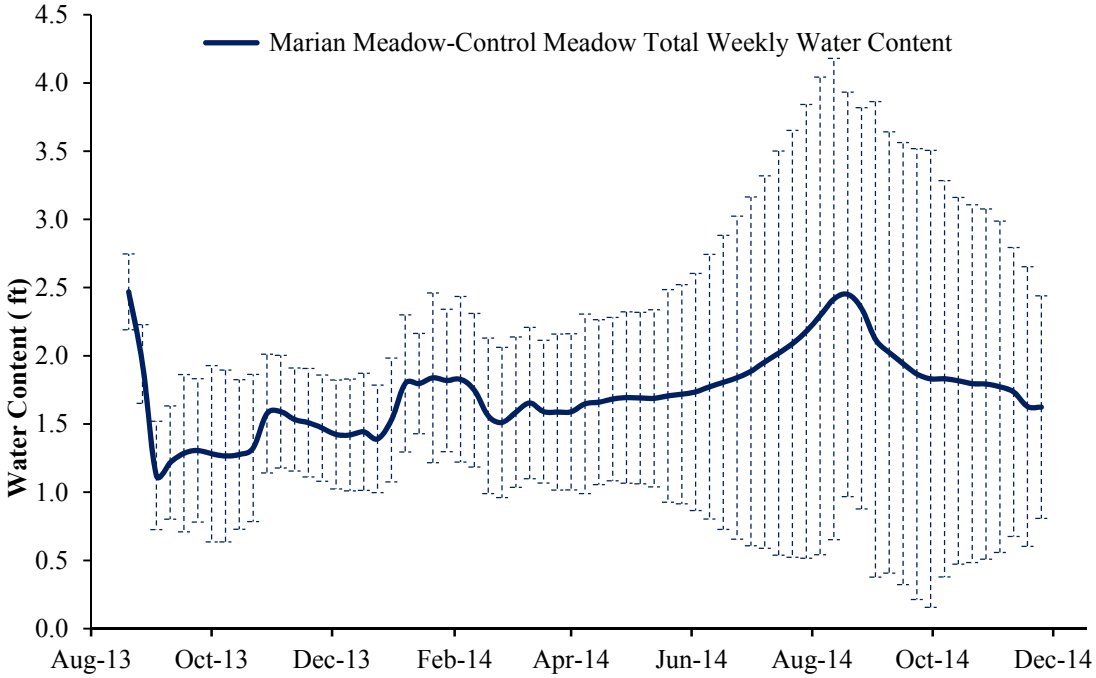

Figure 4.15 The difference between the total water content on Marian Meadow and the Control Meadow

4.4.5 Monthly Comparison Figures

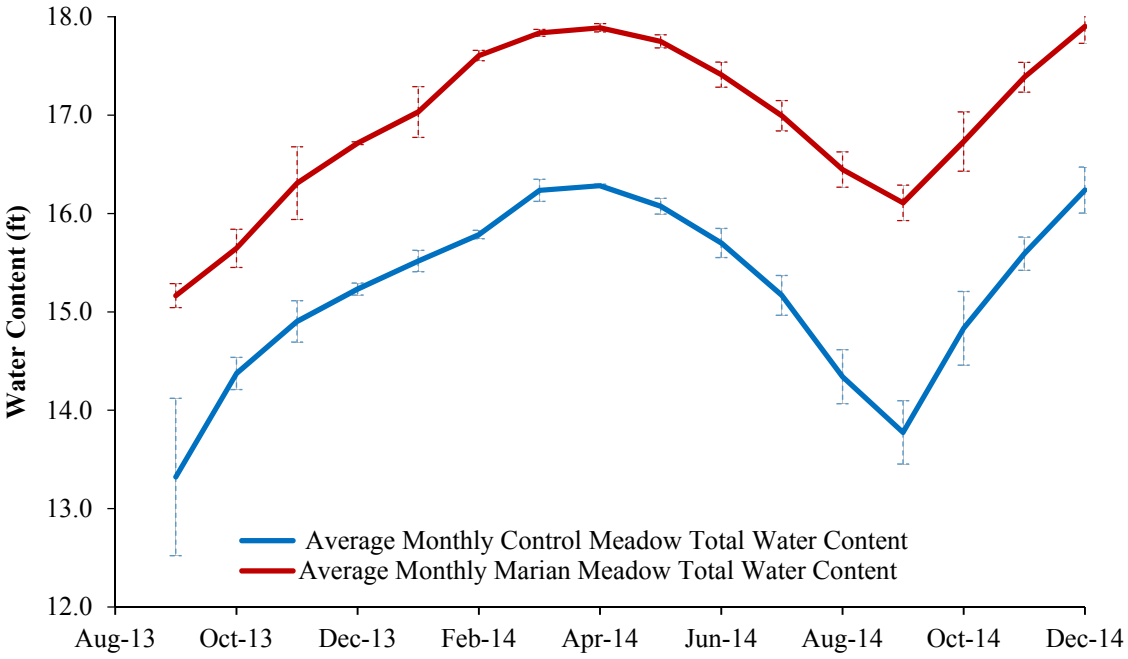

Figure 4.16 Average monthly quantity of water on Marian Meadow and the Control Meadow

4.5 Priestley Taylor Evapotranspiration, Temperature, and Precipitation

The average mean daily air temperature of nearby Chester, California during the analysis period and first year of study was 49.10 °F (9.47 °C) and 49.53 °F (9.74 °C) respectively (Fig 4.17). In the two months preceding initial data collection in 2013, 0.11 inches (3 mm) of precipitation was measured in Chester, California (CDEC, 2013). The total precipitation during the analysis period and first year of study was 36.34 in. (0.92 m) and 19.85 in. (0.50 m) respectively. The precipitation measured during the 2014 water year (September 30th –October 1st) was 19.85 in. (0.5 m), constituting approximately 60% of the historical average annual precipitation measured in the region encompassing the study site (CCSS, 2002 and Skinner and Taylor, 2004). Snow course and snow water content data were not readily available adjacent to the study area. Consequently, the effect that snow and snowmelt had on the MM and CM water balance analysis could not considered.

The sum of the PT actual evapotranspiration (AET) over the analysis period on CM was 4.34±1.10 ft (1.32±0.34 m). The sum of the PT AET on MM during this period was 4.33±1.10 ft (1.31±0.34 m). The only difference in the determination of the AET on MM and CM was the elevation component in the equations used to calculate the psychrometric constant and atmospheric pressure (see Equation 23 and Equation 25). For the purposes of this thesis, the ET from MM and CM will be considered to be the same. The AET during the first year of study was 3.93±1.00 ft (1.20±0.30 m). During, the first year of study 73.3% of the total AET occurred from April 1st –September 1st (Fig 4.18). The average net daily radiation input into the PT model during this period was $12.84\frac{\mathrm{mJ}}{(\mathrm{day})\mathrm{m}^2}$. The average daily net radiation over the first year of study was $7.77\frac{\mathrm{mJ}}{(\mathrm{day})\mathrm{m}^2}$.

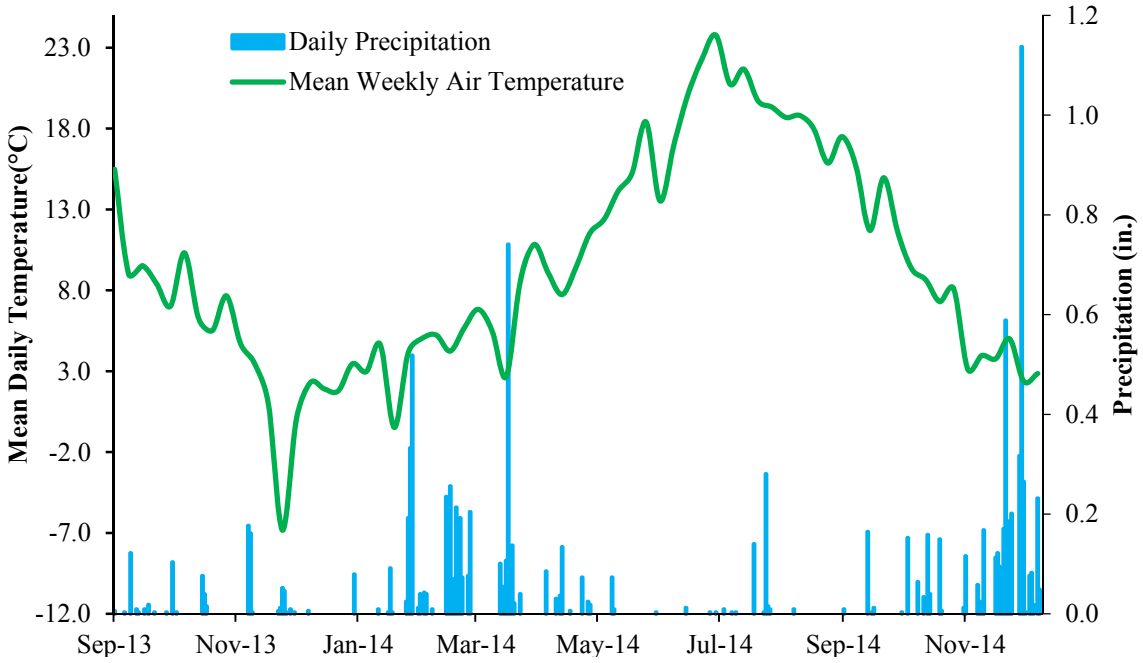

Figure 4.17 Daily precipitation and daily mean air temperature measured in and near Chester California

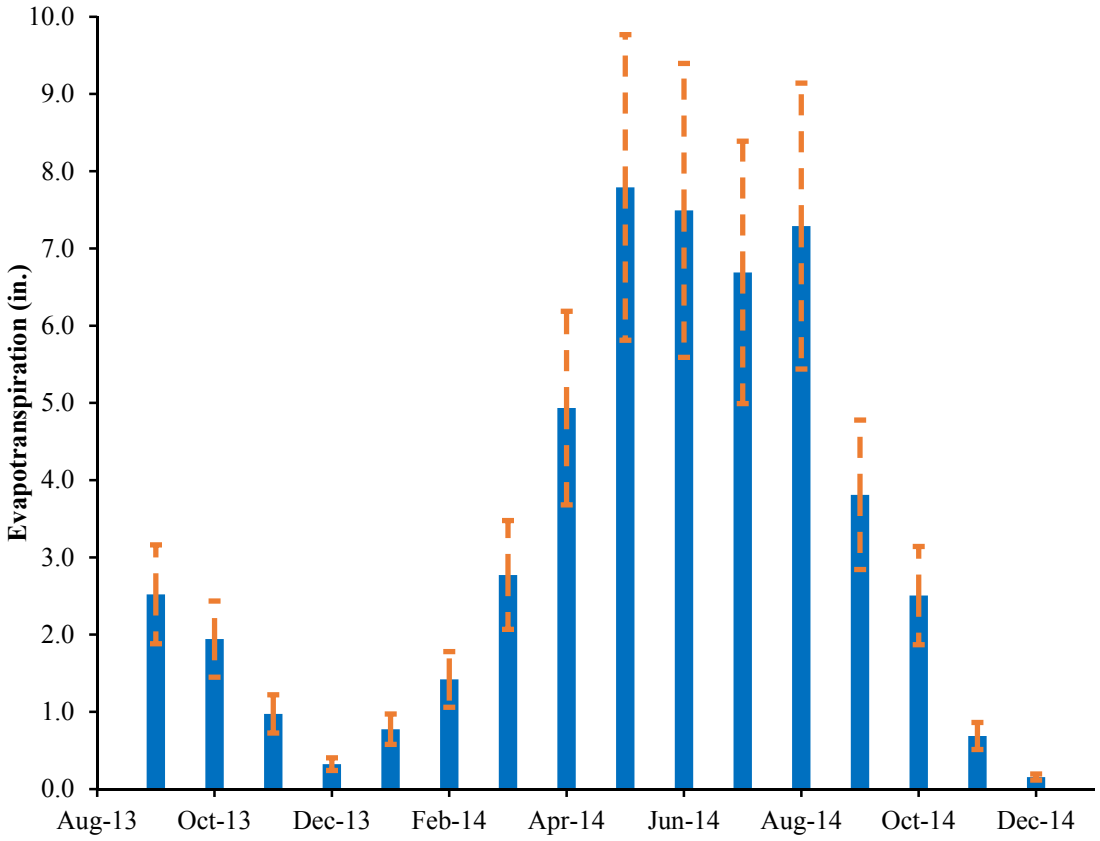

Figure 4.18 Monthly evapotranspiration (PT AET) from Marian Meadow

4.6 Water Budget

Relative to the reference datum, water stored as groundwater comprised an average of 94.4% of the total water stored on CM and an average of 94.8% of the total water stored on MM. The average weekly change in groundwater storage was approximately twice the average weekly change in soil moisture storage on both CM and MM: 0.18 vs 0.09 ft (0.06 vs 0.03 m) and 0.14 vs 0.07 ft (0.04 vs 0.02 m) respectively. During periods of low ET, weekly changes in groundwater recharge had the greatest influence on the balance of hydrologic inputs and outputs on both CM and MM. Due to the design of the water budget analysis; there is a direct inverse relationship between water stored as soil moisture and volumetric soil moisture (Fig 4.19). Similarly, as the depth to groundwater decreases, groundwater content increases because more water is stored within the zone of saturation. This relationship occurs because increases in volumetric soil moisture are simultaneously associated with precipitation inputs that raise the water table.

On MM and CM hydrologic outputs exceeded hydrologic inputs by 1.31 ft (0.40 m) and 1.28 ft (0.39 m) respectively during the first year of study (Table 4.1). On MM hydrologic inputs exceeded inputs from September 2013-March 2014 and September 2014–December 2014. Relative to the reference datum, MM contained at least 1.0 ft (0.3 m) more of water during the entire analysis period (Fig 4.14 and 4.15). The only time period when the equivalent depth of water stored as soil moisture on CM and MM ranged more than 0.3 ft (0.1 m) from the latter was a two month period between September - November 2013. The values recorded during this period may have been caused by an anomaly associated with the installation of the soil moisture probes (see Section 4.3.2).

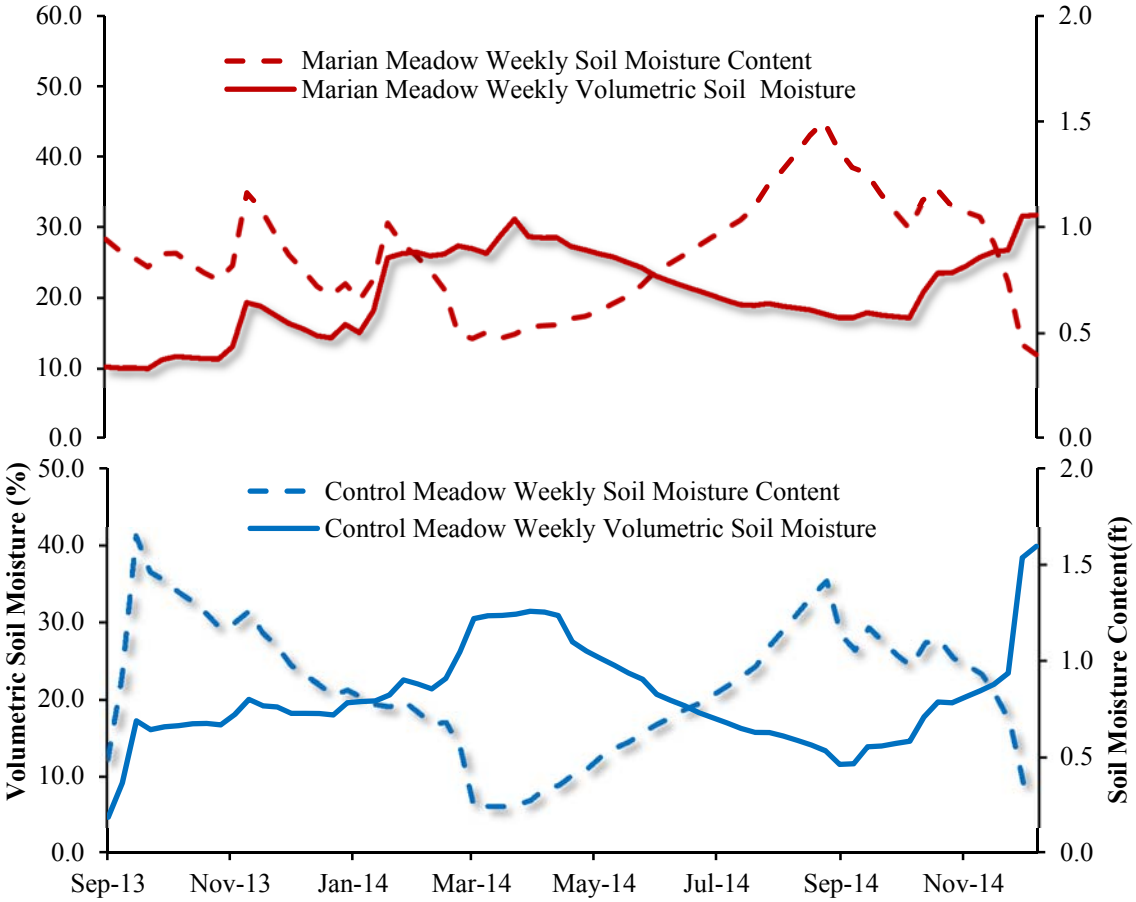

Figure 4.19 Comparison of volumetric soil moisture and the quantity of water stored as soil moisture on the Control Meadow

Table 4.1 Summary of the compiled hydrologic outputs and inputs on the Control Meadow and Marian Meadow during the analysis period and first year of study.

Control Meadow		
Hydrolgic Inputs - Ouputs (ft)	**9/13/2013-9/14/2014**	**9/13/2013-12/21/2014**
Groundwater Storage	0.35	4.00
Priestley AET	-3.93	-4.33
Soil Moisture Storage	0.65	-0.19
Precipitation	1.65	3.03
Total Inputs - Outputs	-1.28	2.60
Marian Meadow		
Hydrolgic Inputs - Ouputs (ft)	**9/13/2013-9/14/2014**	**9/13/2013-12/21/2014**
Groundwater Storage	0.55	3.51
Priestley AET	-3.93	-4.34
Soil Moisture Storage	0.43	-0.54
Precipitation	1.65	3.03
Total Inputs - Outputs	-1.31	1.66

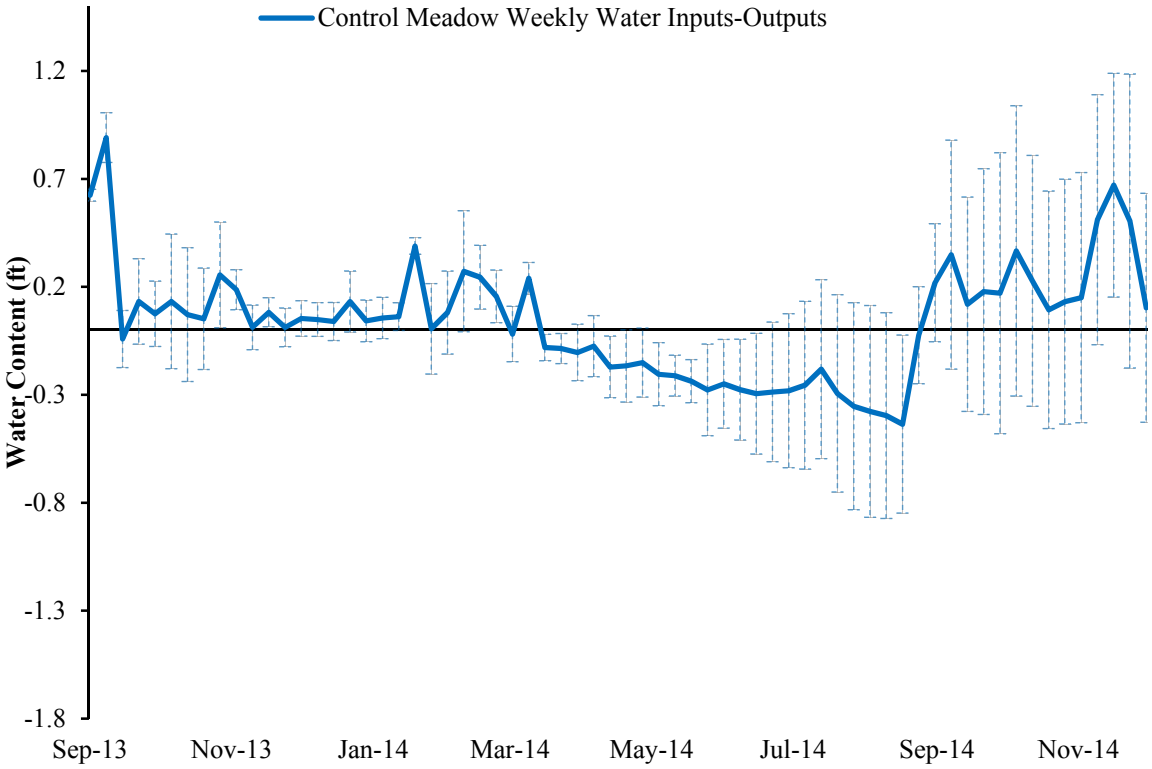

Figure 4.20 The weekly water balance of the Control Meadow

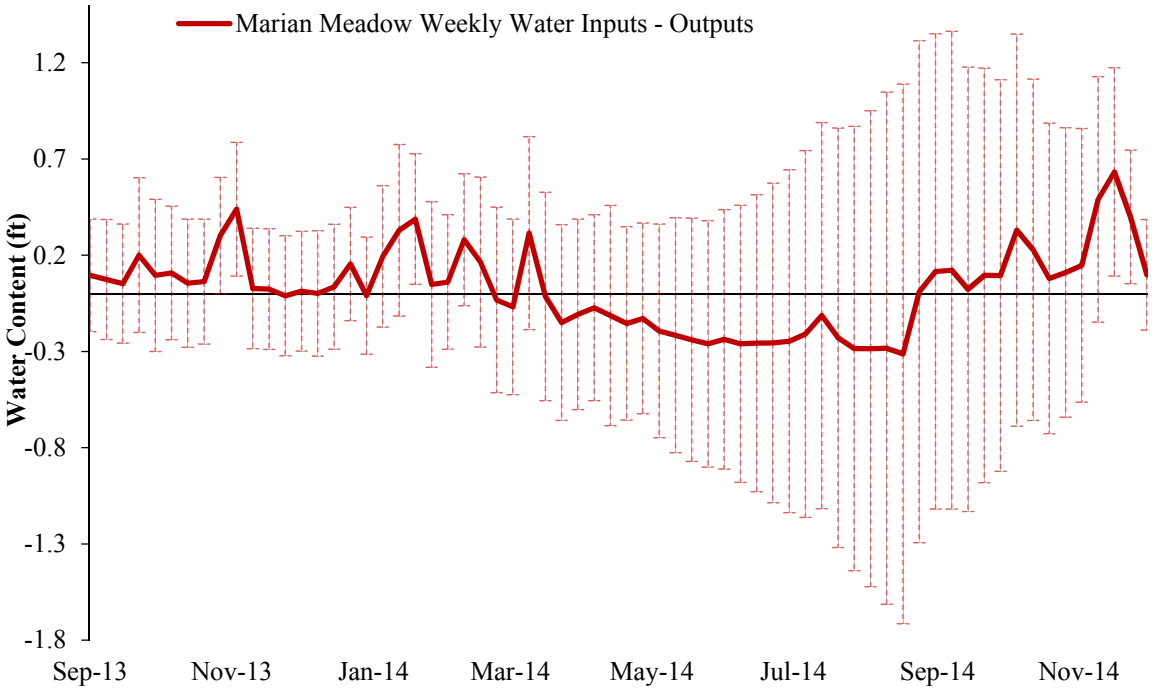

Figure 4.21 The weekly water balance of Marian Meadow

4.7 Electrical Resistivity

The subsurface electrical resistivity below CM was generally higher and had a wider range compared to the subsurface resistivity below MM. On MM, during periods of maximum groundwater depth below the ground surface, 4 ‘zones’ of electrical resistivity were correlated with corresponding subsurface hydrologic zones (Table 4.2). A similar categorization was developed for CM, but no base of the aquifer could be determined using electrical resistivity (Table 4.3). The average resistivity within what was considered the middle of the saturated zone below CM and MM was about 140-160Ω · m and 30- 45Ω · m respectively. The electrical resistivity of the near surface on CM was often high (>1000 Ω · m). The electrical resistivity below the ecotone boundary on CM had an even higher range of values (1000-3000Ω · m). The electrical resistivity of soil below areas of CM farther from the ecotone boundary ranged from 300-1400Ω · m (Fig 4.22). On MM, a range of depths to the base of the aquifer were inferred from surveys taken on varying dates and locations. The minimum depth to the base of the aquifer below MM, inferred from ERT on the Lower MM Transect was chosen to represent the depth to base of the aquifer across all of MM. This resulted in a degree of uncertainty concerning where the true transition from the aquifer to an impermeable layer occurred actually occurred. However, it should be expected that geologic units will not have a consistent bedding or depth of occurrence in the subsurface over a large spatial extent. For the purposes of this water budget, these distinctions are not important because the changes in hydrologic inputs and outputs occur far above the reference datum.

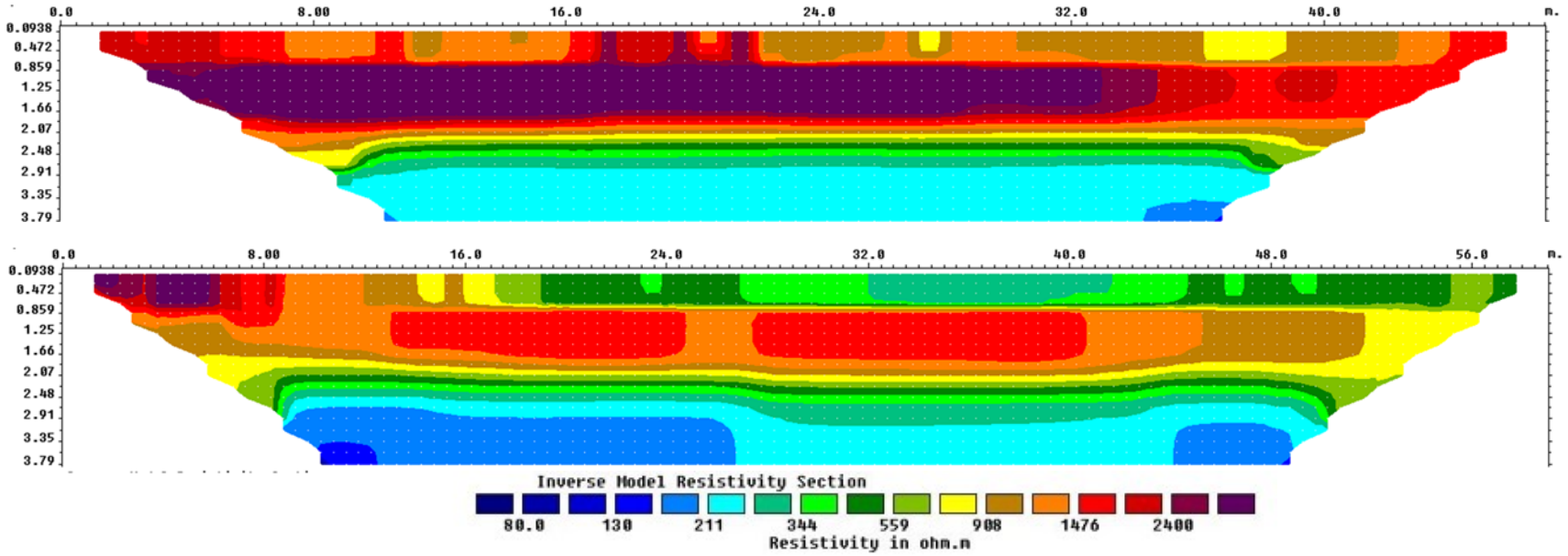

Figure 4.22 Resistivity survey performed on the Control Meadow ecotone boundary during September 2014 and May 2014 respectively Top: (Abs error = 1.94%) Bottom: (Abs Error 1.60 %)

Table 4.2 The resistivity of the hydrologic zones below Control Meadow on September 6 2014

Control Meadow*	
Zone	**9/6/2014**
Near Surface (0-2 ft)	2000Ω•m
Vadose Zone(2 -10 ft)	350-1200 Ω•m
Saturated Zone	80-200 Ω•m
*= does not include ecotone boundary	

Table 4.3 The resistivity of hydrologic zones in Marian Meadow's subsurface measured during September 2013 and September 2014

Marian Meadow		
Zone	**9/10/2013**	**9/7/2014**
Near Surface (0-2 ft)	180-650 Ω•m	130-650 Ω•m
Vadose Zone (2 - 8 ft)	160-350 Ω•m	120-500 Ω•m
Saturated Zone (8-48 ft)	26-70 Ω•m	23-55 Ω•m
Lower Confing Layer (48 ft)	120-240 Ω•m	140-220 Ω•m

4.8 IRIS Tubes

IRIS tubes installed on the MM did not show significant signs of reduction (more than 5% reduction) during any of the periods they were installed. In order for a definite sign of reduction to be present, three of the five tubes must possess 25-30% reduction (see Section 2.6). On CM, IRIS tubes installed from 6/13/15 to 12/21/14 did show minor signs of reduction, but were not formally analyzed because three of the five tubes did not possess a significant indication of reduction. Unless a very high percentage of reduction has occurred, reduction generally appears as splotches rather than total paint removal (which is generally caused by abrasion). Some removal of paint on IRIS tubes deployed in this study was caused by abrasion from installing and removing the tubes in the soil. The loss of paint to abrasion on some tubes may have disguised indicators of reduction. The lack of reduction observed on IRIS tubes is still significant because the incidence of

hydric soil conditions following conifer removal from MM may be indicative of progress towards restoration. However, given the observation of near surface groundwater on CM, and a subsequent lack of reduction on installed IRIS tubes, it seems unlikely that IRIS tubes will indicate the presence of hydric soils on MM following conifer removal. However, the presence of a different soil type on MM may facilitate conditions more favorable to the development of hydric soils if near surface groundwater occurs following conifer removal.

Figure 4.23 One of the IRIS tube sets installed on CM from 6/13/15-12/21/14

CHAPTER 5 DISCUSSION

5.1 Discussion Overview

This discussion will address the individual components of the water budget analysis, the possible sources of uncertainty stemming from the methodology implemented to quantify these parameters and the implications of the data collected prior to conifer removal from MM. In a water budget, uncertainty may come from a variety of sources: omission of data, measurement errors stemming from both the instrument or improper instrument calibration, and the spatial extrapolation of point measurements of parameters such as precipitation (Sloto and Baxton, 2005). In this study, errors of a non-systemic nature such as the loss of individual soil moisture probes or groundwater wells to instrument malfunction played a significant role in adding uncertainty to the water balance. On CM, the loss of soil moisture probes dramatically reduced the number of probes available for an arithmetic average of volumetric soil moisture and soil moisture storage, even following installation of additional soil moisture probes. Other uncertainties in this water balance approach may be inherent to methodology used to quantify its parameters to the extent that any assumptions used to quantify these parameters were unwarranted.

5.2 Water Budget Approach Evaluation

5.2.1 Evapotranspiration

The ET component of the water budget analysis exceeded measured precipitation totals by 2.26 ft (0.69 m) during the analysis period and by 1.30 ft (0.40 m) during the first year of study. In this study, a significant source of error in modeled AET may stem

from dependence on climate data collected by weather stations located several miles from the study area. The calculated PT AET is particularly sensitive to the R_n (net radiation) and α (the PT coefficient) terms. Net radiation primarily controls ET rates because it provides the primary source of the energy needed to vaporize water. In order to rectify uncertainty associated with dependence on climate data collected off-site, a weather station was installed near CM during the spring of 2015. However, the weather station will not rectify any error within the water balance associated with uneven precipitation distribution or net radiation between CM and MM.

The application of a fixed PT coefficient developed from studies of ET from temperate coniferous forests to both meadows adds uncertainty to the water balance. CM is bounded by coniferous forest, but has minimal tree cover within its defined boundaries. Consequently, its low density of plant biomass and minimal canopy cover should lower transpiration rates, but increase evaporation rates. An appropriate fixed PT coefficient for cleared sites in temperate coniferous forests was not observed in the literature reviewed as part of this thesis. The fixed PT coefficient used in the PT equation thus far may also not be appropriate for MM following conifer removal. The physical characteristics of soils directly affect their heat capacity and albedo, which in in turn influence evaporation rates. The faster drainage of plant available water from the near surface of CM (due to its higher sand content, see Appendix E) would theoretically reduce the quantity of surface moisture that could be evaporated compared to MM. The disparities in soil composition between the two meadows should therefore also play a role in increasing the disparity between the ET rates of both meadows.

An alternative method to quantify ET, such as the physical measurement of ET using the eddy covariance method should be considered. This alternative method would allow ET rates to conform to post conifer removal soil moisture and canopy cover on MM. Alternately, a comprehensive analysis of previous research may yield an appropriate fixed PT coefficient for cleared forest sites in the study region. The continued use of a fixed PT coefficient to quantify ET in this study will rely on the assumption that ET rates are unaffected by conifer removal, which runs counter to the studies hypothesis that conifer removal will re-distribute transpired water to subsurface storage. Studies directly addressing ET from forest clearcuts in the study region suggest that the PT coefficient should be modified from a fixed value when soil water content falls below a critical value (Flint and Childs, 1987 and Flint and Childs 1991). Specifically, these studies on small forest clearcuts in the Sierra Nevada Mountains indicated that near surface volumetric soil moisture on small clearcuts does not act as a limiting factor on ET until volumetric soil moisture has decreased below approximately 14.00%. If CM and post-removal MM behave similarly in terms of hydrology, ET may only be limited by low soil water in the near surface during a few months of the year (see Fig 4.8-4.10).

Modifications to the original PT coefficient(α=1.26) that account for leaf area index (LAI) and the ratio of measured volumetric soil moisture to volumetric soil moisture at field capacity were initially considered to account for the hydrologic and vegetative differences between CM and MM (Sumner and Jacobs, 2005 and Fisher et al., 2005). These modifications to the PT model were not implemented in this study because of a lack of sufficient data pertaining to these parameters. A rigorous determination of the field capacity of soil on both meadows would enable the use of a modified PT model that

accounts for weekly soil moisture to quantify ET. An evaluation of the water balance approach applied in this study in terms of how closely weekly or monthly inputs matched outputs is discouraged. On a weekly basis, precipitation will rarely match ET. It should also be noted that groundwater inflow will affect ET rates, thus, facilitating a scenario where more ET than precipitation occurs in some regions within a watershed. This is especially true in watersheds that occur in Mediterranean climates because periods of high precipitation generally occur during the winter and spring months when solar radiation is at a minimum. On CM, surface groundwater or near surface groundwater was only measured during periods of the year when net radiation was relatively low ($<3.0\frac{\mathrm{mJ}}{(\mathrm{day})\mathrm{m}^2}$). It is therefore unlikely that the presence of a freely evaporating surface during this time would dramatically increase daily ET.

5.2.2 Soil Moisture

A number of uncertainties exist concerning the determination of the weekly quantity of water stored as soil moisture on both meadows. The determination of weekly volumetric soil moisture relied on the assumption that the quantity of soil moisture stored at a 1.0 ft (0.3 m) depth constituted the average quantity of water stored throughout the portion of the soil column above the water table at any given time. The calculation of volumetric soil moisture at each site relied on an average of bulk density collected at three separate locations (see Section 3.4). In the future, measuring the bulk density of soil near each soil moisture probe may improve the accuracy of individual volumetric soil moisture calculations (see Equation 7). Average weekly measurements of soil moisture made on CM prior to the installation of additional soil moisture probes on the lower portion of CM are biased towards the drier portion of CM. For example, the average

volumetric soil moisture measured on lines C-1 and C-2 following additional instrumentation from 6/13/14-12/21/14 was 16.29%. The average volumetric soil moisture measured of lines C-3 and C-4 during this period was 20.57%. A more representative average of soil moisture for CM prior to June 2014 may have significantly altered the character of CM's weekly water balance prior to the installation of additional soil moisture probes.

5.2.3 Groundwater Recharge

In a similar future study, the use of deeper groundwater wells may decrease the ambiguity associated with groundwater recharge following large precipitation events. A dataset that quantifies a larger distribution of points between groundwater depths inferred from ERT may improve the performance of each recession curve analysis in terms of accurately modeling recharge. The recession curve analysis assumes an exponential relationship between groundwater recharge and precipitation. In reality, the rate of inflow into an aquifer is controlled by a number of factors: the vertical hydraulic conductivity of the vadose zone, the thickness of the aquifer, the potentiometric gradient of the saturated area and the transmissivity of the saturated area. The recession curve analysis used in this study also assumes that the maximum depths to groundwater occurred during the survey dates conducted during September 2013 and 2014. There is uncertainty concerning how well this assumption conforms to the actual date of maximum groundwater depth. However, this assumption may be justified by comparing the surveys dates to antecedent precipitation (see Appendix G). In the two months prior to September 2013, 0.11 in. of precipitation occurred. In the two months prior to September 2014, about 1.5 in. of precipitation occurred, but only 0.03 in. of precipitation was measured during the month

of August in 2014. Precipitation events began to occur with increased frequency shortly after the resistivity surveys conducted in September 2013 and 2014. Therefore, if groundwater recharge is primarily precipitation driven, the assumption of maximum groundwater depth in September 2013 and 2014 is reasonable.

The assumption of uniform bulk density and porosity within the extent of the saturated zone also caused uncertainty because it is known that compaction from lithostatic pressure affects these parameters at depth. In some groundwater wells, significant discrepancies between depths to groundwater measured by water level loggers and by a well sounder were observed (Tables 5.1-5.3). Currently, the source of these discrepancies is ambiguous because the well sounder used in the field was observed to have difficulty measuring groundwater within wells on several occasions due to issues with its battery. In a few blank wells on both meadows, during a period of near surface groundwater in December 2014, the well sounder did not detect any groundwater. This suggests that water may have had difficulty entering these wells.

Table 5.1 Comparison of measured groundwater depths and groundwater depths measured by water level loggers on Marian Meadow (9/7/14)

Site	Well Sounder Measurement (ft)	Groundwater Well Measurement (ft)
3-1	0.68	1.04
3-2	1.25	x
3-4	0.00	0.69
4-1	0.47	1.27
4-2	2.77	x
6-3	0.94	1.64
6-4	0.86	1.00
9-2	x	1.77
9-3	0.15	1.00
Averages	0.89±0.87	1.20±0.39

Table 5.2 Comparison of measured groundwater depths to groundwater depths measured by water level loggers on Marian Meadow (5/3/14)

Site	Well Sounder Measurement (ft.)	Groundwater Well Measurement (ft.)
3-1	3.56	3.10
3-2	2.03	x
3-4	1.55	1.29
4-1	2.11	1.94
4-2	3.74	x
4-3	3.62	x
6-1	3.54	x
6-2	3.15	x
6-3	3.74	3.55
6-4	2.66	1.75
9-2	3.86	2.49
9-3	1.97	1.83
9-4	2.37	x
Averages	2.91±0.83	2.28±0.75

Table 5.3 Comparison of measured groundwater depths with groundwater depths measured by water level loggers on the Control Meadow (5/3/14)

Site	Well Sounder Measurement (ft.)	Groundwater Well Measurement (ft.)
C1-2	1.12	1.43
C1-3	1.44	1.54
C2-2	1.43	x
C2-3	0.79	x
C2-4	2.13	x
Averages	1.38±0.49	1.48±0.08

5.3 Electrical Resistivity

Using electrical resistivity and its known relation to soil composition and water content, a strong inference could be made in regards to the presence of conifers and soil moisture. On CM, the region of the subsurface that was influenced by the presence of conifers in terms of soil moisture ranged from approximately 2-7.2 ft (0.6-2.2 m) below the ground surface. On 9/6/14, in the aforementioned region below the CM ecotone boundary, a higher resistivity in the first two-thirds (0-36 m) (2600Ω · m) of the ecotone

boundary cross section (starting from eastern edge) was observed relative the last one-third (36-54 m) (1600Ω · m).The resistivity below the ecotone was also higher than resistivity measured in this region elsewhere on CM. However, below approximately 7.2 ft (2.2 m), the presence of conifers did not seem to have a significant effect on the measure of the electrical resistivity of the subsurface. The electrical resistivity below this zone was relatively uniform across CM during surveys conducted on 9/6/14. A comparison between the electrical resistivity from 2-7.2 ft (0.6-2.2 m) below the ecotone on 5/5/2014 and elsewhere on CM could not be done because no other surveys were conducted on CM during this time. However, the same relationship of lower resistivity values seen near the edge of the ecotone boundary was observed. In this case the resistivity of the last one-third was about 600 Ω · m lower than the first two-thirds of the cross section.

Although the highest electrical resistivity on MM was measured in the first few meters of soil below the ground surface on all surveys, the effect that conifers had on the resistivity of the first 7.2 ft (2.2 m) of soil was not easily distinguished. On both meadows, the relationship between electrical resistivity and soil moisture in the first 2 ft (0.6 m) of soil below the ground surface was ambiguous. Future work to relate the electrical resistivity of the near surface to soil moisture may aid in the development of a more sophisticated model of the variation of soil moisture with depth. This work may be able directly address the validity of the assumption that soil moisture at a 1 ft (0.3 m) depth represented the average soil moisture above the water table.

Several factors may be responsible for the disparity between the electrical resistivity of the subsurface on CM and MM (see Section 4.7). Many of these factors

relate to soil moisture, as it is the primary determinant of electrical resistivity in soils. The electrical resistivity of pure clay with a saturation percentage above 10% is lower than the resistivity of pure sand with a similar saturation content (see Section 2.6). Consequently, the higher sand content of soil on CM relative to MM may be responsible for heightened electrical resistivity measured within the saturated zone below CM. On CM, the lack of conifers, contributing to over-story cover (which dissipates incoming solar radiation) may reduce soil temperature throughout the day and contribute to higher evaporation rates near the soil surface thereby increasing electrical resistivity near the ground surface.

However, even with more sophisticated resistivity data processing techniques, it may be difficult to interpret the electrical resistivity of the first few feet of soil below the ground surface of both meadows during the summer. All soils nearing a hygroscopic state (<5-10% volumetric soil moisture with little to no gravitational water) will be very high (>1000 $\Omega \cdot m$). Lastly, the layer that was interpreted as the base of the aquifer below MM is unlikely to be a bedrock contact given its low resistivity (150- 200 $\Omega \cdot m$) It is possible that a portion layer forming the base of the aquifer is actually still saturated, but has a higher resistivity due to soil compaction or a change in soil composition. Given the known geology of the region, it is likely that a bedrock contact will consist of a volcanic unit that may be fractured and porous enough to contain a large volume of water. Consequently, a bedrock contact may have a low electrical resistivity.

5.4 Restoration Implications

Although understanding the pre-encroachment conditions of an encroached meadow is important, restoration should not necessarily constitute a return to pre-

encroachment species distribution and hydrology. Any attempted restoration of a meadow must be understood within the context, of what is possible in terms of an achievable steady state given current intrinsic and extrinsic factors governing ecosystem distribution. On MM, there is a paucity of information in regards to pre-encroachment vegetation composition and hydrology. Analysis of historical imagery indicates that CM had a slightly higher concentration of trees prior to conifer removal in 2012 than the conifer density currently observed on MM (Fig 5.1). Analysis of historical imagery collected in 1993 also indicates that the density of conifers on MM has increased in the last three decades (Fig 5.2).

The restoration of a meadow may be signaled by the return of certain 'keystone' indicator species as a consequence of a change in hydrologic conditions that favors their re-establishment. Alternatively, these species may be re-introduced via re-seeding following removal of encroaching vegetation. In the case of dry and mesic meadows very few if any of the species will be species associated with riparian or wetland habitat. An understanding of the current species present on MM and CM should aid in identifying changes in species distribution following conifer removal from MM. Previous research shows that the seed banks of encroached meadows often consist primarily of ruderal and forest understory species (see Section 2.8). Following the removal of trees from MM, previous research concerning this region strongly indicates that continued removal of conifer seedlings and ruderal species is required to preserve any resulting hydrologic response to vegetation removal (see Section 2.8). In theory, if conifer seedlings and other vegetation not targeted for restoration are continually removed immediately following removal of conifers, the influx of meadow species along with an increased incidence of

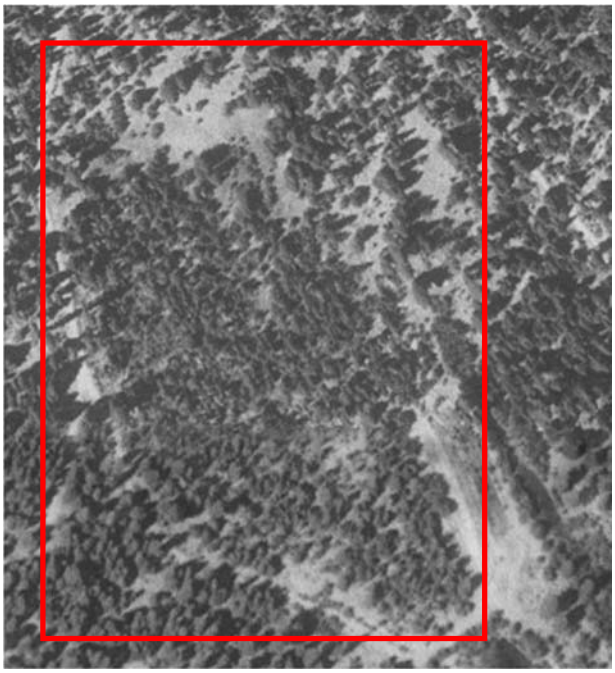

Figure 5.1 Control Meadow prior to conifer removal in 2012 (historic imagery from Google Earth (7/1993))

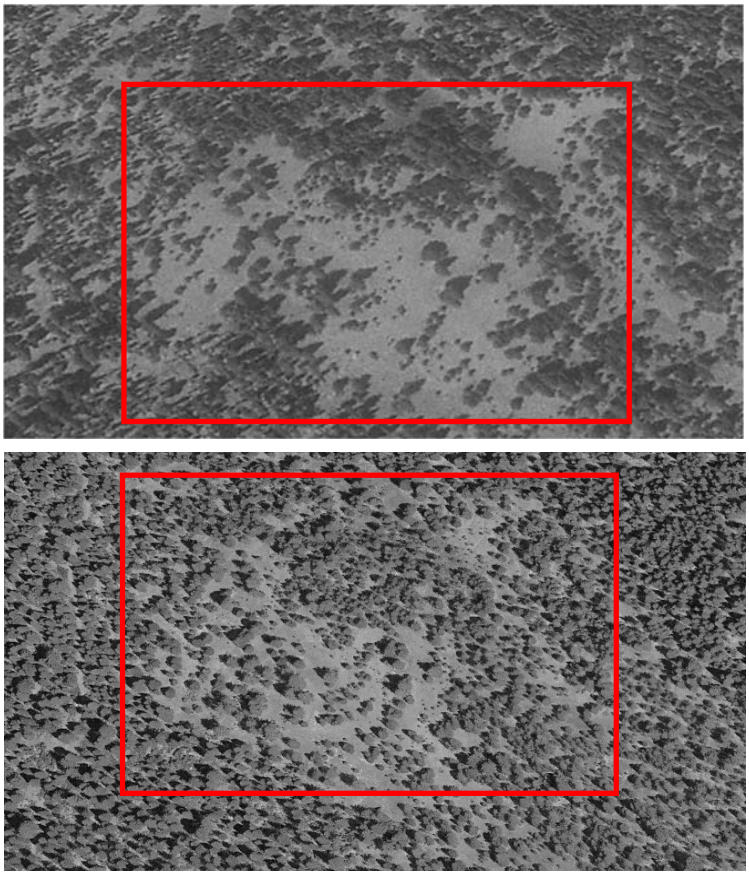

Figure 5.2 Marian Meadow prior to conifer removal Top: 7/1993 Bottom: 5/2014. The red box delineates similar respective areas (historic imagery from Google Earth)

near surface groundwater and more plant available water will discourage the re-encroachment of conifers on MM. Given the appropriate resources, further work is suggested to assess the soil seed bank of MM in terms of species distribution. Future research should also be done to identify the effectiveness of re-seeding of key indicator species on past restorations of dry and mesic meadows in the study region. If past re-seeding efforts on encroached meadows in the study region have been successful, re-seeding should be advocated for as part of restoration efforts on MM.

5.5 Hydrologic Implications

Marian Meadow and CM had a similar range of groundwater depths throughout the analysis period. However, the shallowest seasonal groundwater depth on CM was about a 1.0 ft (0.3 m) closer to ground surface than the MM during the same period during December 2014. During a period spanning from August 2014–October 2014 modeled groundwater depth was 1.0-2.0 ft (0.3-0.6 m) closer to the ground surface on MM compared to modeled depths on CM. This may be an indication that CM has a stronger response to precipitations inputs but also drains gravitational water more quickly than MM. On MM, volumetric soil moisture was lower than CM from May-November and higher than CM from May-November. The range of the average weekly volumetric soil moisture on CM was about 160% higher than the range measured on MM (Δ35.28% vs Δ21.67%).

If CM and MM have historically been dry or mesic meadows soil moisture may be an important index of conditions favorable to restoration because near surface groundwater may be a strictly seasonal event regardless of conifer removal, except for years of very high precipitation. The higher soil moisture observed on MM during the

summer is advantageous to the restoration of MM because plant species will experience less water stress during times of high water demand. Additionally, although soils on both meadows were observed to be above estimated field capacity for a similar period, soils on MM were closer to estimated field capacity during the summer months than CM. It remains to be seen if increases in soil moisture associated with conifer removal will out measure the expected losses of water to increased evaporation from the soil surface due to the lack of canopy cover following removal of conifers.

One key difference between the two meadows not observed in the data collected as part of this research was the quantity of plant available water that could be stored within the first 140 cm of soil. Plant available water is the equivalent depth of soil water at permanent wilting point subtracted from the equivalent depth of soil water at field capacity. The plant available water determined in the region encompassing MM was 0.65 ft (19.6 cm). In comparison, CM is only able to retain about half of the plant available water available on MM (0.30 ft (9.1 cm)) (USDA-NRCS, 2015). The larger capacity to store water available to plants on MM may mean that restoration efforts will be more successful on MM than CM. It should also be noted that although MM is considered to contain more total water than CM, this distinction is arbitrary to the extent that this statement only applies to water stored above the reference datum of 41.0 ft (12.5 m) below the ground surface. Considering the depth to the base of the aquifer below CM, CM probably stores more water than MM. Total water content above the reference datum is being used as a comparative tool rather than a diagnostic of successful restoration. The hydrologic changes in the first few meters of soil below MM will ultimately determine if restoration by means of conifer removal was successful.

A water balance analysis comprising a period of several years must be understood within the context of fluctuations in climate. In this study, the use of a control meadow will aid in separating which changes in the hydrology of MM are associated with conifer removal and which changes are associated with fluctuations in climate. Although the term "control meadow" is used, CM may also be considered a 'reference meadow' because its soil is distinctly different from the soil underlying MM. Ideally, the climate following removal of conifers will approximate the climate antecedent to removal. A dramatic change in climate will inevitably complicate the post-removal analysis by making it harder to recognize which changes are associated with climate which are related to conifer removal from MM. Ultimately, continued collection of hydrologic and ERT data following conifer removal, will aid in in isolating which hydrologic changes are fundamentally tied to removal of conifers and which changes are related to changes in climate. Lastly, the watershed scale removal of conifers in 2016 may temporarily augment groundwater recharge and near-surface soil moisture on MM, thereby accelerating the return of meadow flora if initial restoration efforts are successful.

CHAPTER 6 CONCLUSIONS AND SUMMARY

A large body of research exists pertaining to meadow restoration and the hydrologic response to tree removal from managed forests, but little research has been done to determine the effectiveness of tree removal on restoration of meadows encroached by conifers in terms of hydrology. Several studies have demonstrated that water yield, stream discharge and soil moisture increase when tree density or canopy cover is reduced (Sahin and Hall, 1996; Adams et al., 1991; Keppeler and Ziemer, 1990). Therefore, the hypothesis guiding this research is that increases in soil moisture and decreases in water table depth following conifer removal from meadows can promote meadow restoration by discouraging re-encroachment by conifers (conifers do not tolerate high soil moisture and near surface groundwater well). Increases in plant available water would also create a hydrologic environment favorable to the return of characteristic meadow flora.

The goal of this research is to determine if conifer removal from an encroached meadow in the Sierra Nevada Mountains, occurring in two phases, will increase seasonal soil moisture and decrease seasonal groundwater depths such that post-removal hydrologic conditions will favor meadow restoration. Phase one of conifer removal consists of a clearcut on the encroached meadow (Marian Meadow) in 2015. Phase 2 will consist of a partial removal of timber from the surrounding watershed (approximately 2000 acres) scheduled in 2016. The portion of this research addressed in this thesis constitutes the first half of this study as it is currently planned.

A robust method for evaluating the water balance before and after conifer removal from Marian Meadow was established by implementing a before and after control

intervention study design. Soil moisture probes and water level loggers were installed in a randomized spatially balanced scheme to quantify volumetric soil moisture and seasonal water table characteristics on Marian Meadow and a nearby restored meadow referred to as Control Meadow. A methodology was also established to quantify stream discharge thorough a road culvert on an ephemeral stream that drains Marian Meadow (Marian Creek). The Priestley Taylor model was implemented to quantify daily evapotranspiration from Marian Meadow and Control Meadow.

Electrical resistivity tomography was implemented to characterize the subsurface hydrology of both meadows. Electrical resistivity tomography is a well-established tool in studies investigating subsurface hydrology (Frohlich, 1994 and Ravindran and Prabhu, 2012). Electrical resistivity tomography was demonstrated to improve the spatial interpretation of groundwater recharge and facilitated the use of a recession curve analysis to model groundwater recharge when water level loggers installed in groundwater wells were not able detect groundwater. Electrical resistivity also allowed the effect of conifer encroachment on meadow ecotone subsurface hydrology to be understood. IRIS (Indicators of Reduction in Soils) were also used to determine the incidence of hydric soils on Control Meadow and Marian Meadow prior to conifer removal. IRIS tubes were not formally analyzed because they did not indicate significant signs of Fe^{3+} reduction. However, IRIS tubes may be used following conifer removal from Marian Meadow because the presence of hydric soils on Marian Meadow following conifer removal would be indicative of a favorable hydrologic response to conifer removal.

It should be noted that the presence of drought conditions in California during the time of study may have altered the hydrologic regime observed on Marian Meadow and the Control Meadow in this study. The hydrologic response to conifer removal from Marian Meadow during a wetter climactic period may differ distinctly from what will be observed in this research. It is important to understand that conifer encroachment is not a phenomenon restricted to promotion through changes in subsurface hydrology. Conifer encroachment is also related to a number of other factors intrinsic and extrinsic to each encroached meadow such as soil biogeochemistry, fire regime and slope aspect (Haugo et al., 2011; Griffiths et al., 2005; Miller and Halpern, 1998). If current climate trends continue, it may become increasingly difficult to restore encroached meadows, as conifer encroachment into meadows may be indicative of a transition to a new stable state (Haugo and Halpern, 2007). Consequently, successful meadow restoration may not be limited to inducing hydrologic changes favorable to restoration. Lastly, although the term restoration in used in this study, it does not imply that restoration constitutes a return to pre encroachment hydrologic or vegetative conditions on Marian Meadow.

The lack of a soil seed bank consisting of endemic meadow flora on encroached meadows is a known impediment to meadow restoration (Lett and Knapp, 2005 and Lang, 2006). Future work should be done to determine the key indicator species of dry and mesic meadows in the region and if re-seeding of key indicator species on Marian Meadow would aid restoration efforts. Previous research indicates that the establishment of conifer seedlings and ruderal vegetation following conifer removal reverses increases in soil moisture, stream flow and water yield associated with conifer removal (Keppeler et al., 1994 and Wright et al., 1990). Consequently, if a hydrologic response favorable to

meadow restoration occurs due to conifer removal on Marian Meadow the maintenance of this response will most likely be contingent on continued removal of seedlings and unwanted vegetation.

Analysis of the pre-removal hydrologic characteristics from September 2013 to December 2014 indicates that Marian Meadow appears to be a favorable candidate for restoration (in terms of hydrology). On Marian Meadow, volumetric soil moisture was higher than the Control Meadow from May-November. Sufficient soil moisture in the summer months is crucial to maintenance of meadow biotic communities. The water table depth on Marian Meadow and the Control Meadow was similar throughout the analysis period with two notable exceptions. First, from March to May the water table was shallower on Control Meadow. Second, from mid-August to October the water table was 1.0-2.0 ft (0.3-0.6 m) closer to the ground surface on Marian Meadow. If conifer removal from Marian Meadow causes an increase in volumetric soil moisture and a decrease in seasonal groundwater depth, an augmented version of the stable hydrologic system already present on Marian Meadow may result in conditions favorable to meadow restoration.

REFERENCES

"A Quick Derivation Relating Altitude to Air Pressure." Portland State Aerospace Society. Web. 2 May 2014. <http://psas.pdx.edu/RocketScience/PressureAltitude_Derived.pdf>.

Adams, Paul W., Alan L. Flint, and Richard L. Fredriksen. "Long-Term Patterns in Soil Moisture and Revegetation after a Clearcut of a Douglas-Fir Forest in Oregon." *Forest Ecology and Management* 41.3 (1991): 249-263. Print.

Adli, Zulfadhli H., Mohd H. Musa, and MN Khairul Arifin."Electrical resistivity of subsurface: Field and laboratory assessment." *World Academy of Science, Engineering and Technology* 69 (2010): 805-808. Print.

Agam, Nurit, William P. Kustas, Martha C. Anderson, John M. Norman, Paul D. Colaizzi, Terry A. Howell, John H. Prueger, Tilden P. Meyers, and Tim B. Wilson. "Application of the Priestley-Taylor approach in a two-source surface energy balance model." *Journal of Hydrometeorology* 11.1 (2010): 185-198. Web.

Allen, Richard G., Luis S. Pereira, Dirk Raes, and Martin Smith. "Crop evapotranspiration-Guidelines for computing crop water requirements-FAO." *Irrigation and Drainage Paper 56* 300.9 (1998):1-281. Print.

Amidu, Sikiru A., and John A. Dunbar."Geoelectric Studies of Seasonal Wetting and Drying of a Texas Vertisol." *Vadose Zone Journal* 6.3 (2007): 511-523. Print.

Anderson, R. Scott., and Susan J. Smith. "Paleoclimatic Interpretations of Meadow Sediment and Pollen Stratigraphies from California." *Geology* 22.8 (1994): 723-726. Web.

Archie, G. E. "The electrical resistivity log as an aid in determining some reservoir characteristics." *Well Logging Technology* 31.3 (1942): 197-202. Print.

Aylward, Bruce., and Amy Merrill. "An Economic Analysis of Sierra Meadow Restoration." *A report for Environmental Defense Fund under the National Fish and Wildlife Foundation's Sierra Meadows Initiative*. (2012): 76 Web.

Bernard, Jean. "Multi-electrode Resistivity Imaging for Environmental and Mining Applications." IRIS Instruments, 2006. Web. 4 Feb. 2015. <http://www.iris-instruments.com/Pdf file/5-Resistivity_Imaging/Resistiivty_Imaging_text.pdf>.

Bigelow, Seth W., and Malcolm P. North. "Microclimate Effects of Fuels-Reduction and Group-Selection Silviculture: Implications for Fire Behavior in Sierran Mixed-Conifer Forests." *Forest Ecology and Management* 264. (2012): 51-59. Web.

Black, C.A, D.D Evans, and J.L White. *Methods of Soil Analysis*. Madison: American Society of Agronomy, 1965. Print.

Bohn, Carolyn C. "Guide for fabricating and installing shallow ground water observation wells." *US Department of Agriculture, Forest Service, Rocky Mountain Research Station*, (2001): 1-5. Web.

Brunet, Pascal, Rémi Clément, and Christophe Bouvier. "Monitoring soil water content and deficit using Electrical Resistivity Tomography (ERT)–A case study in the Cevennes area, France." *Journal of Hydrology* 380.1. (2010): 146-153. Web

Brunt, David. *Physical and Dynamical Meteorology*. Cambridge: University Press, 1939. Print.

Burger, Henry R, Anne F. Sheehan, and Craig H. Jones. *Introduction to applied geophysics: Exploring the shallow subsurface.* New York City*:* WW Norton, 2006. Print.

Burns, Russell M., and Barbara H. Honkala. *Silvics of North America: 1. Conifers; 2. Hardwoods. Agriculture Handbook 654* Washington, DC: U.S. Department of Agriculture, Forest Service, 1990. Print.

California Data Exchange Center. California Department of Water Resources. Web. 29 Jan. 2015. <http://cdec.water.ca.gov/misc/DailyPrecip.html>.

Capacitive Water Level Logger." Dataflow Systems Pty Limited Web. 11 Jan. 2015. <http://odysseydatarecording.com/download/Odyssey%20Capacitive%20Water%20Level%20Logger%202013.pdf>.

Caprio, Anthony C., and David M. Graber. "Returning Fire to the Mountains: Can We Successfully Restore The Ecological Role of Pre-Euroamerican Fire Regimes to the Sierra Nevada." Proceedings of the wilderness science in a time of change conference USDA Forest Service (2000):1-12. Print.

Carter, Martin R. Soil Sampling and Methods of Analysis. Boca Raton: Lewis, 1993. Print.

Cassel, D. K., and D. R. Nielsen. "*Field capacity and available water capacity Methods of Soil Analysis: Part 1—Physical and Mineralogical Method 1.* Madison, Wisconsin: Soil Science Society of America, 1986. 901-926. Print.

Chambers, Jeanne. C., Jerry. R. Miller and Dru Germanoski, "Geomorphology, hydrology, and ecology of Great Basin meadow complexes – implications for management and restoration." *U. S. Department of Agriculture Forest Service. General Technical Report* (2011): 152. Web.

Chambers, Jeanne. C., Robin J. Tausch, John L. Korfmacher, Jerry R. Miller, D.G Jewett. *Effects of geomorphic processes and hydrologic regimes on riparian vegetation.* In: Chambers, J.C, Miller, J.R., eds. Great Basin Riparian Ecosystems—Ecology, Management and Restoration. Covelo: Island Press, 2004. 196-231. Web.

"Chester, California." Period of Record Monthly Climate Summary. Web. 7 Feb. 2014. <http://www.wrcc.dri.edu/cgi-bin/cliMAIN.pl?caches nca>.

Chesworth, Ward. *Encyclopedia of Soil Science.* Dordrecht: Springer, 2008. Print.

Christensen, Peter, and William Peacock. Chapter 15 Interpretation of Soil and Water Analysis. In: Raisin Production Manual. Oakland: University of California, Agriculture & Natural Resources, Communication Services, 2000. 115-120. Print.

CIMIS Station Reports." CIMIS. California Irrigation Management Information System. Web. 24 May 2014. <www.cimis.water.ca.gov/WSNReportCriteria.aspx>

Dancey, Christine P., and John Reidy. Statistics without Maths for Psychology: Using SPSS for Windows. 4th ed. Harlow: Pearson/Prentice Hall, 2007. Print.

"DD11 Hydraulic Capacity of Culverts." Design Data. American Concrete Pipe Association. Web. 8 Sept. 2014. <https://www.concrete-pipe.org/pdfdd/DD_11.pdf>

DeAngelis, K. M. "Measurement of soil moisture content by gravimetric method." *American Society of Agronomy* (2007): 1-2.Web.

Dettinger, Michael D., and Daniel R. Cayan. "Large-scale atmospheric forcing of recent trends toward early snowmelt runoff in California." *Journal of Climate* 8.3 (1995): 606-623. Web.

Durrell, Cordell. *Geologic History of the Feather River Country*, *California.* Berkeley: University of California, 1987. Print.

Engelhardt, Blake Meneken. *Geomorphic controls on Great Basin riparian vegetation at the watershed and process zone scales*. Diss. University of Nevada, Reno, 2009.

Environmental Geophysics. United States Environmental Protection Agency, 12 Dec. 2011. Web. 24 Feb. 15. <http://www.epa.gov/esd/cmb/Geophysics Website/pages/reference/_img/fig270.jpg>.

Fisher, Joshua B., Terry A. DeBiase, Ye Qi, Ming Xu, and Allen H. Goldstein. "Evapotranspiration models compared on a Sierra Nevada forest ecosystem." *Environmental Modelling & Software* 20.6 (2005): 783-796. Web.

Fites-Kaufman, Jo Ann, Phillip Rundel, Nathan Stephenson, and Dave A. Weixelman. "Chapter 17 Montane and subalpine vegetation of the Sierra Nevada and Cascade Ranges." *Terrestrial Vegetation of California.* Berkeley: University of California Press, 2007. 456-501. Print.

Flint, A. L. and Childs, S. W. "Modification of the Priestley-Taylor evaporation equation for soil water limited conditions". In: *18th Conference on Agricultural and Forest Meteorology*, Lafayette IN, 1987. Boston: American Meteorological Society, 1987. 70-73. Print.

Flint, Alan L., and Stuart W. Childs. "Use of the Priestley-Taylor evaporation equation for soil water limited conditions in a small forest clearcut." *Agricultural and Forest Meteorology* 56.3 (1991): 247-260. Web.

Franklin, J.F., and J Fites-Kaufmann, "Assessment of late-successional forests of the Sierra Nevada." In: Sierra Nevada Ecosystem Project, Final Report to Congress, Vol. II. *University of California, Water and Wildlands Resources Center*, Davis, CA, (1996): 627–657. Web.

Fritschen, Leo, and Lloyd Wesley Gay. Environmental Instrumentation. New York: Springer-Verlag, 1979. Print.

Frohlich, Reinhard K., Daniel W. Urish, James Fuller, and Mary O'Reilly. "Use of geoelectrical methods in groundwater pollution surveys in a coastal environment." *Journal of Applied Geophysics* 32.2 (1994): 139-154. Web.

Fukue, M., T. Minatoa, H. Horibe and N. Taya "The micro-structure of clay given by resistivity measurements." *English Geology* 54 (1999): 43-53 Web.

Goyal, V. C., P. K. Gupta, S. M. Seth, and V. N. Singh. "Estimation of temporal changes in soil moisture using resistivity method." *Hydrological processes* 10.9 (1996): 1147-1154. Web.

Griffin, James R. *Soil Moisture and Vegetation Patterns in Northern California Forests. Berkeley: Pacific Southwest Forest and Range Experiment Station*, Forest Service, U.S. Dept. of Agriculture, 1967. Print.

Griffin, James R., and William Burke Critchfield. The Distribution of Forest Trees in California with Supplement. Berkeley: Pacific Southwest Forest and Range Experiment Station, 1976. Print.

Griffiths, Robert., Michael Madritch, and Alan Swanson. "Conifer invasion of forest meadows transforms soil characteristics in the Pacific Northwest." *Forest Ecology and Management* 208.1 (2005): 347-358. Web.

Gross, Shana, and Michelle Coppoletta. *Historic Range of Variability for Meadows in the Sierra Nevada and South Cascades*. Rep. United States Department of Agriculture Forest Service, n.d. Web. 24 July 2014. <http://www.fs.usda.gov/Internet/FSE_DOCUMENTS/stelprdb5434345.pdf>.

Hadley, Keith S. "Forest history and meadow invasion at the Rigdon Meadows Archaeological site, western Cascades, Oregon." *Physical Geography* 20.2 (1999): 116-133. Print.

Halpern, Charles B., Joseph A. Antos, Janine M. Rice, Ryan D. Haugo, and Nicole L. Lang. "Tree invasion of a montane meadow complex: temporal trends, spatial patterns, and biotic interactions." *Journal of Vegetation Science* 21.4 (2010): 717-732.Web.

Halpern, Charles B., Ryan D. Haugo, Joseph A. Antos, Sheena S. Kaas, and Allyssa L. Kilanowski. "Grassland restoration with and without fire: evidence from a tree-removal experiment." *Ecological Applications* 22.2 (2012): 425-441. Web.

Hanson RL., "Evapotranspiration and droughts". In: Paulson RW, Chase EB, Roberts RS, Moody DW, Compilers, National Water Summary 1988-89-hydrologic events and floods and droughts: *U.S. Geological Survey Water-Supply Paper 2375*(1991): 99–104

Harrison, Louis P. "Fundamental concepts and definitions relating to humidity." *Humidity and moisture* 3 (1963): 3-70. Print

Haugo, Ryan D., and Charles B. Halpern. "Vegetation Responses to Conifer Encroachment in a Western Cascade Meadow: A Chronosequence Approach." *Botany* 85.3 (2007): 285-298. Web.

Haugo, Ryan D., Charles B. Halpern, and Jonathan D. Bakker. "Landscape context and long-term tree influences shape the dynamics of forest-meadow ecotones in mountain ecosystems." *Ecosphere* 2.8 (2011): 91. Web.

Haugo, Ryan D., Jonathan D. Bakker, and Charles B. Halpern. "Role of biotic interactions in regulating conifer invasion of grasslands." *Forest Ecology and Management* 289 (2013): 175-182. Web.

Herman, Rhett. "An introduction to electrical resistivity in geophysics." American Journal of Physics 69.9 (2001): 943-952. Web.

Hill, Barry, and Sherry Mitchell-Bruker. "Comment on "A Framework For Understanding the Hydroecology of Impacted Wet Meadows in the Sierra Nevada and Cascade Ranges, California, USA": paper published in Hydrogeology Journal (2009) 17: 229–246, by Steven P. Loheide II, Richard S. Deitchman, David J. Cooper, Evan C. Wolf, Christopher T. Hammersmark, Jessica D. Lundquist." *Hydrogeology Journal* 18.7 (2010): 1741-1743. Web.

"Historical Course Data." *California Cooperative Snow Surveys*. California Department of Water Resources, 2002. Web. 24 May 2014. <http://cdec.water.ca.gov/snow/>.

Hong-Jing, J., Shun-qun, L., and Lin, L. "The Relationship between the Electrical Resistivity and Saturation of Unsaturated Soil." *The Electronic Journal of Geotechnical Engineering* 19 (2014): 3739–3746. Web.

"Iron Oxide Paint - Indicator of Reduction in Soil (IRIS) Tubes. *Laboratory Analyses Procedures*. University of Idaho Pedology Laboratory, Web. 11 June 2014. <http://www.uidaho.edu/cals/pses/pedology/resources/Analyses>.

Jayawickreme, Dushmantha H., Celina S. Santoni, John H. Kim, Esteban G. Jobbágy, and Robert B. Jackson. "Changes in hydrology and salinity accompanying a century of agricultural conversion in Argentina." *Ecological Applications* 21.7 (2011): 2367-2379. Web.

Jayawickreme, Dushmantha H., Remke L. Van Dam, and David W. Hyndman. "Subsurface imaging of vegetation, climate, and root-zone moisture interactions." *Geophysical Research Letters* 35.18 (2008). Web.

Jenkinson, B. J., and D. P. Franzmeier. "Development and evaluation of iron-coated tubes that indicate reduction in soils." *Soil Science Society of America* 70.1 (2006): 183-191. Web

Keppeler, Elizabeth T and Robert R. Ziemer. "Logging effects on streamflow: water yield and summer low flows at Caspar Creek in northwestern California." *Water Resources Research* 26.7 (1990): 1669-1679. Web.

Keppeler, Elizabeth T.; Ziemer, Robert R.; Cafferata, Peter H. 1994. Changes in soil moisture and pore pressure after harvesting a forested hillslope in Northern California. In: Marston, Richard A., and Victor R. Hasfurther (eds). Proceedings, Annual Summer Symposium of the American Water Resources Association: Effects of Human-Induced Changes on Hydrologic Systems, 26-29 June 1994, Jackson Hole, Wyoming. American Water Resources Association, Bethesda, Maryland. p. 205-214.

Knowles, Noah., Michael D. Dettinger, and Daniel R. Cayan. "Trends in snowfall versus rainfall in the western United States." *Journal of Climate* 19.18 (2006): 4545-4559. Web.

Komatsu, Hikaru., "Forest categorization according to dry-canopy evaporation rates in the growing season: comparison of the Priestley–Taylor coefficient values from various observation sites." *Hydrological Processes* 19.19 (2005): 3873-3896. Web.

Kremer, Nicolas J., Charles B. Halpern, and Joseph A. Antos. "Conifer reinvasion of montane meadows following experimental tree removal and prescribed burning." *Forest Ecology and Management* 319 (2014): 128-137. Web.

Lang, Nicole L. The soil seed bank of an Oregon montane meadow: consequences of conifer encroachment and implications for restoration. Diss. University of Washington, 2006. Web.

Lett, Michelle S., and Alan K. Knapp. "Woody plant encroachment and removal in mesic grassland: production and composition responses of herbaceous vegetation." *The American midland naturalist* 153.2 (2005): 217-231. Web.

Loheide, Steven P., and Jessica D. Lundquist. "Snowmelt-Induced Diel Fluxes through the Hyporheic Zone." *Water Resources Research* 45. (2009): 1–9. Web.

Loheide, Steven P., and Steven M. Gorelick. "Riparian hydroecology: a coupled model of the observed interactions between groundwater flow and meadow vegetation patterning." *Water Resources Research* 43.7 (2007):1-16 Web.

Lord, Mark L., David G. Jewett, Jerry R. Miller, Dru Germanoski, and Jeanne C. Chambers. "Hydrologic processes influencing meadow ecosystems." *Geomorphology, Hydrology, and Ecology of Great Basin Meadow Complexes—Implications for Management and Restoration* (2011): 44. Web.

Lowry, Christopher S., Steven P. Loheide, Courtney E. Moore, and Jessica D. Lundquist. "Groundwater controls on vegetation composition and patterning in mountain meadows." *Water Resources Research* 47.10 (2011) Web.

Lundquist, J., and J. Roche. 2009. "Climate change and water supply in western national parks." *Park Science* 26.1: 31–34. Web.

McNeill, J. D. *Electrical conductivity of soils and rocks*. Geonics Limited: 1980.

Miles, Scott R., and Charles Goudey. Ecological Subregions of California Section & Subsection Descriptions. San Francisco, California: United States Department of Agriculture Forest Service, Pacific Southwest Region, 1997. Print.

Miller, Eric A., and Charles B. Halpern. "Effects of environment and grazing disturbance on tree establishment in meadows of the central Cascade Range, Oregon, USA." *Journal of Vegetation Science* 9.2 (1998): 265-282. Web.

Murray, Francis W. "On the computation of saturation vapor pressure." *Journal of Applied Meteorology* 6.1 (1967): 203-204. Web.

Neyamadpour, Ahmad, WAT Wan Abdullah, Samsudin Taib, and Behrang Neyamadpour. "Comparison of Wenner and dipole–dipole arrays in the study of an underground three-dimensional cavity." *Journal of Geophysics and Engineering* 7.1 (2010): 30. Web.

"NOAA Climate Data Online." National Oceanic and Atmospheric Administration. Web. 25 Feb. 2014. <http://www.ncdc.noaa.gov/cdo-web>.

Oberdörster, Christoph. "Hydrological characterization of a forest soil using electrical resistivity tomography." *Forschungszentrum* Jülich, 76. (2010)

Palacky, G. J. "Resistivity characteristics of geologic targets." *Electromagnetic Methods in Applied Geophysics* 1 (1988): 53-129. Web.

Priestley, C. H. B., and R. J. Taylor. "On the assessment of surface heat flux and evaporation using large-scale parameters." *Monthly weather review* 100.2 (1972): 81-92. Web.

Pupacko, A. "Variations in northern Sierra Nevada streamflow: implications of climate change." *Water Resources Bulletin* 29 (1993): 283-290. Web

Rabenhorst, M C., "Protocol for using and interpreting IRIS tubes." *Soil survey horizons* 49 (2008):74-77. Web.

Rabenhorst, Martin C. "Visual Assessment of IRIS Tubes in Field Testing for Soil Reduction." *Wetlands* 30.5 (2010): 847–852. Web.

Rabenhorst, Martin C. "Biologic zero: A soil temperature concept." *Wetlands* 25.3 (2005): 616-621. Web.

Rabenhorst, Martin C., and S. N. Burch. "Synthetic iron oxides as an indicator of reduction in soils (IRIS)." *Soil Science Society of America Journal* 70.4 (2006): 1227-1236. Web.

Ratliff, Raymond D. *Meadows in the Sierra Nevada of California: State of Knowledge*. Berkeley, California: United States Department of Agriculture, Forest Service, Pacific Southwest Forest and Range Experiment Station, 1985. Print.

Ravindran, Antony, and H. Mohd Abdul Kadar Prabhu. "Groundwater exploration study using Wenner-Schlumberger electrode array through W-4 2D Resistivity Imaging systems at Mahapallipuram, Chennai, Tamilanadu, India." *Research Journal of Recent Sciences* 1.11 (2012): 36-40. Web.

Rice, Janine M., Charles B. Halpern, Joseph A. Antos, and Julia A. Jones. "Spatio-temporal patterns of tree establishment are indicative of biotic interactions during early invasion of a montane meadow." *Plant Ecology* 213.4 (2012): 555-568.Web

"Sacramento River Basin Watersheds". Sacramento River Basin Watershed Program. Web. 13 May 2014. < http://www.sacriver.org/aboutwatershed/ roadmap/watersheds.>

Sahin, Vildan., and Michael J. Hall. "The Effects of Afforestation and Deforestation on Water Yields." *Journal of Hydrology* 178 (1996): 293–309. Web.

Samouëlian, Anatja, Isabelle Cousin, Alain Tabbagh, Ary Bruand, and Guy Richard. "Electrical resistivity survey in soil science: a review." *Soil and Tillage Research* 83.2 (2005): 173-193. Web.

Shevock, J.R., Chapter 24 Status of rare and endangered plants. In: Sierra Nevada Ecosystem Project: Final Report to Congress, Vol. II. Centers for Water and Wildland Resources, *University of California, Davis*, (1996): 691–707. Web.

Shuttleworth, W. James, and Ian R. Calder. "Has the Priestley-Taylor equation any relevance to forest evaporation?." *Journal of Applied Meteorology* 18.5 (1979): 639-646. Web.

Sibbett, Steven, and Louise Ferguson. Olive Production Manual. 2nd ed. Oakland: University of California, Agriculture and Natural Resources, 2005. Print.

Skinner C. N., A.H. Taylor Southern Cascade Bioregion. Fire in California's Ecosystems J.W. Van Wagtendonk, J. Fites-Kaufmann, K.E. Shaffer, A.E. Thode, N.S. Sugihara (Eds.) Berkley: University of California Press. 2006, 195–224. Print.

Skinner, Carl N., CHI-RU Chang C., Fire regimes, past and present. In: Sierra Nevada Ecosystem Project: Final report to Congress, vol. II: Assessments and Scientific Basis for Management Options. Centers for Water and Wildland Resources, University of California, Davis, Water Resources Center Report No. 37, 1996 1041‑1069. Web.

Sloto, Ronald A., and Debra E. Buxton. "Water Budgets for Selected Watersheds in the Delaware River Basin, eastern Pennsylvania and western New Jersey." *Scientific Investigations Report. United States Geological Survey* (2005): 50. Web.

"SoilWeb." Online Soil Survey Browser. Natural Resources Conservation Service Soils. Web. 25 Aug. 2014. < http://casoilresource.lawr.ucdavis.edu/gmap/.>

Spittlehouse, D. L., and T. A. Black. "A growing season water balance model applied to two Douglas fir stands." *Water Resources Research* 17.6 (1981): 1651-1656. Web.

Stevens Jr, Don L., and Anthony R. Olsen. "Spatially balanced sampling of natural resources." *Journal of the American Statistical Association* 99.465 (2004): 262-278. Web.

Stewart, Iris T., Daniel R. Cayan, and Michael D. Dettinger. "Changes in snowmelt runoff timing in western North America under a business as usual climate change scenario." *Climatic Change* 62.1-3 (2004): 217-232. Web.

Stewart, Iris T., Daniel R. Cayan, and Michael D. Dettinger. "Changes toward earlier streamflow timing across western North America." *Journal of climate* 18.8 (2005): 1136-1155. Web.

Stillwater Sciences. "A Guide for Restoring Functionality to Mountain Meadows of the Sierra Nevada." Web. 17 Nov. 2014. < http://www.stillwatersci.com/resources/2012meadowrestguide.pdf>

Sumner, David M., and Jennifer M. Jacobs. "Utility of Penman–Monteith, Priestley–Taylor, reference evapotranspiration, and pan evaporation methods to estimate pasture evapotranspiration." *Journal of Hydrology* 308.1 (2005): 81-104. Web.

Surfleet, Christopher G., and Arne E. Skaugset. "The Effect of Timber Harvest on Summer Low Flows, Hinkle Creek, Oregon." *Western Journal of Applied Forestry* 28.1 (2013): 13-21. Print.

Swanson, Frederick J., Charles B. Halpern, and John H. Cissel. "Restoration of dry, montane meadows through prescribed fire, vegetation and fuels management: A program of research and adaptive management in western Oregon." *Project 01C--3--3--10 Final Report to the Joint Fire Science Program* (2007):63. Web.

Taylor Alan H., "Tree invasion in meadows of Lassen Volcanic National Park." *California Professional Geographer* 42 (1990): 457–470. Web.

Taylor, Alan H. "Fire regimes and forest changes in mid and upper montane forests of the southern Cascades, Lassen Volcanic National Park, California, USA." *Journal of Biogeography* 27.1 (2000): 87-104. Web.

Tetens, Otto. "Uber einige meteorologische Begriffe." 6 *Z. Geophysics* (1930): 297-309. Print.

U.S. Geological Survey, 1990, National Water Summary Hydrologic Events and Water Supply and Use: *U.S. Geological Survey Water-Supply Paper* 2350 (1987): 553. Web.

"US Department of Transportation Federal Highway Administration "Identifying Roadbed Underlain by Expansive Clays." Central Federal Lands Highway Division, Jan. 2015. Web. 08 Mar. 2015. <http://www.cflhd.gov/resources/agm/eng Applications/ RoadwaySubsidence/522IndentRoadbedExpanClays.cfm/>

Utset, Angel., Imma Farre, Antonio Martínez-Cob, and José Cavero. "Comparing Penman–Monteith and Priestley–Taylor approaches as reference-evapotranspiration inputs for modeling maize water-use under Mediterranean conditions." *Agricultural Water Management* 66.3 (2004): 205-219. Web.

Vankat John L., "Fire and Man in Sequoia National Park." *Annals of the Association of American Geographers*. 67.1 (1977): 17-27. Print.

Vasilas, L. M., G.W. Hurt, and C.V Noble. Field Indicators of Hydric Soils in the United States a Guide for Identifying and Delineating Hydric Soils. Version 7.0, 2010. ed. Washington, D.C.: U. S. Dept. of Agriculture, Natural Resources Conservation Service, 2010. Print.

Viers, J. H., S. E. Purdy, R. A. Peek, A. Fryjoff-Hung, N. R. Santos, J. V. E. Katz, J. D. Emmons, D. V. Dolan, and S. M. Yarnell "Montane Meadows In The Sierra Nevada: Changing Hydroclimatic Conditions and Concepts For Vulnerability Assessment." *Center for Watershed Science Technology Report. CWS-2013-01* (2013):63 Web.

Weixelman, Dave, and Desiderio C. Zamudio. *Central Nevada Riparian Field Guide* Ogden: U.S. Department of Agriculture Forest Service. 1996. Print.

Weixelman, Dave, Barry Hill, David Cooper, Eric Berlow, Joshua Viers, Sabra Purdy, Amy Merrill, and Shana Gross. *Meadow Hydrogeomorphic Types for the Sierra Nevada and Southern Cascades Ranges in California: A Field Key Gen. Tech. Rep. R5-TP-034.* Vallejo: USDA Forest Service, 2011. Print.

Wood, S.H. *Holocene Stratigraphy and Chronology of Mountain Meadows, Sierra Nevada, California*. Diss. California Institute of Technology, 1975 Pasadena, California. Print.

Wright, Kenneth A., Karen H. Sendek, Raymond M. Rice, and Robert B. Thomas. "Logging effects on streamflow: storm runoff at Caspar Creek in Northwestern California." *Water Resources Research*. 26.7 (1990):1657–1667. Print.

Ziemer, Robert R., "Soil Moisture Depletion Patterns around Scattered Trees." U.S.D.A. Forest. Service Note PSW-166 Pacific Southwest Forest and Range Experiment Station (1968): 13. Print.

Appendix A

Marian Meadow Apparent Resistivity Pseudosections, Calculated Apparent Resistivity Pseudosections and Inverse Model Resistivity Sections

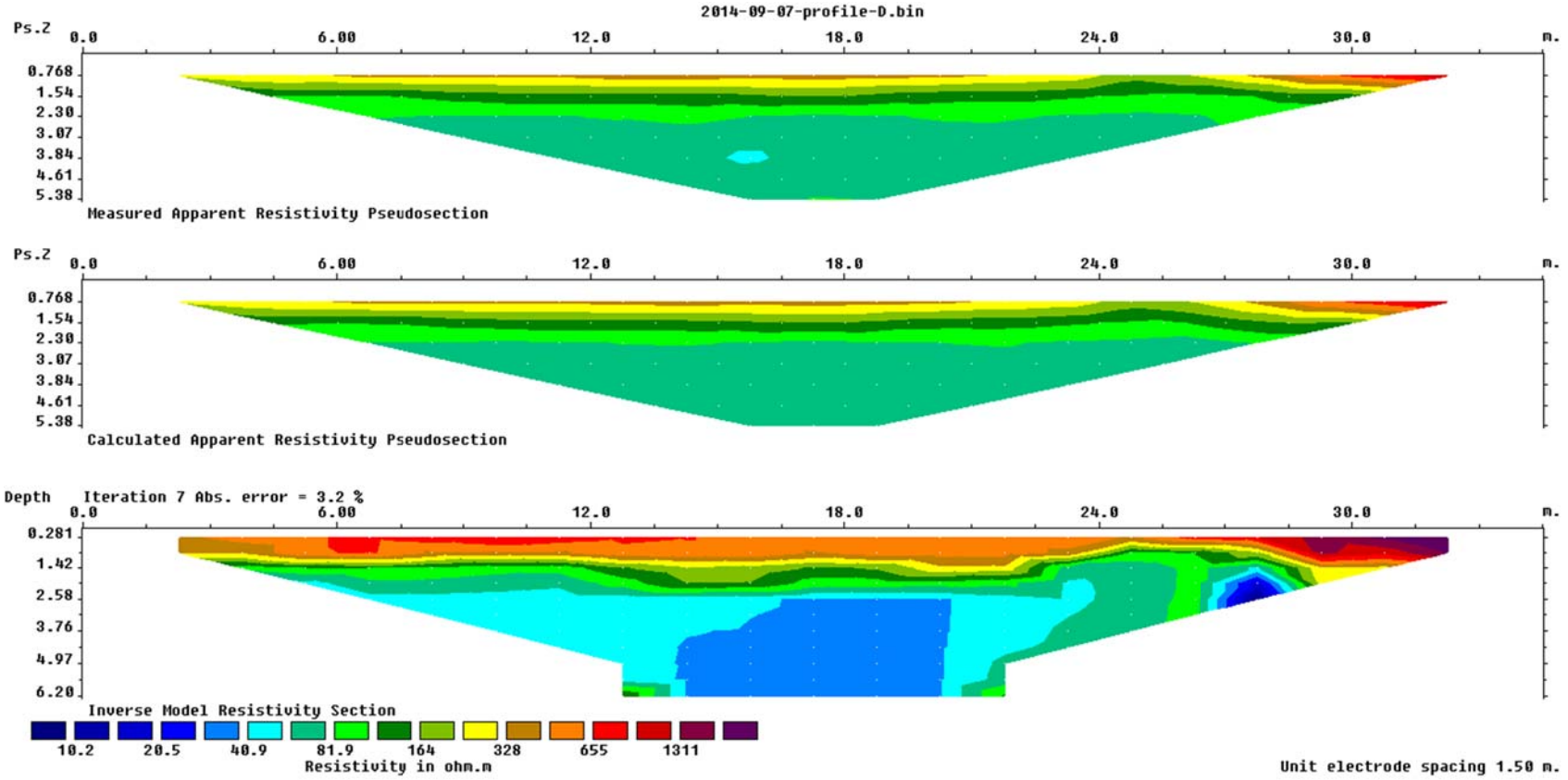

Date	Survey Line	Survey Center Latitude and Longitude	Orientation	Survey Length(m)
9/7/2014	Lower Marian Creek Transect Bisecting Line	40.2610, -121.3117	278°	34.5

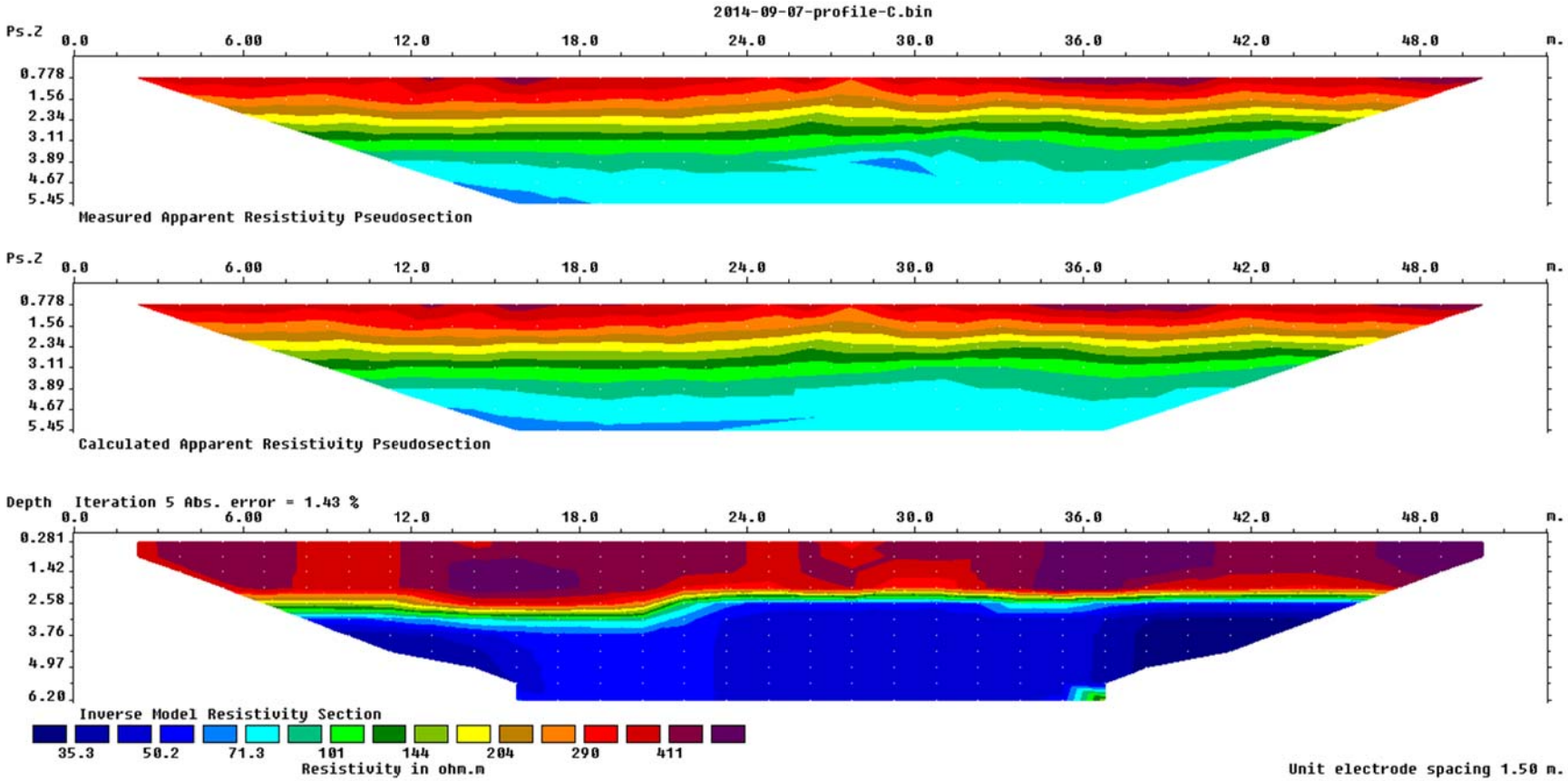

Date	Survey Line	Survey Center Latitude and Longitude	Orientation	Survey Length(m)
9/7/2014	Lower MM Transect Bisecting Line	40.2633, -121.3153	25°	51.75

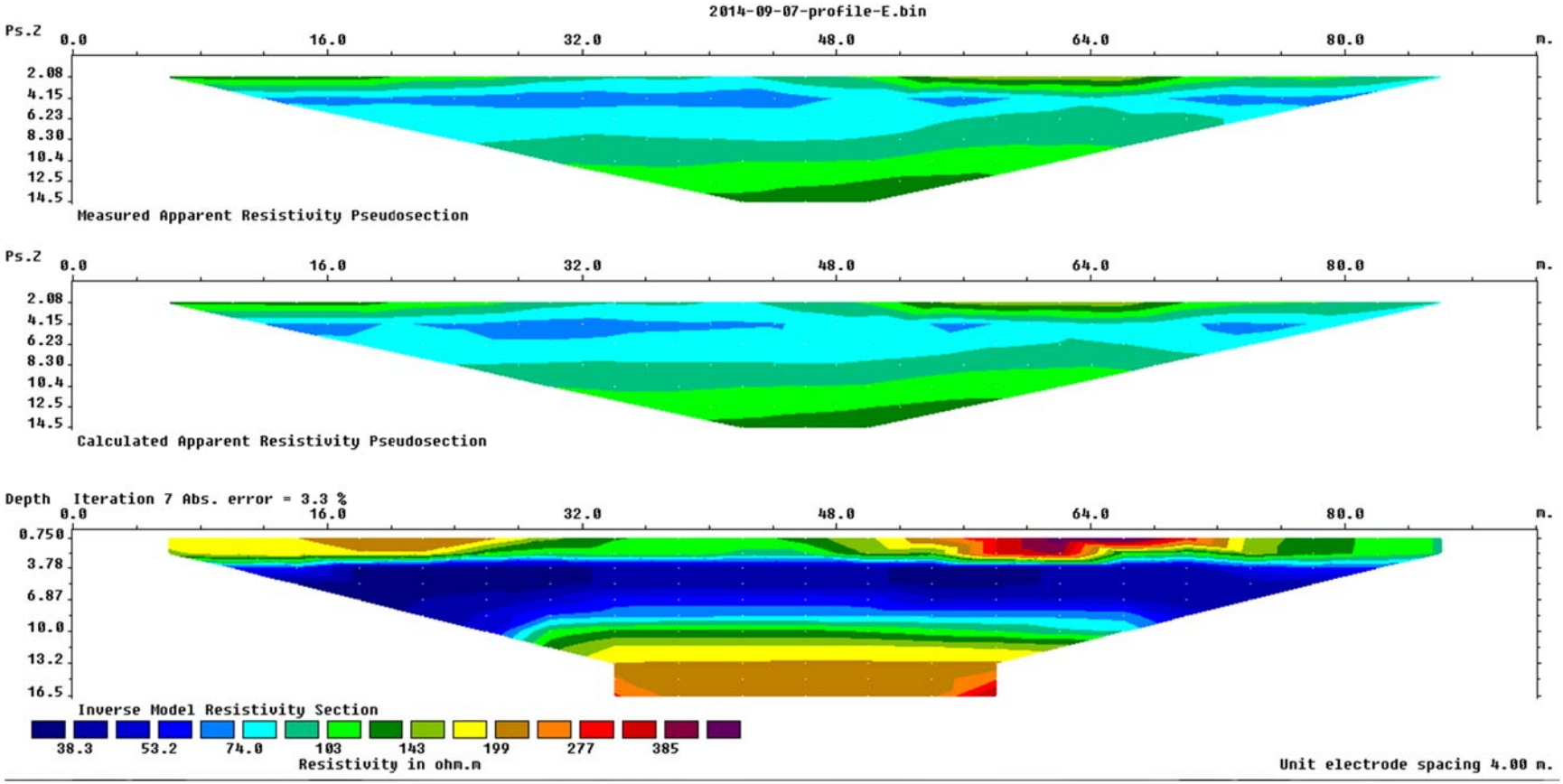

Date	Survey Line	Survey Center Latitude and Longitude	Orientation	Survey Length(m)
9/7/2014	Lower Marian Creek Meadow Transect	40.2614, -121.3116	15°	92 m

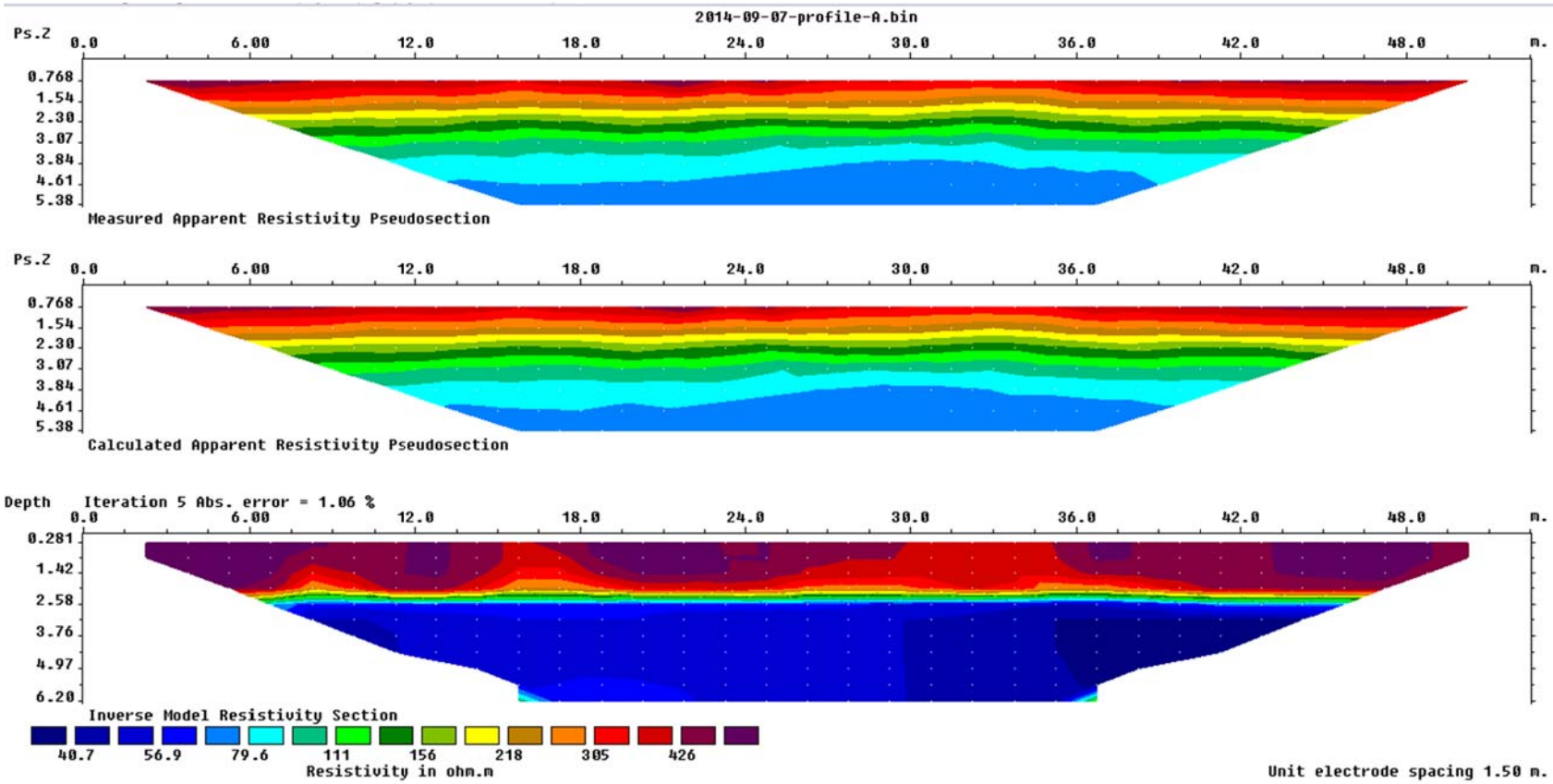

Date	Survey Line	Survey Center Latitude and Longitude	Orientation	Survey Length(m)
9/7/2014	Upper MM Transect Bisecting Line	40.2640, -121.3160	68°	51.75

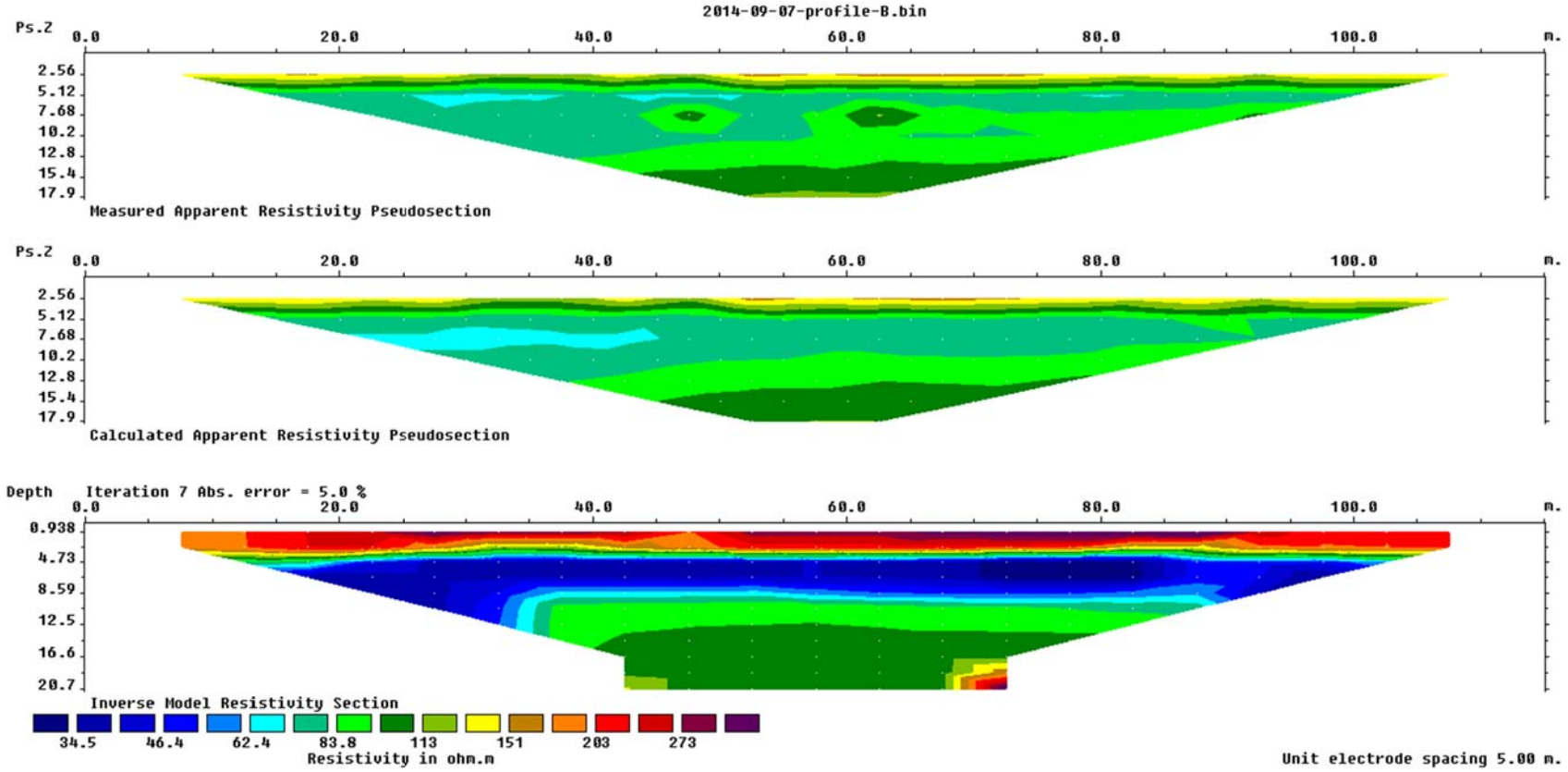

Date	Survey Line	Survey Center Latitude and Longitude	Orientation	Survey Length(m)
9/7/2014	Marian Meadow Transect	40.2635, -121.3156	345°	115

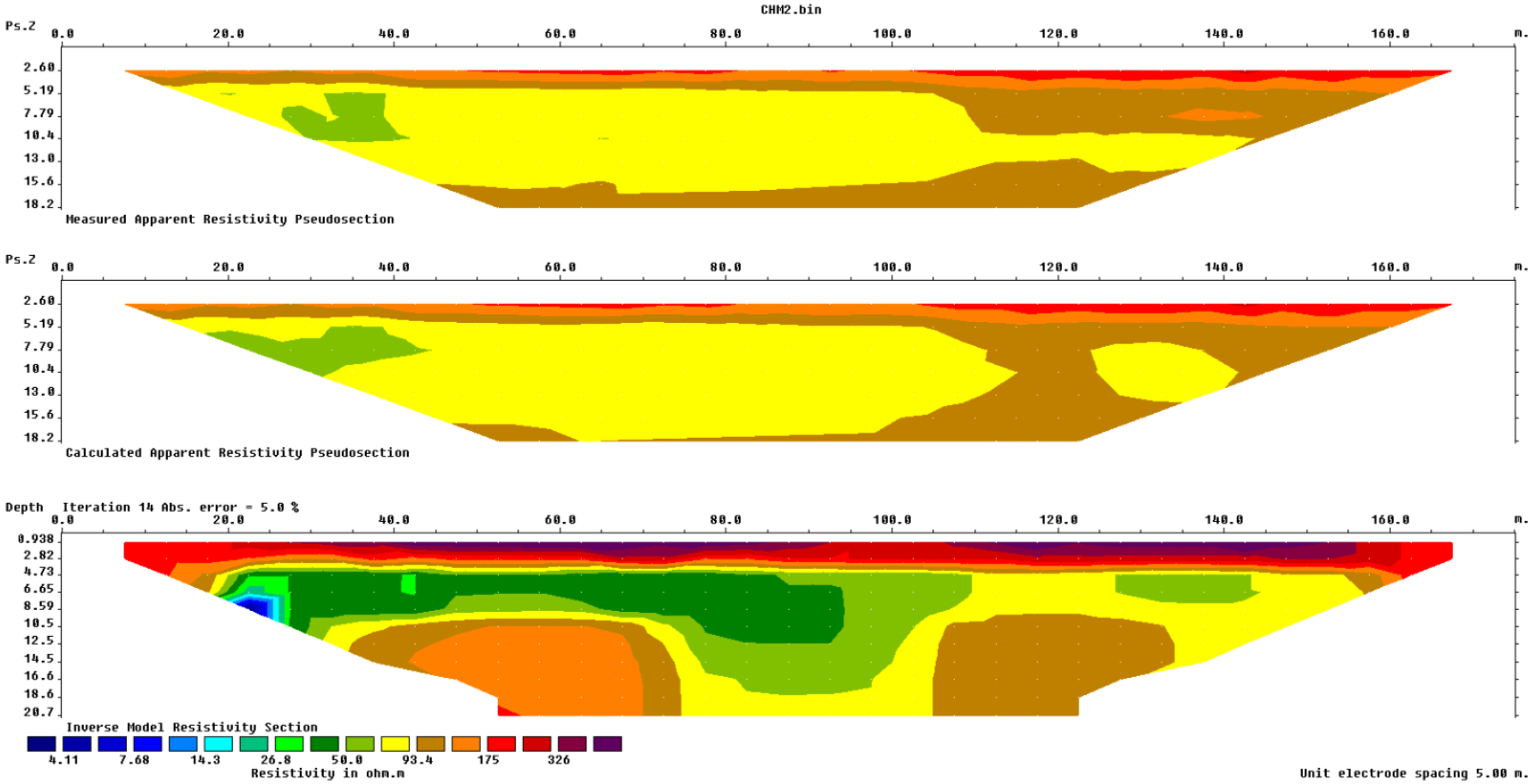

Date	Survey Line	Survey Center Latitude and Longitude	Orientation	Survey Length(m)
5/6/2014	Marian Meadow Transect	40.2633, -121.3141	40°	175

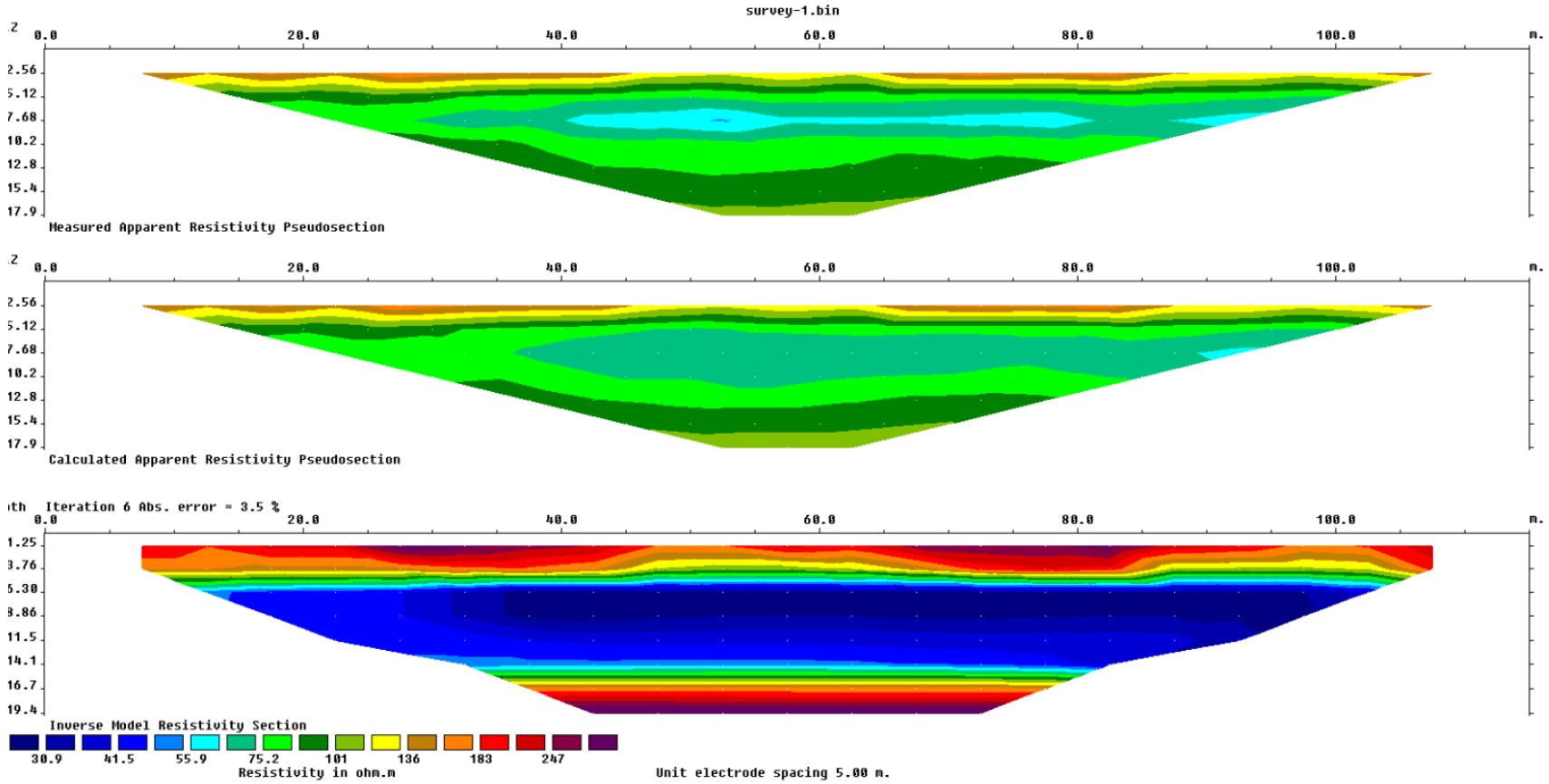

Date	Survey Line	Survey Center Latitude and Longitude	Orientation	Survey Length(m)
9/10/2013	Upper MM Transect Bisecting Long Line	40.2641, -121.3163	65°	115

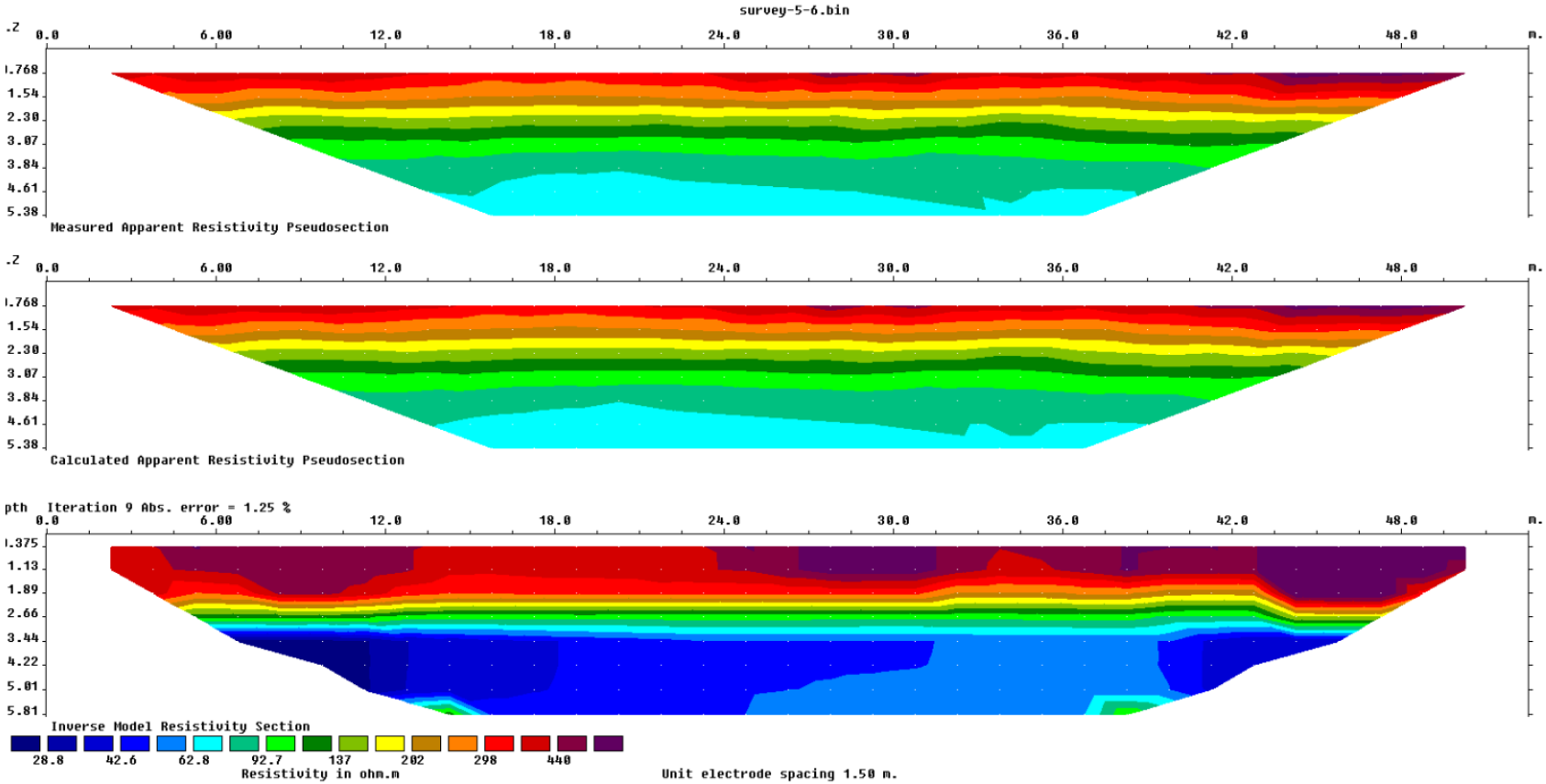

Date	Survey Line	Survey Center Latitude and Longitude	Orientation	Survey Length(m)
9/10/2013	Upper MM Transect Bisecting Line	40.2641, -121.3163	65°	34.5

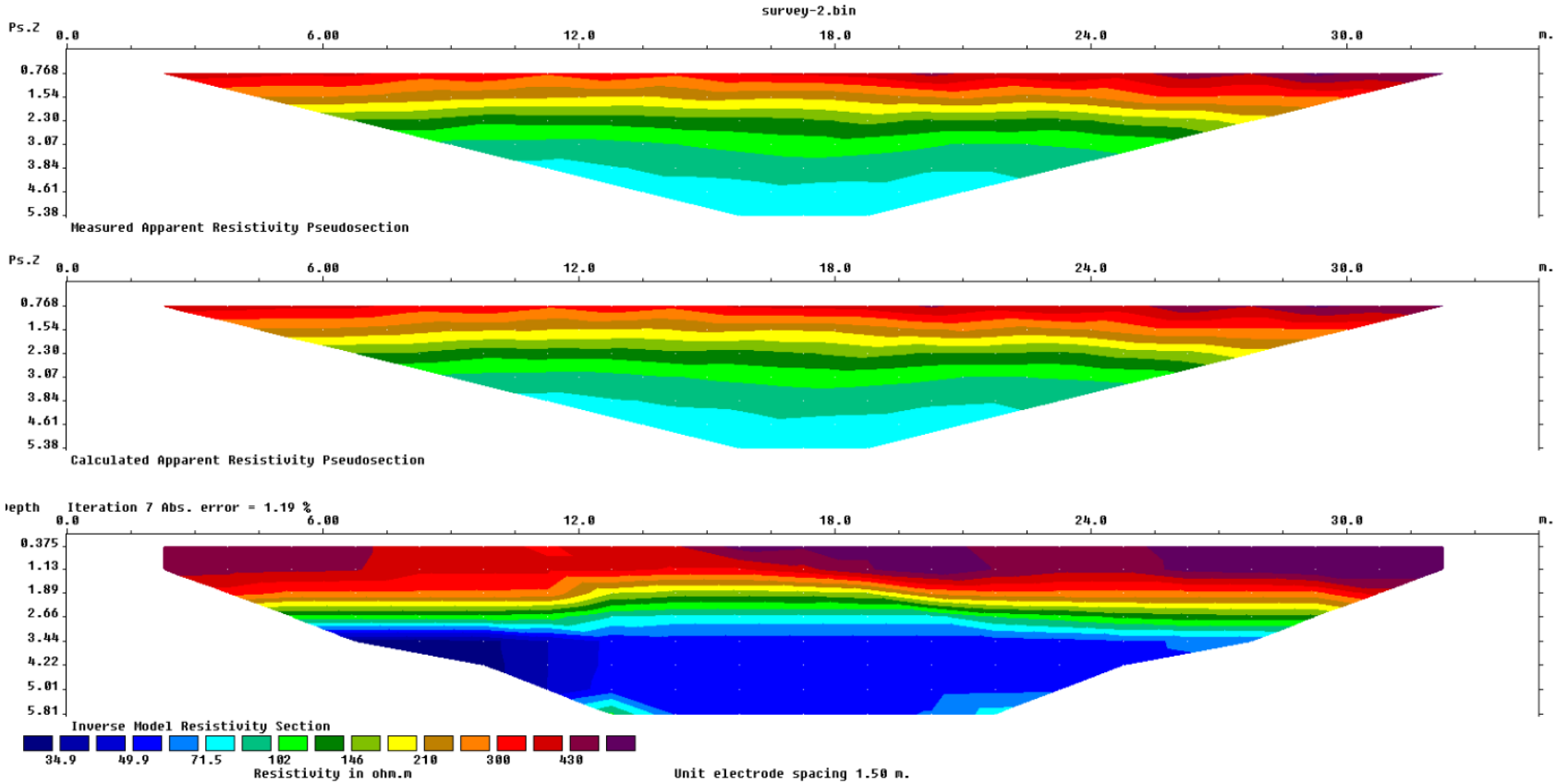

Date	Survey Line	Survey Center Latitude and Longitude	Orientation	Survey Length(m)
9/10/2013	Upper MM Transect Bisecting Short Line	40.2641, -121.3163	65°	34.5

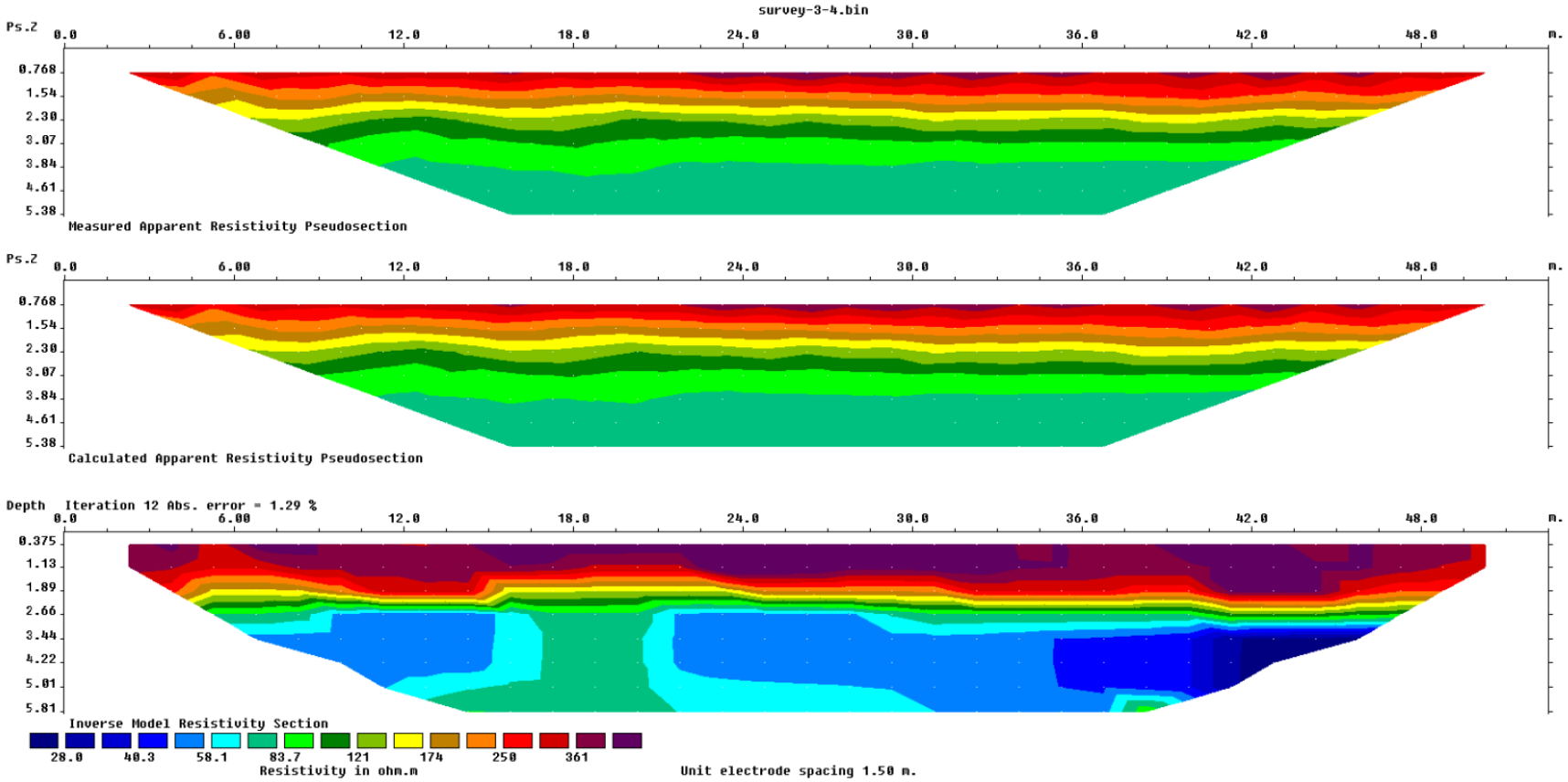

Date	Survey Line	Survey Center Latitude and Longitude	Orientation	Survey Length(m)
9/10/2013	Marian Meadow Transect	40.2642,-121.3164	340°	51.75

Appendix B:

Control Meadow Apparent Resistivity Pseudosections, Calculated Apparent Resistivity Pseudosections and Inverse Model Resistivity Sections

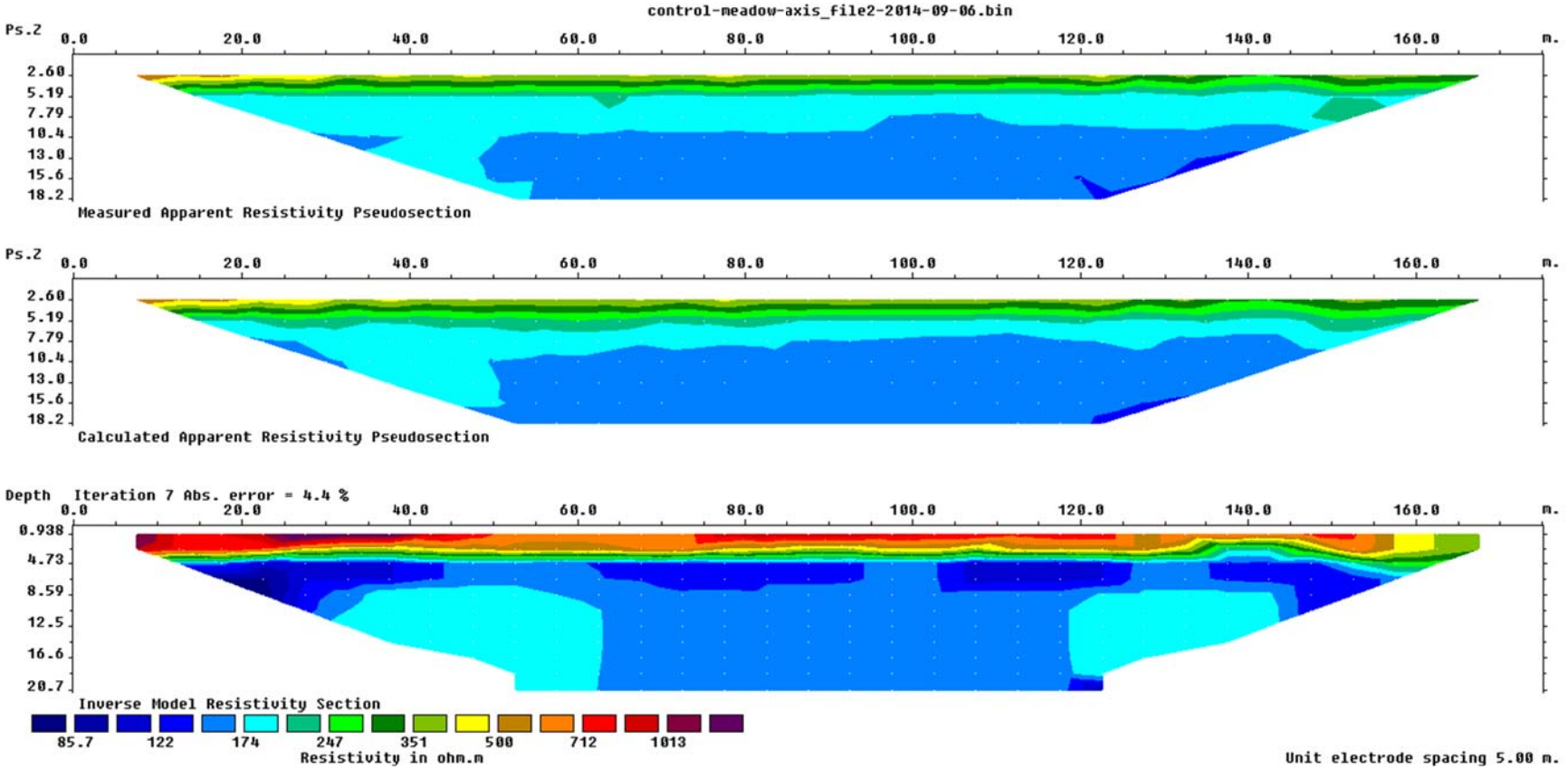

Date	Survey Line	Survey Center Latitude and Longitude	Orientation	Survey Length(m)
9/6/2014	CM Transect	40.2640, -121.3944	335°	170

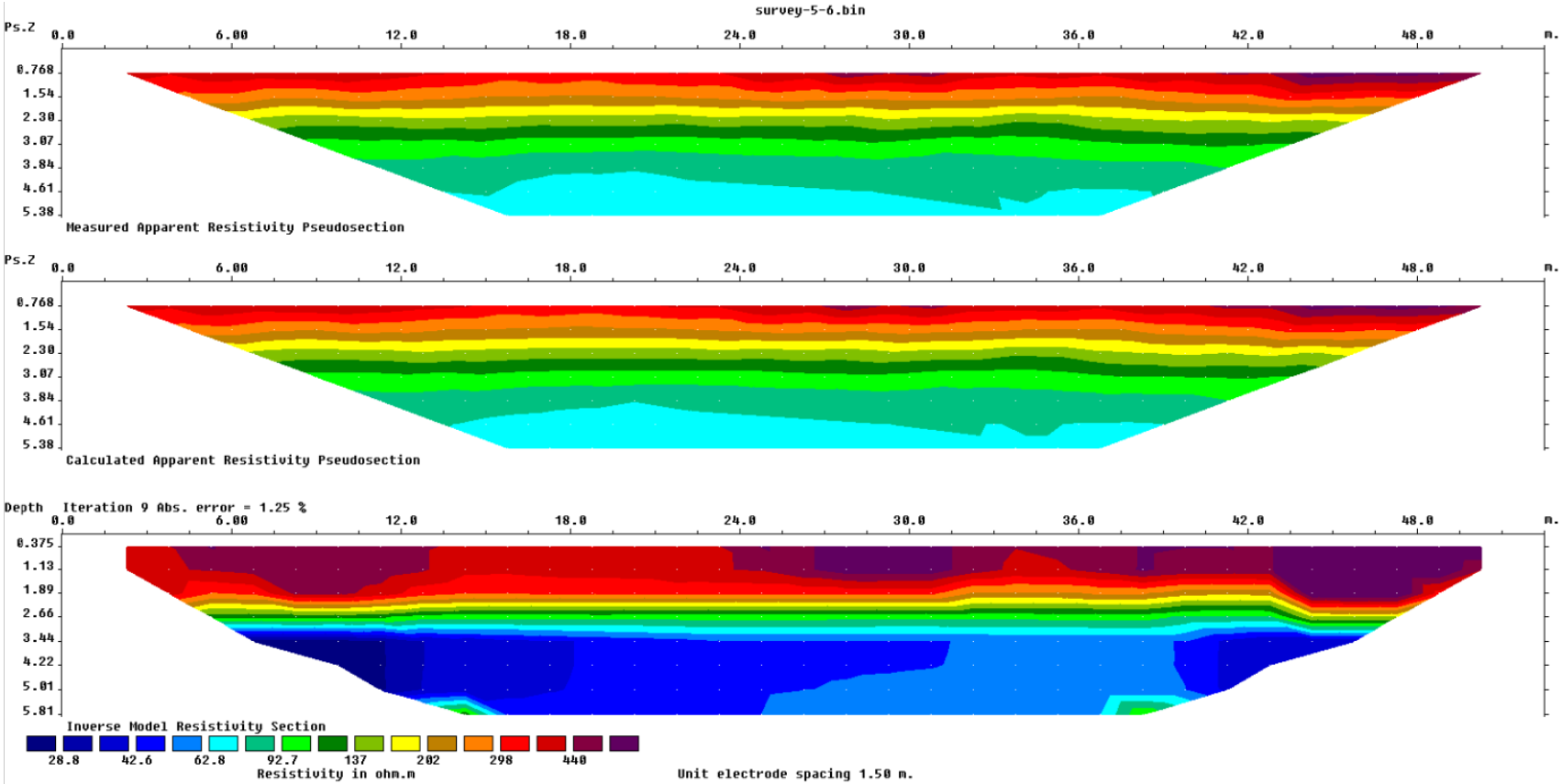

Date	Survey Line	Survey Center Latitude and Longitude	Orientation	Survey Length(m)
9/10/2013	Upper MM Transect Bisecting Line	40.2641, -121.3163	65°	34.5

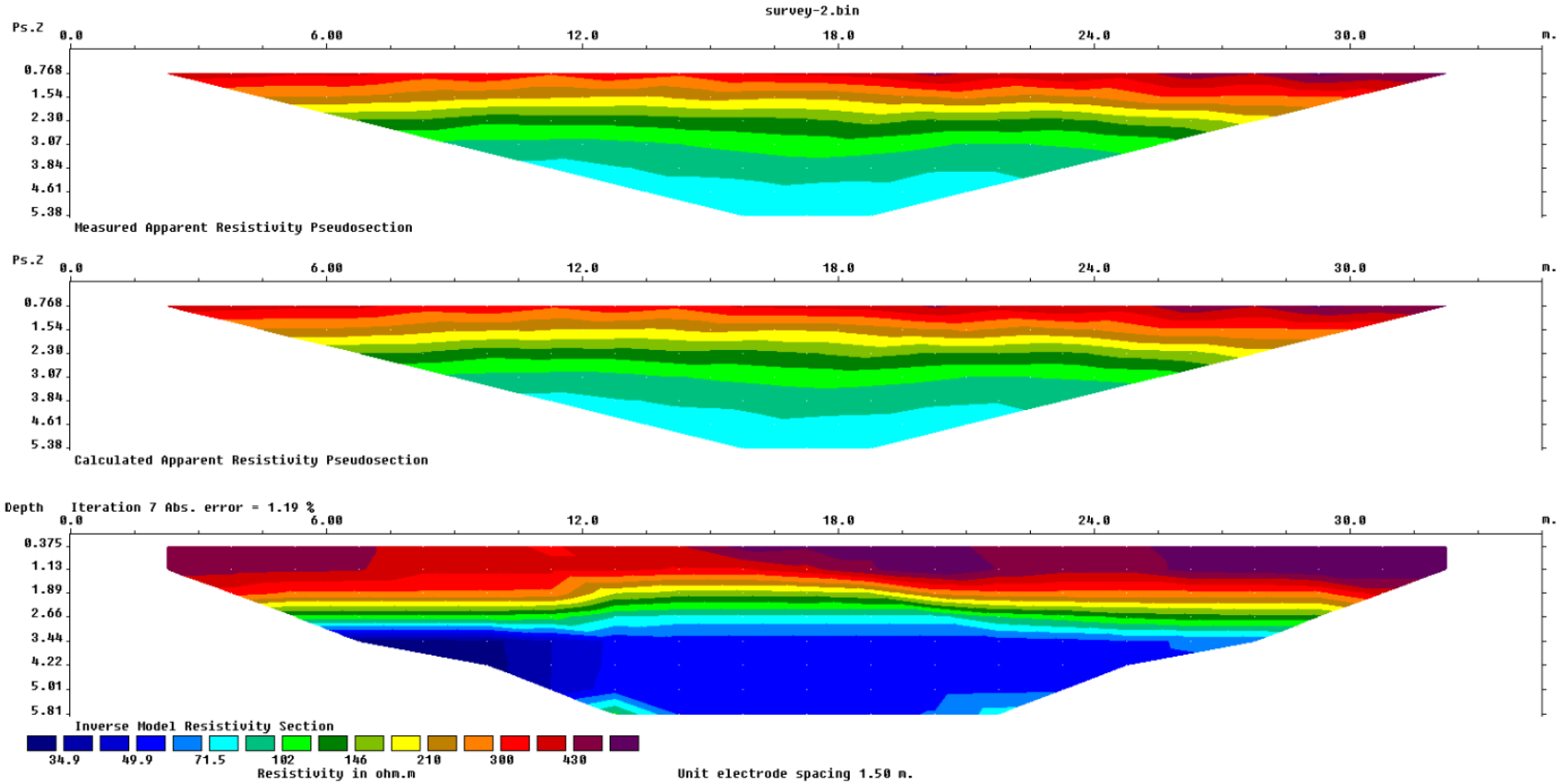

Date	Survey Line	Survey Center Latitude and Longitude	Orientation	Survey Length(m)
9/10/2013	Upper MM Transect Bisecting Short Line	40.2641, -121.3163	65°	34.5

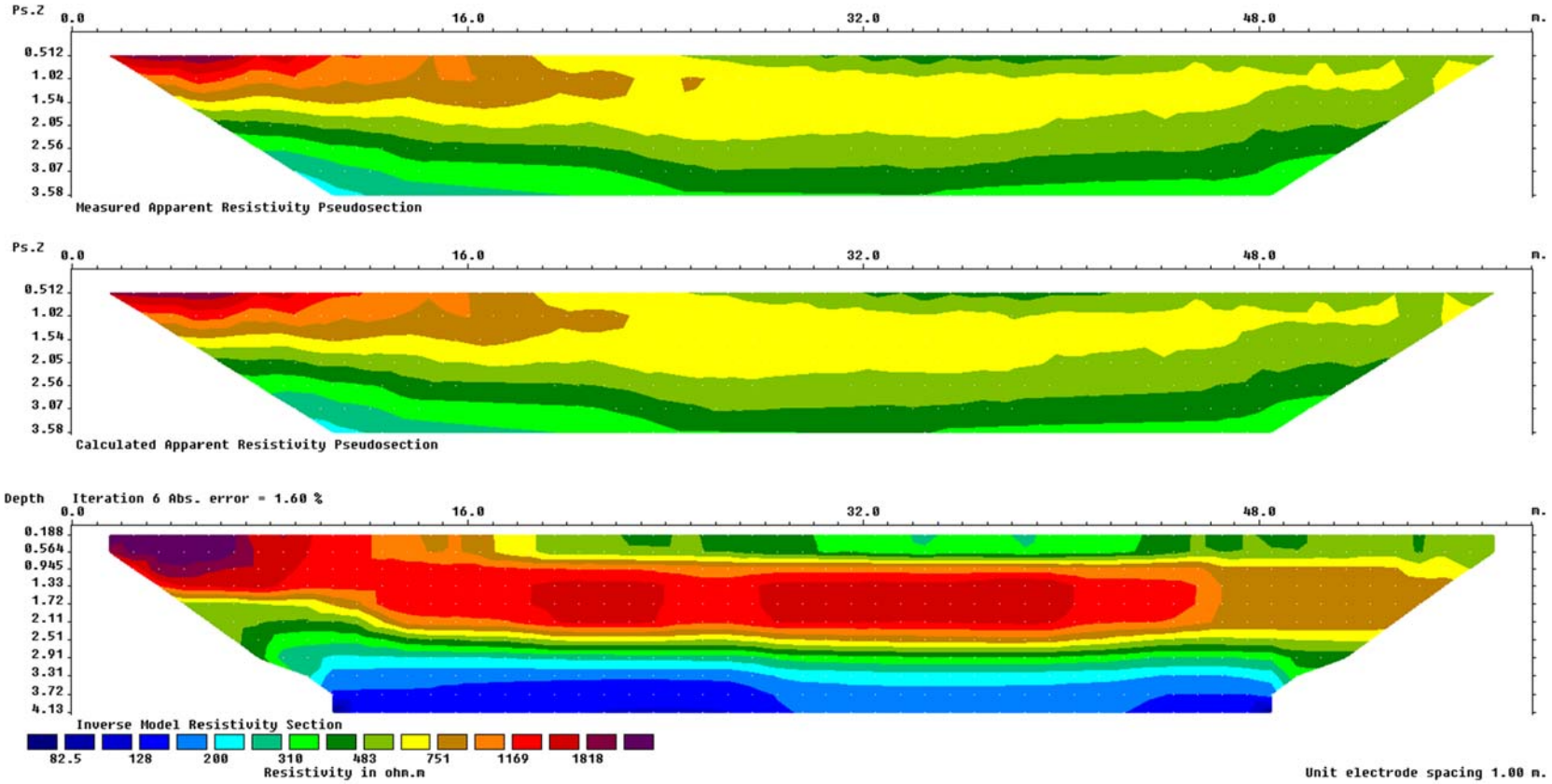

Date	Survey Line	Survey Center Latitude and Longitude	Orientation	Survey Length(m)
5/6/2014	Ecotone Boundary	40.2650, -121.3940	55°	72

Appendix C

Marian Meadow Hydrologic Data

Marian Meadow Soil Moisture Storage (ft)										
Week	**3-1**	**3-4**	**4-1**	**4-2**	**6-3**	**6-4**	**9-2**	**9-3**	**Average**	**St Dev(±)**
9/13/2013	0.93	0.53	0.86	1.26	1.22	0.87			0.94	0.27
9/20/2013	0.87	0.50	0.80	1.22	1.14	0.82			0.89	0.26
9/27/2013	0.83	0.48	0.76	1.22	1.08	0.77			0.86	0.26
10/4/2013	0.79	0.46	0.72	1.15	1.03	0.73			0.81	0.25
10/11/2013	0.75	0.57	0.73	1.48	0.99	0.73			0.87	0.33
10/18/2013	0.73	0.63	0.72	1.47	0.96	0.76			0.88	0.31
10/25/2013	0.70	0.60	0.69	1.29	0.93	0.75			0.83	0.25
11/1/2013	0.68	0.56	0.66	1.20	0.89	0.72			0.78	0.23
11/8/2013	0.66	0.54	0.63	1.13	0.86	0.69			0.75	0.21
11/15/2013	0.89	0.60	0.67	1.12	0.83	0.81			0.82	0.18
11/22/2013	1.38	0.95	0.99	1.39	0.94	1.31			1.16	0.22
11/29/2013	1.27	0.86	0.91	1.27	1.03	1.18			1.09	0.18
12/6/2013	1.16	0.74	0.80	1.15	0.94	1.04			0.97	0.18
12/13/2013	1.08	0.66	0.69	1.01	0.84	0.93			0.87	0.17
12/20/2013	1.02	0.59	0.63	0.90	0.80	0.85			0.80	0.16
12/27/2013	0.97	0.50	0.56	0.84	0.75	0.71			0.72	0.17
1/3/2014	0.93	0.46	0.54	0.80	0.72	0.63			0.68	0.17
1/10/2014	0.88	0.58	0.60	0.90	0.74	0.70			0.73	0.14
1/17/2014	0.85	0.55	0.52	0.82	0.66	0.56			0.66	0.14
1/24/2014	0.84	0.58	0.64	1.12	0.76	0.60			0.76	0.20
1/31/2014	0.89	0.72	0.94	1.49	1.22	0.86			1.02	0.28
2/7/2014	0.93	0.73	0.82	1.20	1.05	0.82			0.92	0.17
2/14/2014	0.91	0.52	0.77	1.12	1.08	0.80			0.87	0.22
2/21/2014	0.85	0.52	0.69	0.98	1.02	0.73			0.80	0.19
2/28/2014	0.80	0.45	0.61	0.80	0.93	0.66			0.71	0.17
3/7/2014	0.76	0.32	0.42	0.52	0.60	0.38			0.50	0.16
3/14/2014	0.76	0.25	0.41	0.49	0.57	0.37			0.48	0.18
3/21/2014	0.76	0.27	0.43	0.52	0.62	0.43			0.51	0.17
3/28/2014	0.81	0.25	0.43	0.44	0.58	0.37			0.48	0.19
4/4/2014	0.81	0.22	0.59	0.43	0.57	0.35			0.50	0.21
4/11/2014	0.80	0.25	0.54	0.50	0.66	0.42			0.53	0.19
4/18/2014	0.80	0.26	0.52	0.51	0.68	0.44			0.54	0.19
4/25/2014	0.79	0.27	0.53	0.51	0.69	0.46			0.54	0.18
5/2/2014	0.49	0.32	0.53	0.54	1.01	0.50	0.60		0.57	0.21
5/9/2014	0.43	0.35	0.56	0.57	0.91	0.54	0.69		0.58	0.18
5/16/2014	0.45	0.39	0.56	0.61	0.92	0.58	0.72		0.60	0.17
5/23/2014	0.46	0.42	0.60	0.63	0.99	0.62	0.76		0.64	0.19
5/30/2014	0.46	0.46	0.64	0.66	1.05	0.65	0.79		0.67	0.20
6/6/2014	0.55	0.50	0.72	0.72	1.09	0.68	0.82		0.73	0.19

6/13/2014	0.76	0.55	0.81	0.80	1.10	0.67	0.85		0.79	0.17
6/20/2014	0.79	0.59	0.86	0.85	1.12	0.71	0.87		0.83	0.16
6/27/2014	0.83	0.63	0.90	0.90	1.15	0.76	0.91		0.87	0.16
7/4/2014	0.86	0.65	0.95	0.95	1.20	0.80	0.94		0.91	0.17
7/11/2014	0.90	0.68	1.00	1.01	1.26	0.83	0.98		0.95	0.18
7/18/2014	0.93	0.70	1.05	1.08	1.32	0.86	1.02		0.99	0.19
7/25/2014	0.96	0.73	1.09	1.13	1.36	0.90	1.05		1.03	0.20
8/1/2014	1.14	0.77	1.13	1.19	1.41	0.93	1.08		1.09	0.20
8/8/2014	1.35	0.85	1.22	1.29	1.50	0.99	1.16		1.19	0.22
8/15/2014	1.30	0.94	1.31	1.38	1.60	1.10	1.23		1.27	0.21
8/22/2014	1.31	1.01	1.40	1.48	1.70	1.21	1.31		1.35	0.22
8/29/2014	1.37	1.09	1.49	1.59	1.80	1.32	1.38		1.43	0.23
9/5/2014	1.44	1.17	1.59	1.69	1.75	1.43	1.42		1.50	0.20
9/12/2014	1.34	1.08	1.50	1.59	1.45	1.33	1.30		1.37	0.17
9/19/2014	1.30	0.98	1.41	1.48	1.33	1.29	1.18		1.28	0.17
9/26/2014	1.60	0.90	1.33	1.41	1.19	1.29	1.07		1.26	0.23
10/3/2014	1.39	0.84	1.26	1.34	1.10	1.19	0.99		1.16	0.20
10/10/2014	1.26	0.78	1.19	1.25	1.02	1.10	0.91		1.07	0.18
10/17/2014	1.18	0.72	1.11	1.16	0.93	1.02	0.83		0.99	0.17
10/24/2014	1.38	0.90	1.20	1.33	0.87	1.35	0.85		1.12	0.24
10/31/2014	1.36	0.99	1.25	1.42	0.96	1.28	0.99		1.18	0.19
11/7/2014	1.22	0.91	1.17	1.31	1.02	1.16	0.92		1.10	0.16
11/14/2014	1.15	0.87	1.14	1.27	1.03	1.14	0.90		1.07	0.15
11/21/2014	1.18	0.83	1.11	1.21	0.99	1.14	0.87		1.05	0.15
11/28/2014	1.10	0.71	0.98	1.06	0.84	1.02	0.75		0.92	0.16
12/5/2014	0.90	0.56	0.81	0.87	0.64	0.83	0.58		0.74	0.14
12/12/2014	0.43	0.24	0.64	0.39	0.59	0.34	0.50		0.45	0.14
12/19/2014	0.44	0.22	0.45	0.36	0.55	0.33	0.46		0.40	0.11

Marian Meadow Volumetric Soil Moisture (%)										
Week	3-1	3-4	4-1	4-2	6-4	6-3	9-2	9-3	Average	St Dev(±)
9/13/2013	10.10	5.78	9.35	13.67	9.43	13.28			10.27	2.91
9/20/2013	9.81	5.67	9.10	13.84	9.32	12.87			10.10	2.93
9/27/2013	9.70	5.69	8.95	14.51	9.27	12.67			10.13	3.09
10/4/2013	9.60	5.65	8.86	14.19	9.19	12.57			10.01	3.01
10/11/2013	9.47	7.34	9.45	19.13	9.61	12.52			11.25	4.20
10/18/2013	9.54	8.52	9.61	19.68	10.41	12.67			11.74	4.13
10/25/2013	9.59	8.49	9.64	18.16	10.82	12.83			11.59	3.54
11/1/2013	9.62	8.25	9.61	17.52	10.91	12.65			11.42	3.33
11/8/2013	9.67	8.19	9.58	17.12	10.99	12.74			11.38	3.20
11/15/2013	13.77	9.71	10.71	18.04	13.55	12.85			13.10	2.91
11/22/2013	22.13	15.91	16.53	23.21	23.11	15.20			19.35	3.84
11/29/2013	21.03	14.95	15.77	22.13	21.80	17.19			18.81	3.22
12/6/2013	19.97	13.48	14.59	21.00	20.15	16.31			17.58	3.21
12/13/2013	19.31	12.49	13.16	19.21	18.85	15.24			16.38	3.15
12/20/2013	18.93	11.69	12.35	17.82	17.95	15.07			15.63	3.09
12/27/2013	18.64	10.20	11.55	17.22	15.79	14.52			14.65	3.26
1/3/2014	18.44	9.93	11.49	17.15	14.60	14.48			14.35	3.24
1/10/2014	18.33	12.94	13.51	20.17	16.95	15.59			16.25	2.80
1/17/2014	18.18	12.74	12.01	19.05	14.24	14.32			15.09	2.88
1/24/2014	18.77	14.08	15.68	27.27	16.09	17.31			18.20	4.72
1/31/2014	20.69	18.38	24.03	37.90	24.11	28.72			25.64	6.96
2/7/2014	24.19	20.96	23.52	34.40	26.65	27.71			26.24	4.66
2/14/2014	24.73	20.12	23.20	33.80	27.21	29.77			26.47	4.88
2/21/2014	24.53	19.64	22.45	31.96	26.99	29.99			25.93	4.64
2/28/2014	25.79	20.56	22.51	29.41	28.11	30.71			26.18	4.00
3/7/2014	26.15	25.94	23.22	28.86	28.42	31.41			27.33	2.84
3/14/2014	26.03	24.87	23.20	28.25	27.97	31.41			26.96	2.89
3/21/2014	25.75	22.55	22.60	27.82	27.76	31.13			26.27	3.34
3/28/2014	28.38	27.80	27.54	28.37	28.72	31.98			28.80	1.62
4/4/2014	28.36	29.30	39.09	28.41	28.92	32.61			31.12	4.22
4/11/2014	27.15	24.44	30.73	28.39	28.45	32.61			28.63	2.83
4/18/2014	27.21	24.40	29.34	28.61	28.68	32.68			28.49	2.71
4/25/2014	26.98	24.76	29.53	28.62	28.81	32.41			28.52	2.56
5/2/2014	26.53	24.40	27.93	28.37	27.56	32.59	23.54		27.28	2.96
5/9/2014	26.18	23.66	27.67	28.17	26.57	32.26	23.06		26.80	3.08
5/16/2014	26.10	23.17	25.74	27.72	25.70	32.34	22.84		26.23	3.19
5/23/2014	25.70	22.71	25.66	27.04	24.65	32.01	22.69		25.78	3.18

5/30/2014	24.99	21.94	25.33	25.96	23.53	31.19	22.10		25.01	3.14
6/6/2014	24.31	21.16	24.84	24.92	22.82	30.25	21.67		24.28	3.03
6/13/2014	23.13	19.86	24.13	23.89	21.73	28.37	20.85		23.14	2.80
6/20/2014	22.30	18.82	23.49	23.27	21.27	27.15	20.23		22.36	2.69
6/27/2014	21.52	17.94	22.95	22.76	20.64	26.15	19.71		21.67	2.64
7/4/2014	20.63	17.02	22.39	22.34	20.10	25.50	19.24		21.03	2.70
7/11/2014	19.76	16.14	21.78	21.98	19.13	25.03	18.81		20.38	2.84
7/18/2014	18.88	15.24	21.05	21.62	18.16	24.40	18.31		19.66	2.96
7/25/2014	18.11	14.60	20.34	21.16	17.52	23.82	17.87		19.06	2.98
8/1/2014	20.12	14.22	19.76	20.86	16.85	23.30	17.50		18.94	2.99
8/8/2014	22.03	14.49	19.73	20.84	16.57	23.24	17.61		19.22	3.14
8/15/2014	19.61	14.51	19.57	20.65	16.81	23.13	17.63		18.84	2.80
8/22/2014	18.26	14.29	19.29	20.52	16.95	23.00	17.62		18.56	2.77
8/29/2014	17.62	14.03	19.04	20.32	16.99	22.78	17.35		18.31	2.77
9/5/2014	17.09	13.76	18.79	20.00	16.90	20.75	16.84		17.73	2.41
9/12/2014	16.74	13.56	18.68	19.77	16.75	18.46	16.52		17.21	1.94
9/19/2014	17.24	13.21	18.62	19.63	17.35	18.25	16.18		17.21	1.99
9/26/2014	22.38	12.95	18.62	19.67	18.42	17.62	15.75		17.92	3.20
10/3/2014	20.56	12.97	18.55	19.66	18.03	17.57	15.70		17.58	2.82
10/10/2014	19.73	12.92	18.53	19.50	17.72	17.54	15.62		17.37	2.67
10/17/2014	19.63	12.75	18.31	19.29	17.61	17.29	15.44		17.19	2.74
10/24/2014	24.46	17.17	21.20	23.40	24.87	17.59	17.12		20.83	3.44
10/31/2014	25.53	20.51	23.44	26.66	25.38	21.21	21.59		23.48	3.46
11/7/2014	24.42	20.10	23.27	26.19	24.59	24.39	21.76		23.53	4.88
11/14/2014	24.42	20.73	24.12	26.89	25.63	26.64	22.89		24.47	2.18
11/21/2014	26.76	21.38	24.90	27.24	27.54	27.94	24.20		25.71	2.36
11/28/2014	28.84	21.72	25.39	27.51	28.82	28.36	25.01		26.52	2.64
12/5/2014	28.83	21.90	25.67	27.60	29.47	28.61	25.14		26.75	2.68
12/12/2014	31.72	29.81	45.85	28.21	30.28	29.88	24.98		31.53	6.66
12/19/2014	39.20	30.25	35.99	28.55	31.04	31.57	25.12		31.68	4.66

Marian Meadow Depth to Groundwater(ft)									
Week	**3-1**	**3-4**	**4-1**	**6-3**	**6-4**	**9-2**	**9-3**	**Average**	**St Dev (±)**
9/13/2013	9.18	9.18	9.18	9.18	9.18	9.18	9.18	9.18	0.00
9/20/2013	8.83	8.79	8.79	8.82	8.74	8.82	8.72	8.79	0.04
9/27/2013	8.51	8.43	8.43	8.50	8.35	8.50	8.31	8.43	0.08
10/4/2013	8.21	8.10	8.10	8.19	7.98	8.20	7.93	8.10	0.11
10/11/2013	7.89	7.75	7.76	7.87	7.60	7.88	7.53	7.76	0.14
10/18/2013	7.62	7.45	7.45	7.59	7.27	7.60	7.18	7.45	0.17
10/25/2013	7.31	7.12	7.12	7.28	6.91	7.30	6.82	7.12	0.20
11/1/2013	7.06	6.84	6.84	7.02	6.61	7.04	6.50	6.85	0.22
11/8/2013	6.81	6.57	6.58	6.77	6.32	6.79	6.20	6.58	0.24
11/15/2013	6.48	6.22	6.22	6.44	5.95	6.46	5.82	6.23	0.26
11/22/2013	6.25	5.98	5.98	6.21	5.69	6.23	5.56	5.98	0.28
11/29/2013	6.03	5.74	5.74	5.98	5.43	6.01	5.29	5.75	0.29
12/6/2013	5.79	5.48	5.48	5.74	5.16	5.76	5.02	5.49	0.30
12/13/2013	5.58	5.26	5.27	5.53	4.93	5.56	4.79	5.27	0.32
12/20/2013	5.39	5.06	5.06	5.33	4.72	5.36	4.57	5.07	0.33
12/27/2013	5.20	4.86	4.86	5.14	4.51	5.17	4.36	4.87	0.33
1/3/2014	5.02	4.67	4.67	4.96	4.31	4.99	4.15	4.68	0.34
1/10/2014	4.82	4.46	4.47	4.76	4.10	4.79	3.94	4.48	0.35
1/17/2014	4.65	4.28	4.29	4.59	3.92	4.62	3.76	4.30	0.35
1/24/2014	4.46	4.09	4.09	4.40	3.72	4.43	3.56	4.11	0.36
1/31/2014	4.30	3.92	3.93	4.23	3.55	4.27	3.39	3.94	0.36
2/7/2014	3.85	3.47	3.47	3.78	3.09	3.82	2.93	3.49	0.36
2/14/2014	3.69	2.59	3.31	3.62	2.93	3.66	2.80	3.23	0.45
2/21/2014	3.45	2.63	3.07	3.38	2.69	3.42	3.01	3.09	0.34
2/28/2014	3.10	2.18	2.72	3.04	2.35	3.07	2.54	2.71	0.37
3/7/2014	2.92	1.22	1.79	1.91	1.35	2.58	1.71	1.93	0.62
3/14/2014	2.92	1.00	1.75	1.81	1.34	2.14	1.59	1.79	0.61
3/21/2014	2.97	1.19	1.89	1.99	1.54	2.47	1.74	1.97	0.59
3/28/2014	2.84	0.89	1.55	1.82	1.27	2.31	1.44	1.73	0.66
4/4/2014	2.84	0.76	1.51	1.76	1.21	1.89	1.34	1.62	0.65
4/11/2014	2.96	1.04	1.77	2.02	1.46	2.06	1.56	1.84	0.61
4/18/2014	2.95	1.08	1.78	2.08	1.54	2.21	1.64	1.90	0.59
4/25/2014	2.93	1.09	1.78	2.12	1.59	2.30	1.69	1.93	0.59
5/2/2014	1.85	1.30	1.91	3.09	1.81	2.55	1.85	2.05	0.58
5/9/2014	1.65	1.50	2.04	2.83	2.03	2.98	1.99	2.15	0.56
5/16/2014	1.73	1.69	2.19	2.84	2.25	3.15	2.16	2.29	0.54
5/23/2014	1.78	1.86	2.35	3.10	2.50	3.35	2.41	2.48	0.58
5/30/2014	1.86	2.09	2.55	3.38	2.77	3.57	2.74	2.71	0.62
6/6/2014	2.25	2.38	2.88	3.61	2.99	3.81	3.06	3.00	0.58

6/13/2014	3.29	2.79	3.37	3.86	3.08	4.05	3.41	3.41	0.43
6/20/2014	3.56	3.16	3.64	4.13	3.36	4.32	3.68	3.69	0.41
6/27/2014	3.86	3.51	3.94	4.41	3.66	4.60	3.98	3.99	0.39
7/4/2014	4.19	3.84	4.26	4.72	3.99	4.90	4.30	4.31	0.38
7/11/2014	4.53	4.20	4.61	5.04	4.34	5.21	4.64	4.66	0.36
7/18/2014	4.91	4.60	4.99	5.39	4.73	5.55	5.02	5.03	0.34
7/25/2014	5.29	5.00	5.36	5.73	5.12	5.87	5.39	5.39	0.31
8/1/2014	5.65	5.39	5.71	6.04	5.50	6.17	5.74	5.74	0.28
8/8/2014	6.12	5.90	6.18	6.46	5.99	6.57	6.20	6.20	0.24
8/15/2014	6.63	6.46	6.69	6.91	6.53	7.00	6.70	6.70	0.19
8/22/2014	7.19	7.07	7.23	7.39	7.12	7.46	7.24	7.24	0.14
8/29/2014	7.80	7.74	7.83	7.91	7.76	7.94	7.82	7.83	0.07
9/5/2014	8.45	8.47	8.47	8.45	8.45	8.46	8.46	8.46	0.01
9/12/2014	8.01	7.94	8.03	7.86	7.96	7.87	7.97	7.95	0.06
9/19/2014	7.54	7.39	7.56	7.26	7.46	7.29	7.47	7.42	0.12
9/26/2014	7.14	6.92	7.17	6.75	7.02	6.78	7.04	6.97	0.16
10/3/2014	6.77	6.49	6.79	6.28	6.62	6.31	6.63	6.56	0.21
10/10/2014	6.37	6.04	6.40	5.80	6.19	5.83	6.21	6.12	0.24
10/17/2014	6.01	5.63	6.04	5.37	5.81	5.40	5.83	5.73	0.27
10/24/2014	5.64	5.22	5.67	4.94	5.42	4.98	5.44	5.33	0.30
10/31/2014	5.31	4.85	5.33	4.55	5.06	4.59	5.09	4.97	0.32
11/7/2014	4.99	4.51	5.02	4.19	4.73	4.24	4.76	4.64	0.33
11/14/2014	4.71	4.20	4.74	3.88	4.44	3.92	4.46	4.34	0.35
11/21/2014	4.42	3.89	4.44	3.56	4.13	3.60	4.16	4.03	0.36
11/28/2014	3.83	3.29	3.86	2.95	3.54	3.00	3.57	3.43	0.37
12/5/2014	3.13	2.58	3.15	2.24	2.83	2.29	2.86	2.73	0.37
12/12/2014	1.37	0.81	1.39	1.97	1.12	2.01	1.30	1.42	0.43
12/19/2014	1.12	0.72	1.25	1.74	1.07	1.82	1.09	1.26	0.39

Marian Meadow Groundwater Storage (ft)									
Week	3-1	3-4	4-1	6-3	6-4	9-2	9-3	Average	St Dev (±)
9/13/2013	14.10	14.10	14.10	14.10	14.10		14.10	14.10	0.00
9/20/2013	14.26	14.28	14.28	14.26	14.29		14.31	14.28	0.02
9/27/2013	14.40	14.43	14.43	14.40	14.47		14.49	14.43	0.03
10/4/2013	14.53	14.58	14.58	14.54	14.63		14.66	14.58	0.05
10/11/2013	14.67	14.73	14.73	14.68	14.80		14.83	14.73	0.06
10/18/2013	14.79	14.87	14.87	14.81	14.95		14.99	14.87	0.08
10/25/2013	14.93	15.01	15.01	14.94	15.11		15.15	15.01	0.09
11/1/2013	15.04	15.14	15.14	15.06	15.24		15.29	15.14	0.10
11/8/2013	15.15	15.26	15.26	15.17	15.37		15.42	15.25	0.11
11/15/2013	15.30	15.41	15.41	15.32	15.53		15.59	15.41	0.12
11/22/2013	15.40	15.52	15.52	15.42	15.65		15.71	15.52	0.12
11/29/2013	15.50	15.63	15.63	15.52	15.76		15.82	15.62	0.13
12/6/2013	15.60	15.74	15.74	15.63	15.88		15.95	15.74	0.14
12/13/2013	15.70	15.84	15.84	15.72	15.98		16.05	15.83	0.14
12/20/2013	15.78	15.93	15.93	15.81	16.08		16.15	15.92	0.14
12/27/2013	15.87	16.02	16.01	15.89	16.17		16.24	16.01	0.15
1/3/2014	15.95	16.10	16.10	15.97	16.26		16.33	16.10	0.15
1/10/2014	16.03	16.19	16.19	16.06	16.35		16.42	16.19	0.15
1/17/2014	16.11	16.27	16.27	16.14	16.43		16.50	16.26	0.16
1/24/2014	16.19	16.36	16.36	16.22	16.52		16.59	16.35	0.16
1/31/2014	16.27	16.43	16.43	16.29	16.60		16.67	16.42	0.16
2/7/2014	16.46	16.63	16.63	16.49	16.80		16.87	16.62	0.16
2/14/2014	16.54	17.02	16.70	16.56	16.87		16.93	16.74	0.20
2/21/2014	16.64	17.00	16.81	16.67	16.98		16.83	16.80	0.15
2/28/2014	16.80	17.21	16.96	16.82	17.13		17.04	16.97	0.16
3/7/2014	16.88	17.63	17.38	17.33	17.57		17.41	17.32	0.27
3/14/2014	16.88	17.72	17.39	17.37	17.58		17.47	17.37	0.29
3/21/2014	16.85	17.64	17.33	17.29	17.49		17.40	17.30	0.27
3/28/2014	16.91	17.78	17.48	17.36	17.60		17.53	17.40	0.30
4/4/2014	16.91	17.83	17.50	17.39	17.63		17.58	17.45	0.31
4/11/2014	16.86	17.71	17.39	17.27	17.52		17.48	17.35	0.29
4/18/2014	16.86	17.69	17.38	17.25	17.49		17.44	17.33	0.28
4/25/2014	16.87	17.69	17.38	17.23	17.46		17.42	17.32	0.27
5/2/2014	17.35	17.59	17.32	16.80	17.37	17.90	17.35	17.26	0.33
5/9/2014	17.44	17.51	17.27	16.92	17.27	17.87	17.29	17.22	0.29
5/16/2014	17.40	17.42	17.20	16.91	17.17	17.85	17.21	17.16	0.29
5/23/2014	17.38	17.35	17.13	16.80	17.06	17.83	17.10	17.07	0.33
5/30/2014	17.35	17.24	17.04	16.67	16.94	17.82	16.96	16.97	0.37
6/6/2014	17.17	17.12	16.89	16.57	16.84	17.80	16.81	16.84	0.40

6/13/2014	16.71	16.93	16.68	16.46	16.80	17.80	16.66	16.66	0.44
6/20/2014	16.59	16.77	16.56	16.34	16.68	17.78	16.54	16.53	0.47
6/27/2014	16.46	16.61	16.42	16.21	16.55	17.77	16.41	16.40	0.52
7/4/2014	16.31	16.47	16.28	16.08	16.40	17.75	16.26	16.26	0.56
7/11/2014	16.16	16.31	16.13	15.93	16.24	17.74	16.11	16.11	0.61
7/18/2014	15.99	16.13	15.96	15.78	16.07	17.72	15.95	15.94	0.67
7/25/2014	15.83	15.95	15.80	15.63	15.90	17.70	15.78	15.78	0.72
8/1/2014	15.67	15.78	15.64	15.49	15.73	17.69	15.63	15.62	0.77
8/8/2014	15.46	15.56	15.43	15.30	15.51	17.66	15.42	15.42	0.84
8/15/2014	15.23	15.31	15.21	15.11	15.28	17.62	15.20	15.20	0.91
8/22/2014	14.98	15.04	14.96	14.89	15.02	17.59	14.96	14.96	0.99
8/29/2014	14.72	14.74	14.70	14.67	14.73	17.56	14.70	14.70	1.08
9/5/2014	14.42	14.41	14.42	14.42	14.42	17.54	14.42	14.42	1.18
9/12/2014	14.62	14.65	14.61	14.69	14.64	17.59	14.64	14.65	1.12
9/19/2014	14.83	14.89	14.82	14.95	14.86	17.65	14.86	14.88	1.05
9/26/2014	15.00	15.10	14.99	15.18	15.06	17.70	15.05	15.08	1.00
10/3/2014	15.17	15.29	15.16	15.39	15.24	17.73	15.23	15.26	0.94
10/10/2014	15.35	15.49	15.33	15.60	15.43	17.77	15.42	15.46	0.89
10/17/2014	15.50	15.68	15.49	15.79	15.60	17.80	15.59	15.63	0.83
10/24/2014	15.67	15.86	15.66	15.98	15.77	17.79	15.76	15.81	0.77
10/31/2014	15.82	16.02	15.81	16.15	15.93	17.73	15.92	15.97	0.69
11/7/2014	15.96	16.17	15.94	16.31	16.07	17.76	16.06	16.12	0.65
11/14/2014	16.08	16.31	16.07	16.45	16.20	17.77	16.19	16.25	0.60
11/21/2014	16.21	16.45	16.20	16.59	16.34	17.78	16.33	16.38	0.56
11/28/2014	16.47	16.71	16.46	16.86	16.60	17.84	16.59	16.65	0.48
12/5/2014	16.78	17.03	16.77	17.17	16.91	17.91	16.90	16.96	0.40
12/12/2014	17.56	17.81	17.55	17.30	17.67	17.95	17.59	17.54	0.21
12/19/2014	17.67	17.85	17.62	17.40	17.69	17.97	17.69	17.61	0.18

Marian Meadow Water Balance (ft)					
Week	**Priestley AET**	**Precipitation**	**Δ Soil Moisture Storage**	**Δ Groundwater Storage**	**Inputs-Outputs**
9/13/2013	-0.09	0.00			
9/20/2013	-0.06	0.04	-0.05	0.18	0.10
9/27/2013	-0.06	0.01	-0.03	0.16	0.07
10/4/2013	-0.05	0.00	-0.04	0.15	0.05
10/11/2013	-0.04	0.03	0.06	0.15	0.20
10/18/2013	-0.04	0.00	0.00	0.13	0.10
10/25/2013	-0.02	0.04	-0.05	0.15	0.11
11/1/2013	-0.03	0.00	-0.04	0.12	0.05
11/8/2013	-0.02	0.00	-0.03	0.12	0.06
11/15/2013	-0.01	0.09	0.07	0.16	0.30
11/22/2013	-0.01	0.00	0.34	0.11	0.44
11/29/2013	-0.01	0.01	-0.08	0.11	0.03
12/6/2013	0.00	0.03	-0.12	0.11	0.02
12/13/2013	-0.01	0.00	-0.10	0.10	-0.01
12/20/2013	-0.01	0.00	-0.07	0.09	0.01
12/27/2013	-0.01	0.00	-0.08	0.09	0.00
1/3/2014	-0.01	0.00	-0.04	0.08	0.04
1/10/2014	-0.01	0.02	0.05	0.09	0.15
1/17/2014	-0.01	0.00	-0.08	0.08	-0.01
1/24/2014	-0.02	0.03	0.10	0.09	0.19
1/31/2014	-0.01	0.01	0.26	0.07	0.33
2/7/2014	-0.02	0.30	-0.10	0.20	0.39
2/14/2014	-0.03	0.03	-0.06	0.11	0.05
2/21/2014	-0.04	0.11	-0.07	0.06	0.06
2/28/2014	-0.03	0.23	-0.09	0.17	0.28
3/7/2014	-0.05	0.08	-0.21	0.35	0.16
3/14/2014	-0.07	0.00	-0.02	0.06	-0.03
3/21/2014	-0.07	0.05	0.03	-0.08	-0.07
3/28/2014	-0.04	0.28	-0.03	0.11	0.31
4/4/2014	-0.09	0.01	0.02	0.05	-0.01
4/11/2014	-0.11	0.02	0.03	-0.10	-0.15
4/18/2014	-0.11	0.02	0.01	-0.03	-0.11
4/25/2014	-0.10	0.04	0.00	-0.01	-0.07
5/2/2014	-0.11	0.03	0.03	-0.05	-0.11
5/9/2014	-0.13	0.01	0.01	-0.04	-0.15
5/16/2014	-0.11	0.02	0.02	-0.06	-0.13

5/23/2014	-0.15	0.00	0.04	-0.08	-0.19
5/30/2014	-0.15	0.00	0.03	-0.10	-0.22
6/6/2014	-0.16	0.00	0.05	-0.13	-0.24
6/13/2014	-0.14	0.00	0.07	-0.18	-0.26
6/20/2014	-0.15	0.00	0.04	-0.13	-0.24
6/27/2014	-0.17	0.00	0.04	-0.13	-0.26
7/4/2014	-0.16	0.00	0.04	-0.14	-0.26
7/11/2014	-0.15	0.00	0.04	-0.15	-0.26
7/18/2014	-0.12	0.00	0.04	-0.16	-0.25
7/25/2014	-0.12	0.04	0.04	-0.16	-0.21
8/1/2014	-0.10	0.08	0.06	-0.15	-0.11
8/8/2014	-0.13	0.00	0.10	-0.20	-0.23
8/15/2014	-0.14	0.00	0.07	-0.22	-0.29
8/22/2014	-0.13	0.00	0.08	-0.24	-0.29
8/29/2014	-0.11	0.00	0.09	-0.26	-0.28
9/5/2014	-0.10	0.00	0.07	-0.28	-0.31
9/12/2014	-0.09	0.00	-0.13	0.23	0.01
9/19/2014	-0.07	0.05	-0.09	0.23	0.12
9/26/2014	-0.06	0.00	-0.03	0.20	0.12
10/3/2014	-0.07	0.00	-0.10	0.19	0.02
10/10/2014	-0.05	0.04	-0.09	0.19	0.10
10/17/2014	-0.03	0.03	-0.08	0.17	0.09
10/24/2014	-0.03	0.05	0.13	0.18	0.33
10/31/2014	-0.03	0.04	0.06	0.16	0.23
11/7/2014	-0.03	0.04	-0.08	0.15	0.08
11/14/2014	-0.01	0.02	-0.03	0.13	0.11
11/21/2014	-0.01	0.05	-0.02	0.14	0.15
11/28/2014	0.00	0.35	-0.12	0.26	0.49
12/5/2014	0.00	0.50	-0.18	0.31	0.63
12/12/2014	-0.01	0.12	-0.29	0.58	0.40
12/19/2014	0.00	0.08	-0.05	0.07	0.10

Appendix D

Control Meadow Hydrologic Data

Control Meadow Soil Moisture Storage (ft.)									
Week	**C4-3**	**C4-1**	**C3-2**	**C3-1**	**C2-4**	**C1-3**	**C1-2**	**Average**	**St Dev(±)**
9/13/2013						0.49	0.49	0.49	0.00
9/20/2013						0.92	0.92	0.92	0.00
9/27/2013						1.72	1.58	1.65	0.10
10/4/2013						1.53	1.39	1.46	0.10
10/11/2013						1.31	1.53	1.42	0.16
10/18/2013						1.28	1.44	1.36	0.11
10/25/2013						1.12	1.50	1.31	0.27
11/1/2013						1.05	1.44	1.24	0.27
11/8/2013						1.03	1.30	1.17	0.19
11/15/2013						1.06	1.33	1.20	0.19
11/22/2013						1.20	1.32	1.26	0.08
11/29/2013						1.08	1.20	1.14	0.08
12/6/2013						1.05	1.11	1.08	0.04
12/13/2013						0.92	1.03	0.98	0.07
12/20/2013						0.88	0.97	0.93	0.06
12/27/2013						0.84	0.91	0.88	0.05
1/3/2014						0.79	0.86	0.82	0.05
1/10/2014						0.78	0.92	0.85	0.10
1/17/2014						0.77	0.86	0.81	0.06
1/24/2014						0.74	0.81	0.77	0.05
1/31/2014						0.74	0.79	0.76	0.03
2/7/2014						0.80	0.79	0.79	0.01
2/14/2014						0.79	0.68	0.73	0.07
2/21/2014						0.71	0.64	0.68	0.05
2/28/2014						0.75	0.61	0.68	0.10
3/7/2014						0.56	0.54	0.55	0.01
3/14/2014						0.22	0.25	0.23	0.03
3/21/2014						0.23	0.27	0.25	0.03
3/28/2014						0.24	0.25	0.24	0.01
4/4/2014						0.26	0.24	0.25	0.02
4/11/2014						0.30	0.25	0.28	0.04
4/18/2014						0.38	0.29	0.34	0.06
4/25/2014						0.40	0.31	0.35	0.07
5/2/2014						0.45	0.37	0.41	0.06
5/9/2014						0.48	0.40	0.44	0.06
5/16/2014						0.54	0.46	0.50	0.06
5/23/2014						0.58	0.52	0.55	0.04
5/30/2014						0.59	0.58	0.58	0.01
6/6/2014						0.62	0.64	0.63	0.02

6/13/2014				0.84	0.46	0.67	0.73	0.67	0.16
6/20/2014				0.87	0.51	0.69	0.78	0.71	0.15
6/27/2014				0.96	0.56	0.67	0.82	0.75	0.18
7/4/2014				1.07	0.60	0.62	0.84	0.78	0.22
7/11/2014				1.20	0.65	0.61	0.86	0.83	0.27
7/18/2014				1.32	0.71	0.63	0.84	0.87	0.31
7/25/2014				1.42	0.77	0.66	0.83	0.92	0.34
8/1/2014				1.52	0.84	0.70	0.83	0.97	0.37
8/8/2014				1.69	0.93	0.81	0.90	1.08	0.41
8/15/2014				1.80	1.03	0.86	0.97	1.17	0.43
8/22/2014				1.90	1.15	0.92	1.04	1.25	0.44
8/29/2014				1.97	1.28	0.99	1.13	1.34	0.43
9/5/2014			1.43	2.03	1.35	1.04	1.23	1.42	0.37
9/12/2014			1.24		1.22	0.95	1.13	1.14	0.13
9/19/2014			1.09		1.13	0.86	1.14	1.06	0.13
9/26/2014			0.94		1.05	1.00	1.69	1.17	0.35
10/3/2014			0.86		0.99	1.05	1.49	1.10	0.28
10/10/2014			0.77			0.93	1.39	1.03	0.32
10/17/2014			0.67			0.83	1.41	0.97	0.39
10/24/2014			0.66			1.20	1.42	1.09	0.39
10/31/2014			0.79			1.21	1.33	1.11	0.28
11/7/2014			0.74			1.10	1.21	1.01	0.24
11/14/2014			0.68			1.06	1.18	0.97	0.26
11/21/2014			0.62			1.05	1.12	0.93	0.27
11/28/2014			0.51			0.95	1.01	0.82	0.27
12/5/2014			0.44			0.79	0.82	0.69	0.21
12/12/2014			0.03			0.59	0.43	0.35	0.29
12/19/2014			0.06			0.51	0.33	0.30	0.23

Control Meadow Volumetric Soil Moisture (%)									
Week	C4-3	C4-1	C3-2	C3-1	C2-4	C1-3	C1-2	Average	St Dev(±)
9/13/2013						4.57	4.56	4.56	0.01
9/20/2013						9.06	9.00	9.03	0.05
9/27/2013						17.81	16.39	17.10	1.01
10/4/2013						16.81	15.12	15.96	1.20
10/11/2013						15.16	17.53	16.34	1.68
10/18/2013						15.59	17.37	16.48	1.26
10/25/2013						14.45	19.01	16.73	3.23
11/1/2013						14.28	19.27	16.77	3.53
11/8/2013						14.84	18.33	16.58	2.47
11/15/2013						16.14	19.76	17.95	2.56
11/22/2013						19.00	20.80	19.90	1.27
11/29/2013						18.16	19.97	19.07	1.28
12/6/2013						18.52	19.32	18.92	0.57
12/13/2013						17.21	18.98	18.09	1.25
12/20/2013						17.40	18.77	18.08	0.97
12/27/2013						17.55	18.58	18.06	0.72
1/3/2014						17.32	18.44	17.88	0.80
1/10/2014						18.19	20.73	19.46	1.80
1/17/2014						18.90	20.38	19.64	1.05
1/24/2014						19.07	20.37	19.72	0.92
1/31/2014						20.12	20.87	20.49	0.53
2/7/2014						22.88	22.02	22.45	0.61
2/14/2014						21.98	21.88	21.93	0.07
2/21/2014						20.91	21.63	21.27	0.50
2/28/2014						22.55	22.73	22.64	0.12
3/7/2014						29.12	23.06	26.09	4.28
3/14/2014						33.41	27.44	30.43	4.22
3/21/2014						33.76	27.86	30.81	4.17
3/28/2014						33.77	27.89	30.83	4.16
4/4/2014						33.88	28.16	31.02	4.04
4/11/2014						33.89	28.87	31.38	3.55
4/18/2014						33.44	29.12	31.28	3.05
4/25/2014						32.65	28.97	30.81	2.60
5/2/2014						28.07	26.73	27.40	0.95
5/9/2014						26.89	25.50	26.20	0.98
5/16/2014						25.57	24.95	25.26	0.44
5/23/2014						24.25	24.45	24.35	0.14
5/30/2014						22.72	23.95	23.33	0.87
6/6/2014						21.50	23.53	22.52	1.43

6/13/2014			19.91	25.67	14.10	20.50	22.65	20.57	4.26
6/20/2014			19.95	23.91	14.21	19.01	21.76	19.77	3.63
6/27/2014			19.82	24.01	14.07	16.73	20.72	19.07	3.81
7/4/2014			19.68	24.24	13.65	13.92	19.32	18.16	4.44
7/11/2014			19.54	24.48	13.37	12.48	17.69	17.51	4.88
7/18/2014			19.20	24.36	13.23	11.61	15.75	16.83	5.09
7/25/2014			18.61	23.86	13.15	11.04	14.01	16.13	5.13
8/1/2014			17.90	23.44	13.00	10.82	12.92	15.62	5.09
8/8/2014			17.49	23.51	13.01	11.27	12.67	15.59	5.00
8/15/2014			16.74	22.68	13.12	10.89	12.27	15.14	4.74
8/22/2014			15.62	21.66	13.19	10.49	11.90	14.57	4.39
8/29/2014			14.44	20.23	13.25	10.18	11.66	13.95	3.86
9/5/2014			13.39	18.96	12.60	9.69	11.46	13.22	3.50
9/12/2014			12.80		12.19	9.46	11.34	11.45	1.45
9/19/2014			12.48		12.15	9.22	12.22	11.52	1.54
9/26/2014			11.89		12.01	11.58	19.42	13.72	3.80
10/3/2014			11.89		12.06	13.06	18.30	13.83	3.03
10/10/2014			11.86			12.36	18.30	14.17	3.58
10/17/2014			11.51			11.99	19.88	14.46	4.70
10/24/2014			12.59			18.70	21.53	17.60	4.57
10/31/2014			16.66			20.34	21.72	19.57	2.61
11/7/2014			17.34			19.87	21.17	19.46	1.95
11/14/2014			17.84			20.76	22.19	20.26	2.22
11/21/2014			18.18			22.18	22.74	21.04	2.49
11/28/2014			18.63			23.35	23.67	21.88	2.82
12/5/2014			22.09			24.18	23.67	23.31	1.09
12/12/2014			57.08			33.46	24.54	38.36	16.81
12/19/2014			57.31			33.61	28.63	39.85	15.32

Control Meadow Depth to Groundwater (ft)						
Week	**C4-3**	**C3-2**	**C1-3**	**C1-2**	**Average**	**St Dev(±)**
9/13/2013			10.74	10.72	10.73	0.02
9/20/2013			10.16	10.19	10.18	0.02
9/27/2013			9.65	9.66	9.65	0.01
10/4/2013			9.13	9.18	9.16	0.04
10/11/2013			8.63	8.74	8.68	0.07
10/18/2013			8.19	8.28	8.24	0.06
10/25/2013			7.75	7.88	7.81	0.09
11/1/2013			7.36	7.46	7.41	0.07
11/8/2013			6.96	7.10	7.03	0.10
11/15/2013			6.58	6.75	6.67	0.12
11/22/2013			6.31	6.33	6.32	0.02
11/29/2013			5.97	6.03	6.00	0.04
12/6/2013			5.65	5.73	5.69	0.06
12/13/2013			5.37	5.42	5.39	0.04
12/20/2013			5.08	5.15	5.12	0.05
12/27/2013			4.80	4.90	4.85	0.07
1/3/2014			4.54	4.66	4.60	0.09
1/10/2014			4.29	4.44	4.37	0.10
1/17/2014			4.08	4.20	4.14	0.08
1/24/2014			3.86	3.99	3.93	0.09
1/31/2014			3.68	3.77	3.73	0.07
2/7/2014			3.48	3.58	3.53	0.07
2/14/2014			3.58	3.12	3.35	0.32
2/21/2014			3.41	2.95	3.18	0.32
2/28/2014			3.32	2.70	3.01	0.44
3/7/2014			1.91	2.35	2.13	0.31
3/14/2014			0.64	0.92	0.78	0.20
3/21/2014			0.67	0.96	0.81	0.21
3/28/2014			0.71	0.90	0.80	0.13
4/4/2014			0.78	0.85	0.82	0.05
4/11/2014			0.89	0.87	0.88	0.02
4/18/2014			1.15	1.00	1.07	0.10
4/25/2014			1.23	1.06	1.15	0.12
5/2/2014			1.60	1.39	1.49	0.15
5/9/2014			1.80	1.55	1.68	0.18
5/16/2014			2.12	1.86	1.99	0.19
5/23/2014			2.38	2.13	2.25	0.18

5/30/2014			2.58	2.41	2.50	0.12
6/6/2014			2.89	2.73	2.81	0.11
6/13/2014			3.28	3.23	3.25	0.03
6/20/2014			3.62	3.57	3.60	0.04
6/27/2014			4.00	3.95	3.98	0.04
7/4/2014			4.43	4.37	4.40	0.04
7/11/2014			4.89	4.84	4.87	0.04
7/18/2014			5.41	5.35	5.38	0.04
7/25/2014			5.95	5.89	5.92	0.04
8/1/2014			6.49	6.43	6.46	0.04
8/8/2014			7.18	7.12	7.15	0.04
8/15/2014			7.94	7.88	7.91	0.04
8/22/2014			8.78	8.73	8.75	0.04
8/29/2014			9.71	9.66	9.69	0.04
9/5/2014	10.7	10.7	10.74	10.69	10.71	0.02
9/12/2014	9.7345	9.70	10.01	10.01	9.86	0.17
9/19/2014	8.8134	8.76	9.29	9.32	9.05	0.30
9/26/2014	8.016	7.94	8.66	8.72	8.33	0.41
10/3/2014	7.2946	7.20	8.07	8.17	7.68	0.51
10/10/2014	6.5956	6.49	7.49	7.60	7.04	0.58
10/17/2014	5.9753	5.86	6.95	7.09	6.47	0.64
10/24/2014	5.3834	5.26	6.43	6.58	5.91	0.69
10/31/2014	4.8564	4.73	5.95	6.12	5.41	0.72
11/7/2014	4.3843	4.25	5.51	5.69	4.96	0.75
11/14/2014	3.9672	3.83	5.12	5.31	4.56	0.76
11/21/2014	3.561	3.43	4.72	4.92	4.16	0.77
11/28/2014	2.8872	2.76	4.05	4.25	3.49	0.77
12/5/2014	2.124	2.00	3.27	3.48	2.72	0.77
12/12/2014	0.047	0.06	1.75	1.77	0.91	0.99
12/19/2014	0.0336	0.10	1.53	1.16	0.71	0.75

Control Meadow Groundwater Storage (ft)						
Week	**C4-3**	**C3-2**	**C1-3**	**C1-2**	**Average**	**St Dev (±)**
9/13/2013			12.08	12.09	12.08	0.01
9/20/2013			12.31	12.30	12.31	0.01
9/27/2013			12.52	12.51	12.51	0.00
10/4/2013			12.72	12.70	12.71	0.02
10/11/2013			12.92	12.88	12.90	0.03
10/18/2013			13.10	13.06	13.08	0.03
10/25/2013			13.28	13.22	13.25	0.04
11/1/2013			13.43	13.39	13.41	0.03
11/8/2013			13.59	13.54	13.56	0.04
11/15/2013			13.74	13.67	13.71	0.05
11/22/2013			13.85	13.84	13.84	0.01
11/29/2013			13.99	13.96	13.97	0.02
12/6/2013			14.11	14.08	14.10	0.02
12/13/2013			14.23	14.21	14.22	0.01
12/20/2013			14.34	14.31	14.33	0.02
12/27/2013			14.45	14.41	14.43	0.03
1/3/2014			14.56	14.51	14.53	0.03
1/10/2014			14.65	14.60	14.63	0.04
1/17/2014			14.74	14.69	14.72	0.03
1/24/2014			14.83	14.77	14.80	0.04
1/31/2014			14.90	14.86	14.88	0.03
2/7/2014			14.98	14.94	14.96	0.03
2/14/2014			14.94	15.12	15.03	0.13
2/21/2014			15.01	15.19	15.10	0.13
2/28/2014			15.04	15.29	15.17	0.18
3/7/2014			15.61	15.43	15.52	0.13
3/14/2014			16.11	16.00	16.06	0.08
3/21/2014			16.10	15.99	16.04	0.08
3/28/2014			16.09	16.01	16.05	0.05
4/4/2014			16.06	16.03	16.04	0.02
4/11/2014			16.01	16.02	16.02	0.01
4/18/2014			15.91	15.97	15.94	0.04
4/25/2014			15.88	15.95	15.91	0.05
5/2/2014			15.73	15.81	15.77	0.06
5/9/2014			15.65	15.75	15.70	0.07
5/16/2014			15.52	15.63	15.57	0.07
5/23/2014			15.42	15.52	15.47	0.07
5/30/2014			15.34	15.41	15.37	0.05
6/6/2014			15.22	15.28	15.25	0.04

6/13/2014			15.06	15.08	15.07	0.01
6/20/2014			14.92	14.94	14.93	0.01
6/27/2014			14.77	14.79	14.78	0.02
7/4/2014			14.60	14.62	14.61	0.02
7/11/2014			14.41	14.44	14.43	0.02
7/18/2014			14.21	14.23	14.22	0.02
7/25/2014			13.99	14.02	14.01	0.02
8/1/2014			13.78	13.80	13.79	0.02
8/8/2014			13.50	13.53	13.51	0.02
8/15/2014			13.20	13.22	13.21	0.02
8/22/2014			12.86	12.89	12.87	0.02
8/29/2014			12.49	12.51	12.50	0.01
9/5/2014	12.097	12.097	12.08	12.10	12.09	0.01
9/12/2014	12.483	12.495	12.37	12.37	12.43	0.07
9/19/2014	12.85	12.874	12.66	12.65	12.76	0.12
9/26/2014	13.169	13.2	12.91	12.89	13.04	0.17
10/3/2014	13.457	13.495	13.15	13.11	13.30	0.20
10/10/2014	13.736	13.779	13.38	13.33	13.56	0.23
10/17/2014	13.983	14.031	13.59	13.54	13.79	0.26
10/24/2014	14.22	14.27	13.80	13.74	14.01	0.27
10/31/2014	14.43	14.482	13.99	13.93	14.21	0.29
11/7/2014	14.619	14.672	14.17	14.10	14.39	0.30
11/14/2014	14.785	14.838	14.33	14.25	14.55	0.30
11/21/2014	14.947	15	14.48	14.41	14.71	0.31
11/28/2014	15.216	15.269	14.75	14.67	14.98	0.31
12/5/2014	15.521	15.572	15.06	14.98	15.28	0.31
12/12/2014	16.35	16.346	15.67	15.66	16.01	0.39
12/19/2014	16.356	16.327	15.76	15.91	16.09	0.30

Control Meadow Water Balance (ft)					
Week	Priestley AET	Precipitation	Δ Soil Moisture Storage	Δ Groundwater Storage	Inputs-Outputs
9/13/2013	-0.09	0.00			
9/20/2013	-0.06	0.04	0.43	0.22	0.62
9/27/2013	-0.06	0.01	0.73	0.21	0.89
10/4/2013	-0.05	0.00	-0.19	0.20	-0.04
10/11/2013	-0.04	0.03	-0.04	0.19	0.13
10/18/2013	-0.04	0.00	-0.06	0.18	0.08
10/25/2013	-0.02	0.04	-0.05	0.17	0.13
11/1/2013	-0.03	0.00	-0.06	0.16	0.07
11/8/2013	-0.02	0.00	-0.08	0.15	0.05
11/15/2013	-0.01	0.09	0.03	0.14	0.26
11/22/2013	-0.01	0.00	0.06	0.14	0.19
11/29/2013	-0.01	0.01	-0.11	0.13	0.01
12/6/2013	0.00	0.03	-0.07	0.12	0.08
12/13/2013	-0.01	0.00	-0.10	0.12	0.01
12/20/2013	-0.01	0.00	-0.05	0.11	0.05
12/27/2013	-0.01	0.00	-0.05	0.11	0.05
1/3/2014	-0.01	0.00	-0.05	0.10	0.04
1/10/2014	-0.01	0.02	0.03	0.09	0.13
1/17/2014	-0.01	0.00	-0.04	0.09	0.04
1/24/2014	-0.02	0.03	-0.04	0.09	0.06
1/31/2014	-0.01	0.01	-0.01	0.08	0.06
2/7/2014	-0.02	0.30	0.03	0.08	0.39
2/14/2014	-0.03	0.03	-0.06	0.07	0.01
2/21/2014	-0.04	0.11	-0.06	0.07	0.08
2/28/2014	-0.03	0.23	0.01	0.07	0.27
3/7/2014	-0.05	0.08	-0.13	0.35	0.24
3/14/2014	-0.07	0.00	-0.31	0.54	0.16
3/21/2014	-0.07	0.05	0.01	-0.01	-0.02
3/28/2014	-0.04	0.28	0.00	0.00	0.24
4/4/2014	-0.09	0.01	0.01	-0.01	-0.08
4/11/2014	-0.11	0.02	0.02	-0.02	-0.09
4/18/2014	-0.11	0.02	0.06	-0.08	-0.10
4/25/2014	-0.10	0.04	0.02	-0.03	-0.07
5/2/2014	-0.11	0.03	0.06	-0.14	-0.17
5/9/2014	-0.13	0.01	0.03	-0.07	-0.17
5/16/2014	-0.11	0.02	0.06	-0.13	-0.15

5/23/2014	-0.15	0.00	0.05	-0.11	-0.21
5/30/2014	-0.15	0.00	0.03	-0.10	-0.21
6/6/2014	-0.16	0.00	0.05	-0.13	-0.24
6/13/2014	-0.14	0.00	0.04	-0.18	-0.28
6/20/2014	-0.15	0.00	0.03	-0.14	-0.25
6/27/2014	-0.17	0.00	0.04	-0.15	-0.28
7/4/2014	-0.16	0.00	0.03	-0.17	-0.30
7/11/2014	-0.15	0.00	0.04	-0.19	-0.29
7/18/2014	-0.12	0.00	0.05	-0.21	-0.28
7/25/2014	-0.12	0.04	0.04	-0.21	-0.26
8/1/2014	-0.10	0.08	0.05	-0.22	-0.18
8/8/2014	-0.13	0.00	0.11	-0.27	-0.29
8/15/2014	-0.14	0.00	0.08	-0.30	-0.35
8/22/2014	-0.13	0.00	0.09	-0.34	-0.38
8/29/2014	-0.11	0.00	0.09	-0.37	-0.40
9/5/2014	-0.10	0.00	0.07	-0.41	-0.44
9/12/2014	-0.09	0.00	-0.28	0.34	-0.02
9/19/2014	-0.07	0.05	-0.08	0.33	0.22
9/26/2014	-0.06	0.00	0.12	0.28	0.35
10/3/2014	-0.07	0.00	-0.07	0.26	0.12
10/10/2014	-0.05	0.04	-0.07	0.26	0.18
10/17/2014	-0.03	0.03	-0.06	0.23	0.17
10/24/2014	-0.03	0.05	0.12	0.22	0.37
10/31/2014	-0.03	0.04	0.02	0.20	0.23
11/7/2014	-0.03	0.04	-0.10	0.18	0.09
11/14/2014	-0.01	0.02	-0.04	0.16	0.13
11/21/2014	-0.01	0.05	-0.04	0.16	0.15
11/28/2014	0.00	0.35	-0.11	0.27	0.51
12/5/2014	0.00	0.50	-0.14	0.31	0.67
12/12/2014	-0.01	0.12	-0.33	0.72	0.50
12/19/2014	0.00	0.08	-0.05	0.08	0.10

Appendix E:

Marian Meadow and Control Meadow Soil Survey Information

Table Explanation. This soil series data is taken in its entirety from the UC Davis Soil Web Survey. The area that MM is located within was surveyed as containing 60 Holland and 30% Skalan soil. CM was surveyed as 85% Elam(EmB), an Entisol. A small portion of CM was surveyed as 85% Cohasset (CgD) (see Figure below)

Holland Series				
Depth Range	**Horizon Designation**	**Percent Clay**	**Percent Sand**	**Percent Plant Organic Matter**
0-41	H1	20.00	42.10	2.5
41-112	H2	25.00	38.50	0.75
112-152	H3	31.00	18.10	0.5
Skalan Series				
Depth Range	**Horizon Designation**	**Percent Clay**	**Percent Sand**	**Percent Plant Organic Matter**
0-36	H1	15.00	65.90	2.5
36-152	H2	25.00	38.50	0.75
152-200	H3	x	x	x
Elam Series				
Depth Range	**Horizon Designation**	**Percent Clay**	**Percent Sand**	**Percent Plant Organic Matter**
0-13	H1	7.50	83.50	5
13-102	H2	11.50	65.70	0.35
102-114	H3	x	x	x
114-152	H4	11.50	65.70	0.00
Cohasset Series				
Depth Range	**Horizon Designation**	**Percent Clay**	**Percent Sand**	**Percent Plant Organic Matter**
0-38	H1	20	42.1	4
38-102	H2	30	x	0.75
102-112	H3	x	35.9	x

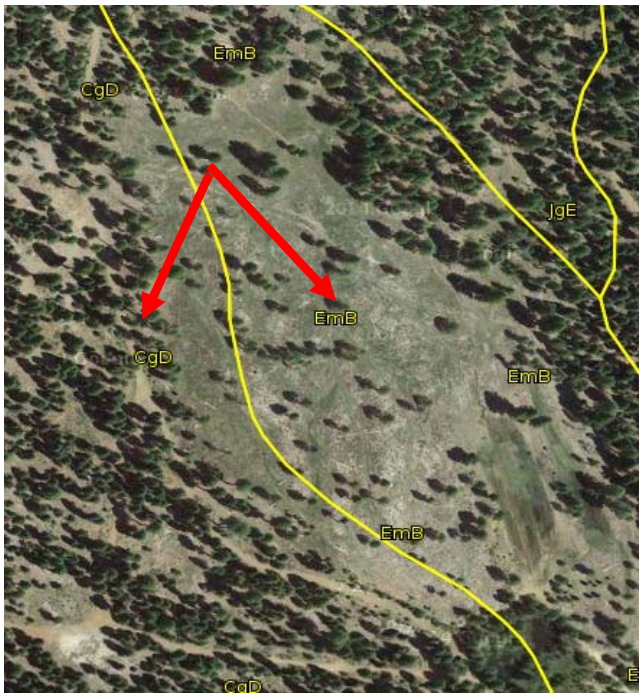

Appendix F

Iron Oxide Paint Fabrication Instructions

(reproduced from: http://www.uidaho.edu/cals/pses/pedology/resources/Analyses See:

Iron Oxide Paint - Indicator of Reduction in Soil (IRIS) tubes

Iron Oxide Paint
Indicator of Reduction in Soil (IRIS) Tubes

Equipment

- distilled water (DW) system
- pH meter
- 7 and 10 pH buffer solutions
- dialysis tubing (~12 ft x 1.5 in.)
- constant water bath in large dish pan
- graduated cylinder
- 2000, 1000, 100-mL volumetric flasks
- 250-mL centrifuge tubes/bottles
- 2 or 4-L glass beaker
- centrifuge
- very fine sand paper (220 grit)
- 2-inch foam brushes
- 1/2 inch, schedule 40 PVC pipe
- drill
- ring stand and clamps
- saw
- refrigerator
- one-liter opaque Nalgene storage containers

Reagents

- Anhydrous $FeCl_3$ (ferric chloride) – Use Baker or Fisher analyzed reagent-grade stock.

- 1 M KOH (potassium hydroxide) – Weigh 56 grams KOH, dissolve, and make to one liter
- volumetrically using TDW. Calculate amount needed and make in a 4-L glass bottle.

- 1 M $AgNO_3$ (silver nitrate) – Weigh 17.0 grams $AgNO_3$ and add to a 100-mL volumetric flask.

- Make the $AgNO_3$ to volume with TDW.

- Acetone – Use Baker or Fisher analyzed reagent-grade stock.

Comments

This procedure was adapted from M. C. Rabenhorst's Quick (7 day) IRIS paint recipe by email communication, March 2006. Paint recipe may be doubled. Calibrate pH meter using pH 7 and 10 (or higher) buffers. Paint should be stored in a cool, dark location, preferably a refrigerator. The suspension should be suitable for painting IRIS tubes approximately 1 week after the initial synthesis of the Fe oxides. Use appropriate precautions when making paint, cutting pipe, and painting. Use goggles and gloves when cutting, sanding, cleaning, and painting.

Procedure

1. Dissolve 16 g of anhydrous $FeCl_3$ in 500-mL distilled water in a 2-L beaker or larger if recipe doubled. Stir solution by placing on a magnetic stirrer. Initial pH will be approximately 1.6. Begin stirring and monitoring pH as you add approximately 370-mL of 1 M KOH until you reach pH 12. Add the KOH slowly as you approach pH 12. Allow the suspension to stand for 30 minutes, then restart the stirring and check the pH. Keep adding 1 M KOH until pH 12 is reached. The total volume of suspension should be approximately 900-mL.

2. Transfer the paint suspension into four 250-mL centrifuge tubes/bottles. Centrifuge at approximately 1000 rpm for 5 min to concentrate the Fe oxides. Discard the supernatant. *If suspension does not separate after centrifugation, re-check pH and add 1 M KOH until pH 12 is reached.* Transfer the contents into two 250-mL centrifuge tubes/bottles. Mix precipitated Fe oxide with distilled water and centrifuge 2 more times. Discard the supernatant each time.

3. After the 3rd centrifugation, re-suspend the Fe oxides with distilled water and transfer to dialysis tubing. Place the dialysis tubing into basins/tubs filled with distilled water. Create a constant water bath with distilled water dripping into basins/tubs to replace water every 6 hrs for the first day and every 12 hrs for 2 additional days. *Test the water bath for the presence of salts by dropping $AgNO_3$ and noting the presence of a white precipitate. Continue with the water bath until the white precipitate no longer appears.*

4. Transfer the paint from the dialysis tubing to an opaque Nalgene storage bottle. Store paint in the refrigerator.

5. To get the correct paint consistency, transfer paint into 250-mL centrifuge tubes/bottles and centrifuge at approximately 1000-1500 rpm for 5 min. Decant the supernatant so there is the same volume of supernatant as the volume of the Fe oxide "cake" at the bottom of the bottle. Thoroughly re-suspend the Fe oxide. Paint should be the appropriate consistency to paint the tubes.

6. Apply paint to the tubes (1/2 inch, schedule 40 PVC that have been cleaned with acetone to remove the ink and lightly sanded with very fine sand paper (~220 grit)) using a 2-inch foam brush, while the tube is spun using a drill (like a lathe). See picture below for actual set-up to paint tubes. Test the paint by painting one or two prepared tubes and allowing the paint to dry overnight. If the paint on the tubes is resistant to abrasion (does not rub off easily on your fingers), then proceed to paint and prepare IRIS tubes.

References

Castenson, K.L. 2004. Hydromorphology of Piedmont floodplain soils. M.S. Thesis. Univ. of
Maryland, College Park, MD.

Castenson, K.L., and M.C. Rabenhorst. 2006. Indicator of reduction in soil (IRIS): Evaluation of a new approach for assessing reduced conditions in soil. Soil Sci. Soc. Am. J. *In Press*.

Jenkinson, B. 2002. Indicators of Reduction in Soils (IRIS): A visual method for the identification of hydric soils. Ph.D. diss. Purdue Univ., West Lafayette.

Jenkinson, B.J., and D.P. Franzmeier. 2006. Development and evaluation of Fe-coated tubes that
indicate reduction in soils. Soil Sci. Soc. Am. J. 70: 183-191.

Rabenhorst, M.C. 2006. Quick (7 day) IRIS paint recipe. Email communication, March 2006.

Rabenhorst, M. C., and K. L. Castenson. 2005. Temperature effects on iron reduction in a hydric
soil. Soil Science 170:734-744.

Schwertmann, U., and R.M. Cornell. 2000. Iron Oxides in the Laboratory: Preparation and
Characterization. 2nd ed. Wiley-VCH, New York.

Calculations

There are not any calculations necessary for this procedure.

Quick (7 day) IRIS Tube Paint Recipe
M. C. Rabenhorst
November 29, 2005
Modified March 2, 2006

1. Dissolve 16g of anhydrous $FeCl_3$ in 0.5 L of distilled water (approximately 0.2M) in a 2 L beaker. Add a magnetic stir bar and place on a magnetic stirrer. The initial pH of this solution will be approximately 1.6. While stirring, monitor the pH as you add approximately 370 mL of 1M KOH until you reach a pH of 12 (use pH buffers of 7 and 10 (or higher) to standardize the pH meter rather than 4 and 7). At around pH 4, the Fe oxides will begin to precipitate rapidly and the suspension will become very thick. You will need to speed up the stir bar and continue to adjust it in order to maintain a stirred suspension. Continue adding the KOH until the pH reaches 12.0, adding it more slowly and carefully as you approach the final pH. Allow the suspension to stand for approximately 30 minutes, then restart the stirring and check the pH. If it has dropped below 12.0, add additional KOH dropwise to bring it back to the target pH. The total volume of suspension should be approximately 900 mL.

2. Transfer the suspension equally into four 250 mL nalgene bottles and centrifuge at approximately 1000 rpm for 5 min to concentrate the Fe oxides. Discard the supernatant. Transfer the contents of the four tubes into two 250 mL tubes and centrifuge wash the precipitated Fe oxide 2 times with distilled water, discarding the supernatant each time.

3. After the 3rd centrifugation, resuspend the Fe oxides with distilled water and transfer to dialysis tubing. Place the dialysis tubing into basins filled with distilled water and replace the water at approximately 6 hr intervals during the first day and then at approximately 12 hr intervals for a total of 3 days. Transfer the Fe oxides from the dialysis tubing to a nalgene storage bottle and keep in the dark. The suspension should be suitable for painting IRIS tubes approximately 1 week (7 days) after the initial synthesis of the Fe oxides.

4. To get the paint to the right consistency, place the paint in a 250 mL centrifuge bottle and centrifuge at approximately 1000- to 1500 rpm for approximately 5 minutes. After centrifugation, decant the supernatant so that there is approximately the same volume of supernatant as the volume of the Fe oxide "cake" at the bottom of the bottle (see figure). Then thoroughly resuspend the Fe oxide and the paint should be at approximately the correct consistency for painting tubes.

5. Paint is applied to the tubes (½ " schedule 40 pvc that has been cleaned with acetone to remove ink and lightly sanded with very fine sandpaper) using a 2" foam brush while the tube is spun using a cordless drill. Test the paint by painting one or two prepared PVC IRIS tubes and allowing the paint to dry overnight. If the paint on the tubes is resistant to abrasion (does not rub off easily on your fingers) then proceed to paint and prepare IRIS tubes.

References:

Rabenhorst, M. C. 2005. Using Synthetic Iron Oxides as an Indicator of Reduction in Soils (IRIS). SSSA Meetings (Salt Lake City, UT) Nov. 6-10. Annual Meeting Abstr.

Rabenhorst, M. C., and S. N. Burch. 2006. Synthetic Iron Oxides as an Indicator of Reduction in Soils (IRIS). Soil Sci. Soc. Am. J. *In Press*.

Rabenhorst, M. C., and K. L. Castenson. 2005. Temperature Effects on Iron Reduction in a Hydric Soil. Soil Sci. 170:734-742.

Castenson, K. L., and M. C. Rabenhorst. 2006. Indicator of Reduction in Soil (IRIS): Evaluation of a New Approach for Assessing Reduced Conditions in Soil. Soil Sci. Soc. Am. J. *In Press*.

Jenkinson, B.J., and D.P. Franzmeier. 2006. Development and evaluation of Fe-coated tubes that indicate reduction in soils. Soil Sci. Soc. Am. J. 70: 183-191.

Appendix G:

Climate Data

Week	Weekly Precipitation Total (in.)	Average Daily Net Radiation $(\frac{mJ}{(day)m^2})$	Average Mean Daily Air Temperature ˚C
9/13/2013	0.03	8.91	18.61
9/20/2013	0.44	7.15	15.48
9/27/2013	0.10	6.73	9.01
10/4/2013	0.01	6.06	9.52
10/11/2013	0.35	5.36	8.41
10/18/2013	0.00	4.64	7.02
10/25/2013	0.43	2.86	10.32
11/1/2013	0.00	3.22	6.27
11/8/2013	0.00	2.74	5.52
11/15/2013	1.12	1.87	7.66
11/22/2013	0.00	1.40	4.72
11/29/2013	0.06	1.14	3.49
12/6/2013	0.37	0.94	0.99
12/13/2013	0.02	1.08	-6.83
12/20/2013	0.00	0.94	0.04
12/27/2013	0.00	1.14	2.30
1/3/2014	0.00	0.99	1.90
1/10/2014	0.26	1.65	1.79
1/17/2014	0.03	1.84	3.45
1/24/2014	0.32	2.24	2.98
1/31/2014	0.08	2.25	4.64
2/7/2014	3.59	2.20	-0.48
2/14/2014	0.30	4.39	4.17
2/21/2014	1.31	4.84	5.04
2/28/2014	2.74	3.82	5.24
3/7/2014	0.92	6.50	4.25
3/14/2014	0.00	8.22	5.67
3/21/2014	0.57	8.48	6.83
3/28/2014	3.38	6.11	5.48
4/4/2014	0.13	10.97	2.66
4/11/2014	0.28	11.95	8.53
4/18/2014	0.22	12.18	10.83
4/25/2014	0.46	11.94	9.09
5/2/2014	0.32	13.14	7.74
5/9/2014	0.06	13.93	9.44
5/16/2014	0.27	11.84	11.55
5/23/2014	0.00	14.98	12.38
5/30/2014	0.00	14.92	14.13
6/6/2014	0.01	15.52	15.24

6/13/2014	0.00	15.00	18.41
6/20/2014	0.04	14.68	13.53
6/27/2014	0.00	15.42	17.02
7/4/2014	0.01	14.30	20.12
7/11/2014	0.04	13.16	22.30
7/18/2014	0.02	11.46	23.77
7/25/2014	0.46	11.34	20.75
8/1/2014	1.01	9.37	21.67
8/8/2014	0.00	12.04	19.72
8/15/2014	0.03	13.05	19.33
8/22/2014	0.00	12.04	18.69
8/29/2014	0.00	10.72	18.81
9/5/2014	0.00	9.87	17.98
9/12/2014	0.03	8.59	15.87
9/19/2014	0.54	7.22	17.50
9/26/2014	0.05	6.07	15.71
10/3/2014	0.00	6.68	11.71
10/10/2014	0.51	5.58	14.96
10/17/2014	0.32	3.32	11.59
10/24/2014	0.65	3.67	9.33
10/31/2014	0.51	3.61	8.65
11/7/2014	0.42	2.99	7.30
11/14/2014	0.27	2.04	8.10
11/21/2014	0.59	1.83	3.13
11/28/2014	4.24	0.39	3.97
12/5/2014	6.04	0.36	3.77
12/12/2014	1.46	0.79	5.00
12/19/2014	0.92	0.59	2.38